Analyses of Desmin Disease Mutants *in vivo* with Emphasis on their Effects on Myoblast Differentiation

Pavle Krsmanovic
Doctoral Thesis
German Cancer Research Centre (DKFZ)

Dissertation

submitted to the
Combined Faculties for the Natural Sciences and for Mathematics
of the Ruperto-Carola University of Heidelberg, Germany
for the degree of
Doctor of Natural Sciences

Presented by: Pavle Krsmanovic,
MSc Molecular and Cellular Biology
Born in: Belgrade, Serbia

Oral-examination: April 2013

Analyses of Desmin Disease Mutants *in vivo* with Emphasis on their Effects on Myoblast Differentiation

Referees: Prof. Dr. Harald Herrmann-Lerdon
Prof. Dr. Peter Lichter

Declaration by the PhD Candidate

I hereby declare that the data described and presented in this thesis are a result of my own work and effort. In cases where other sources of information have been used, they have been appropriately indicated and referenced. The particular experiments performed by others, as well as figures supplemented by them, have been rightfully acknowledged.

Heidelberg, 14.02.2013 _____

Pavle Krsmanovic

Acknowledgments

I would hereby like to acknowledge all the past and present members of the group of Functional Architecture of the Cell (B065) in the German Cancer Research Centre (DKFZ). Their support and advices through the course of my PhD thesis were of great significance for the success of the work.

In particular, I would like to Michaela Hergt for her guidance, help and advices during my work with cells. She not only gave me a lot of advices regarding the work with antibodies in immunecytochemical procedures but also helped me establish the procedures for maintaining the cells in culture. Finally, she performed the staining with hematoxylin-eosin histological dyes on C2C12 cells. In addition, I would also like to thank Thorsten Kolb who has helped with some other laboratory procedures as well as frequently giving me useful tips and technical advices. I have had quite a number of helpful discussions with him on the topic of my work.

I would also like to thank to Dr. Vered Raz, Human and Clinical Genetics, Leiden University Medical Center, The Netherlands, for her suggestion of the differentiation marker to be used in the studies with the C2C12 cells.

I would also like to acknowledge the collaboration with the group Prof. Zentgraf, DKFZ, in an effort to generate monoclonal antibodies specific for human desmin, as well as the work done with Dr. Rackwitz, Peptide specialty laboratories, Heidelberg, which included generation of various rabbit antibodies specific for different types of desmin.

Furthermore, I would like to thank Prof. Stephan Frings, Prof. Gabriele Elisabeth Pollerberg and in particular Prof. Peter Lichter for readily accepting to be my examiners.

On top of all, I would like to thank to Prof. Harald Herrmann-Lerdon, the supervisor of my work, for helping me shape the project and having some quite fruitful discussions with me on the experimental results.

Last but not least, I would like to thank to PD Dr. Karsten Richter and the electron microscopy facility of the DKFZ who have performed electron microscopy images of cells I have been working with and thereby provided me with a useful high-resultion images of the cells.

Abstract

Mutations in genes of various intermediate filament (IF) proteins are the causes of a wide range of diseases. For example, a premature aging disorder, Hutchinson-Gilbert progeria syndrome, is caused by mutation in the nuclear lamins. Mutations in a muscle-specific IF protein desmin cause a wide range of myofibrillar myopathies, and in severe cases cardiomyopathies. The effects of the desmin mutations vary with respect to the severity of their impact on its filament formation capacity. One of the observations on the tissue sections of the patients includes the occurrence of both apparently normal association of desmin filaments with Z-discs as well as the occurrence of desmin accumulations in the muscle cells of patients. However, the exact mechanisms leading to such phenotype remain unknown.

The purpose of this PhD thesis was to analyse the effects of some of the known desmin mutations on cell differentiation. In addition, considering what appears to be concurrent occurrence of desmin aggregation and IFs formation as indicated above we aimed to determine to what extent are normal and mutant desmin proteins segregated in these cells. For that purpose, we have employed C2C12 murine myoblast cell line for analyses of the impacts of desmin mutantions. As these cells can be induced to differentiate they are commonly used as a model in studies on muscle cells. Therefore, we have transfected genes of the normal human desmin (*hDes*WT) and some known desmin mutants into these cells. In order to detect the transfected protein antibodies specific for *hDes* were generated.

Two desmin gene mutations were used for the analyses, namely *hDes*E245D and *hDes*R350P. Whereas the former desmin mutant was found to be incorporated into the IF-system of fibroblasts, the later segregates from it and accumulates in small aggregates through the cell. The analyses performed included cell fractionation and immuno-cytochemistry. *hDes*WT and *hDes*E245D mutant were predominantly found to incorporate into endogenous desmin IFs, whereas the extent of *hDes*R350P mutant incorporation into the filaments varied in the cell population. By subsequent cell passaging the number of *hDes*R350P-expressing cells was reduced, whereas both *hDes*WT and *hDes*E245D were still expressed to a similar extent.

Subsequently transfected C2C12 cells were induced to differentiate. Similarly to the observations in cell passaging, the amount of *hDes*R350P but not *hDes*WT or *hDes*E245D in cells was found to be reduced upon differentiation. Expression of a myosin heavy chain, a C2C12 differentiation marker, was higher in cells expressing either of the mutants than in untransfected or the cells transfected with the *hDes*WT desmin. Finally, the transfected cells were subjected to immuno-cytochemical analyses with respect to the coexpression of myosin heavy chain and of the various transfected desmins. Whereas *hDes*WT and *hDes*E245D were both present in approximately 70% of myosin heavy chain positive cells, about 10% of differentiating cells contained *hDes*R350P.

Additional studies on C2C12 cells included the analyses of distribution of the A-type lamins in undifferentiated and differentiated cells. Whereas in the undifferentiated C2C12 cells some soluble A-type lamins could have been extracted, the differentiated cells appeared to contain very little of such lamins. Furthermore, the A-type lamin distribution in cells transfected with *hDes*R350P, but not *hDes*WT or *hDes*E245D, and subjected to differentiation was the same as in myoblasts, indicating the cells likely fail to undergo differentiation. These results demonstrate a very close connection between cytosolic and nuclear IFs. Finally, they indicate that the late onset of desminopathies could be correlated to the steady *hDes*R350P clearance from the cultured myoblasts leading to their failure of cells to differentiate.

Zusammenfassung

Mutationen in Genen, die für eines der vielen Intermediärfilament-(IF)-Proteine kodieren, sind die Ursache für eine Vielzahl humaner Erkrankungen. Mutationen im muskelspezifischen IF-Protein Desmin verursachen myofibrillärer Myopathien und in schweren Fällen auch Cardiomyopathien (Desminopathien). Sind nukleäre IF-Proteine wie die Lamine betroffen, so beobachtet man ein breites Spektrum von Erkrankungen, und zwar ebenfalls Muskeldystrophien und Cardiomyopathien aber auch systemische Erkrankungen wie die vorzeitigen Alterung oder Progerie. Die verschiedenen Desmin-Mutationen unterscheiden sich hinsichtlich der Schwere ihrer Auswirkungen auf die Fähigkeit des Proteins, geordnete Filamente zu bilden. Übereinstimmend mit dieser aus *in vitro*-Experimenten gewonnenen Erkenntnis beobachtet man auf Gewebeschnitten von Patienten das massive Auftreten von Desmin-Aggregaten sowie eine umfassende strukturelle Degeneration der Sarkomere. Die zugrunde liegenden Pathomechanismen sind weitestgehend nicht bekannt.
Das Ziel dieser Doktorarbeit war es daher, die Auswirkungen einiger der signifikanten Desmin-Mutationen auf die Muskelzell-Differenzierung zu analysieren. Frühere Studien hatten gezeigt, dass Desmin-Aggregate und IFs nebeneinander in Myotuben auftreten können. Daher war es unser Ziel, zu ermitteln in welchem Umfang normales und mutiertes Desmin in Muskelzellen in gemeinsamen Strukturen auftauchen oder ob sie teilweise oder vollständig segregieren. Zu diesem Zweck haben wir die Maus-Zelllinie C2C12, die von Myoblasten abgeleitet ist und die sich in Kultur zu Myotuben differenzieren lässt, zur Analyse der Desmin-Mutanten eingesetzt. Um normales humanes Desmin (*hDes*WT) und von ihm abgeleitete Mutanten nach Transfektion in C2C12-Zellen von endogenem Desmin unterscheiden zu können, haben wir einen für humanes Desmin spezifischen Antikörper erzeugt.
Als beispielhafte Mutanten haben wir *hDes*E245D und *hDes*R350P gewählt. Die erstere inkorporiert in das IF-System von Fibroblasten, die letztere segregiert vollständig und lagert sich in Form kleiner Aggregate ab. In C2C12-Zellen war das Ergebnis deutlich anders: während *hDes*E245D wie *hDes*WT nach Transfektion in endogene IFs inkorporiert wurde, war das Auftreten von *hDes*R350P in unterschiedlichen Zellen einer Kultur sehr variabel. Als wichtigstes Ergebnis aber erhielten wir, dass die Expression von *hDes*R350P im Verlauf nachfolgender Passagen fast vollständig verloren ging - ganz im Gegensatz zu der von *hDes*WT und *hDes*E245D, die relativ stabil exprimiert wurden.
An diese Experimente anschließend wurden transfizierte C2C12-Zellen zur Differenzierung angeregt. Ähnlich zu den Beobachtungen während der fortgesetzten Kultur nicht differenzierender Zellen, wurde die Menge von *hDes*R350P, nicht aber die von *hDes*WT und von *hDes*E245D, in den Zellen während der Differenzierung stark reduziert. Dieser Befund deutet darauf hin, dass die Gegenwart von *hDes*R350P in den Zellen die Differenzierung behindert. Dagegen war die Expression der schweren Kette des Myosins (MHC), einem Differenzierungsmarker für C2C12-Zellen, höher in mit den Mutanten als in den mit *hDes*WT transfizierten Zellen. Weiterhin, während *hDes*WT und *hDes*E245D in etwa 70% der MHC-positiven Zellen gefunden wurde, enthielten weniger als 10% der differenzierenden Zellen *hDes*R350. Basierend auf diesen Beobachtungen mit C2C12-Zellen, könnte man vermuten, dass auch in Patienten bestimmte mutierte Desmin-Varianten die zelluläre Homöostase deutlicher stören als andere und daher zu einem früheren Beginn der Erkrankung führen. Schließlich deutet eine andere Beobachtung, die veränderte Menge an Lamin A im Nukleoplasma als Folge der Anwesenheit mutierter Desmine, auf einen weiteren Aspekt des Pathomechanismus hin, und zwar könnte die Expressionskontrolle einiger Gene durch Reduktion der Menge nukleoplasmatischen Lamins langfristig gestört werden und somit zur Entwicklung einer Desminopathie führen.

Table of Contents

1. Introduction 1
1.1 Intermediate filaments 1
1.1.1 Different filamentous networks in a cell 1
1.1.2 Abundance of the IF proteins 1
1.1.3 Structure of the IF proteins 2
1.1.4 Different classes of the IF proteins 3
1.1.5 Assembly of the IFs 3
1.2 Myocytes and IF-associated diseases 4
1.2.1 IF networks in myocytes 4
1.2.2 Myofibrillar myopathies 6
1.2.3 Desminopathies 7
1.3 Objectives 7
1.3.1 Background of the Study 7
1.3.2 Aims of the Work 9

2. Materials and Methods 11
2.1 Materials 11
2.1.1 List of Chemicals 11
2.1.2 Primary Antibodies 12
2.1.3 Primers 12
2.1.4 Plasmids (Clones) 13
2.1.5 Cell Lines and Bacterial Strains 13
2.1.6 Cell Culture Media and Solutions 13
2.1.7 Buffer Solutions 14
2.1.8 Reagents and enzymes 14
2.1.9 Laboratory Equipment and Software 15
2.2 Methods 15
2.2.1 Maintenance of Cell Cultures 15
2.2.2 Cloning and Mutagenesis 16
2.2.3 Cell Transfection 17
2.2.4 In situ Cell Fractionation: Preparation of Cytoskeletons 17
2.2.5 SDS-Polyacrylamide Gel Electrophoresis and Western Blotting 18
2.2.6 Cell Fixation and Immuno-cytochemistry (ICC) 19
2.2.7 Hematoxylin-Eosin (HE) Staining 20
2.2.8 Microscopy and Image Processing 20
2.2.9 Immunoprecipitation (IP) 20
2.2.10 Electron Microscopy (EM) 21

3. Results 22
3.1 Generating desmin antibodies and the analyses of their specificity 22
3.1.1 Anti-desmin D9 monoclonal antibody detects mouse and human desmin with equal specificity 22
3.1.2 Human desmin 1 antibody is highly specific for human desmin 24
3.1.3 Whereas mouse desmin 1 antibody detects both mouse and human desmin proteins, mouse desmin 2 antibody is specific for mouse desmin on WB 26
*3.1.4 Successful generation of antibodies specific for either Des*WT *or Des*R350P 28
3.1.5 Antibodies binding to different epitopes of IF proteins could have a different staining pattern in ICC 30
3.2 Analyses of the IF proteins in C2C12 cells 32

3.2.1 A-type lamins are differently distributed in C2C12 cultured in growth or differentiation medium 33
3.2.2 Desmin expression increases in C2C12 cells upon differentiation 34
3.2.3 Whereas undifferentiated C2C12 cells are basophilic, they become eosinophilic upon differentiation 36
3.2.4 Electron Microscopy of C2C12 (GM) and (DM) cells revealed distinct patterns of their IFs 38
3.3 Effects of transfection of human desmin in C2C12 myoblasts **38**
*3.3.1 hDes*WT *is readily incorporated into the pre-existing mouse desmin filament network* 41
*3.3.2 hDes*E245D *is largely integrated into the endogenous desmin filaments* 43
3.3.3 hDesR350P is asymmetrically distributed in C2C12 cells 44
3.3.4 Western blotting of the cell extracts revealed that the amount of hDesR350P in C2C12 transfected cells decreases during subsequent passages 51
3.3.5 mCherry-tagged hDesR350P is degraded by the C2C12 cells 53
*3.3.6 Whereas hDes*WT *forms irregular filaments in Vim$^{-/-}$ fibroblasts, hDesR350P forms aggregates* 54
*3.3.7 mDes*WT *does not co-immunoprecipitate with the hDes* 55
3.4 Differentiation of the human desmin transfected C2C12 cells **56**
*3.4.1 The amount of transfected desmin*R350P *reduces upon differentiation of C2C12 cells* 56
3.4.2 C2C12 cells expressing desmin mutants largely fail to fuse 59
3.4.3 Distribution of A-type lamins in C2C12 cells transfected with desminR350P remains myoblast-like after induction of differentiation 62
3.4.4 C2C12 cells transfected with either of the mutant desmins express a higher amount of differentiation marker compared to those expressing wild type desmin 64
3.4.5 C2C12 cells expressing hDesR350P delay their differentiation 65

4. Discussion **68**
4.1 The experimental system employed in the study **68**
4.1.1. Optimisation of the C2C12 growth and differentiation procedures 68
4.1.2. Analyses of colocalisation of different antibodies 69
4.1.3 Other technical obstacles and limitations 72
4.2 The impact of the desmin mutants on the endogenous IF network of C2C12 cells **74**
4.2.1 Mild mutants being incorporated into the filaments 74
4.2.2 Asymmetric distribution of severe mutants upon cell division 74
4.2.3 The mutant desmin protein is not entirely segregated from the wt one 76
4.3 Differentiation of C2C12 cells expressing mutant desmin **77**
4.3.1 Effects of G9a inhibitor and geneticin treatments onto C2C12 differentiation 77
4.3.2 Presence of hDesR350P could stimulate either differentiation or cell proliferation in C2C12 cells 79
4.4 Conclusions and the outlook **80**

5. References **82**

6. Appendices **88**
Appendix 1: List of abbreviations **88**
Appendix 2: h/mDesmin amino acid sequences alignment **90**
Appendix 3: Amino acids **91**

1. Introduction

1.1 Intermediate filaments

1.1.1 Different filamentous networks in a cell

The eukaryotic cytoskeleton represents an elaborate system of filaments, which integrates the cellular organelles into a coordinated system. It primarily consists out of three distinct network types: microfilaments (MFs), microtubules (MTs) and intermediate filaments (IFs). The three filament systems are in addition supported by a large number of associated proteins. Actin and tubulin, which represent principal components of the MFs and MTs respectively, are globular subunits existing in three primary isoforms, α, β, and γ. They are found in cells of all eukaryotic organisms and play a major role in cell contraction and motility, in case of MFs, or represent a transport scaffold for trafficking of various cellular components, as in case of MTs. IFs, on the other hand, which are coded by over 70 genes as in case of humans, are characterised by common domain organisation albeit with high differences in their amino acid composition (Herrmann and Aebi 2004).

1.1.2 Abundance of the IF proteins

Unlike MFs or MTs, which are found throughout the eukaryotic kingdom, IFs are restricted to metazoan cells. The name for IFs stems from their filaments diameter of ~10-12 nm which is intermediate to that of MFs (~5-8 nm) and MTs (~20-25 nm). As such, they have been initially observed in the 1960s upon analysis of metaphase myocytes as filament structures which stained negative for actin and myosin (Ishikawa et al. 1968). The three distinct filament systems can be distinguished by electron microscopy (EM) or immunofluorescence microscopy in different myogenic cultured cells (Franke et al. 1978).

Most metazoans exhibit two distinct IF systems: cytosolic and nucleoplasmic. Cytosolic IFs span the cytoplasm whereby they connect various plasma membrane-associated complexes, such as desmosomes and hemidesmosomes in epithelial cells, or costamers and intercalated discs in striated cardiac muscle. On the other hand, nucleoplasmic IF networks span the chromatin being located primarily adjacent to the inner nuclear membrane (INM). Their main components are the lamins (Herrmann et al. 2007). Nuclear lamina, a meshwork of lamins, further integrates INM proteins, nuclear pores and heterochromatin into a joint functional surface. The lamina network remains stable throughout the cell cycle, except during mitosis

when the nuclear envelope opens up and lamins are phosphorylated leading to their dispersion throughout the cytosol.

1.1.3 Structure of the IF proteins

As indicated above, members of the IF superfamily share their domain organisation. Namely, they exhibit a tripartite structure, consisting of a central α-helical "rod" domain flanked by a non-α-helical amino-terminal "head" and a carboxy-terminal "tail" domain (Geisler et al. 1982). The α-helix of the rod domain consists out of four subdomains, namely 1A, 1B, 2A and 2B, which are connected by non-α-helical linkers, L1 and L12, as well as the helical L2 linker (the model is depicted on figure 1A). The length of the α-helical subdomains is conserved to the very amino acid among vertebrate cytoplasmic IFs.

In addition, the α-helical domain consists out of seven-residue (heptad) repeat with a short discontinuity in the 2B subdomain, the so called "stutter" (Parry 2005). The heptad repeats further leads to the formation of coiled-coil dimers of two IF polypeptides (figure 1B), which represent the building blocks of the IF assembly. The coiled-coil dimmers of IF proteins also exhibit a high stability in buffers containing high concentrations of salt or detergents, indicating that their tight association is likely mediated by a combination of hydrophobic and ionic interactions (Steinert and Roop 1988).

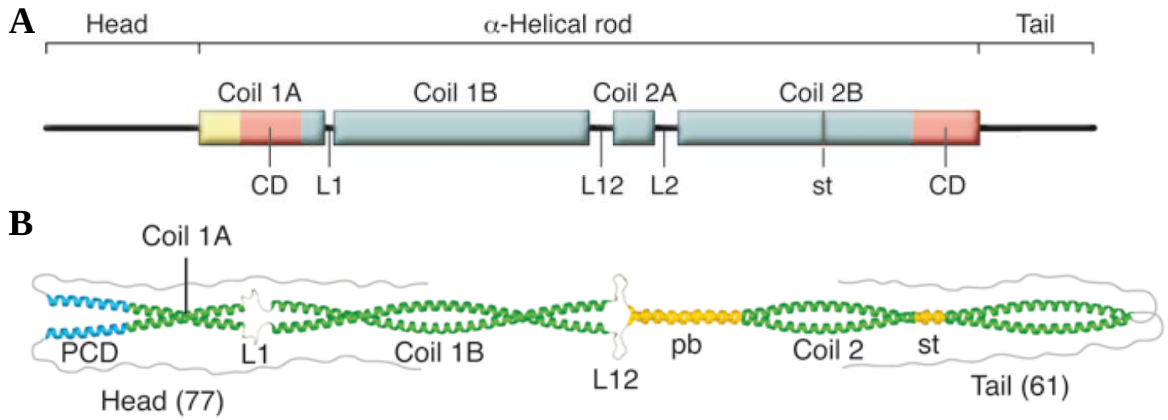

Figure 1. Domain organisation of IF proteins. (A) Scheme of the domain organisation of desmin as an example of an IF protein: the predominantly α-helical rod domain, flanked by largely unstructured head and tail domains. The rod domain of consists of pre-coil domain (PCD, only in vimentin-like IF proteins – marked by yellow box), coils 1A, 1B, 2A and 2B, as well as the linker segments between them: L1, L12 and L2. IF consensus motifs (CD) are marked with red boxes as well as the stutter (st) in the coild 2B. **(B)** Model of the dimeric coiled-coil structure as exhibited by vimentin (adapted from Herrmann et al. 2009).

1.1.4 Different classes of the IF proteins

As previously mentioned, there are over 70 different genes coding for IF proteins, as well as some alternatively spliced variants of the genes. Whereas actin and tubulin are abundant in many different cell types IF proteins are expressed in tissue- and development-specific manner. Based on their amino acid sequences comparison vertebrate IF proteins have been classified into six sequence homology classes (SHCs): SHC1 and SHC2 consist of acidic and basic keratins, respectively; SHC3 includes vimentin, desmin, glial fibrillary acidic protein (GFAP), and peripherin; neurofilament triplet proteins, as well as α-internexin and nestin comprise SHC4; SCH5 includes lamins; and SCH6 consists of beaded filament structural protein 1 (Bfsp1, also known as filensin) and Bsfp2 (also known as phakinin or CP49), two lens-specific proteins (Parry and Steinert 1999). The six SHCs could be further grouped based on their assembly properties, whereby keratins (SHC1 and SHC2 IF proteins, group 1), vimentin-like IFs (SHC3 and SHC4 IF proteins, group 2) and lamins (SCH5 IF proteins, group 3) represent the further three groups of the IF proteins. Members of each group are capable of forming heteropolymers (Herrmann and Aebi 2000).

1.1.5 Assembly of the IFs

The above outlined groups of IF proteins, based on similarities in their coil 2 sequences, further indicate their abilities to co-polymerise (Herrmann and Aebi 2000). On the other hand, the differences in their coil 1 segments allow them to segregate one from the other into distinct IF networks in a cell. In case of the first group of IFs, acidic and basic keratins are obligate heterodimers, i.e., one acidic and one basic type of keratins are required to form a keratin IF dimer. On the other hand, muscle, mesenchymal and neuronal IFs (group 2) could form both homo- and heteropolymers. For example, during the development of myocytes vimentin in those cells is steadily replaced by desmin IFs. Thereby, as the vimentin IFs are typical mesenchymal filaments, during myocyte maturation they are transiently coexpressed with desmin (Granger and Lazarides 1980). In addition, it has been experimentally demonstrated that vimentin and desmin filaments could form heteropolymers *in vitro* (Wickert et al. 2005), which has also been found to occur *in vivo* in hamster kidney cells (Quinlan and Franke 1982). Finally, lamins do not copolymerase with any of the other IF proteins.

Unlike actin or tubulin, IF proteins bind neither ATP nor GTP during filament assembly (Pollard and Borisy 2003, Waterman-Storer and Salmon, 1997). In further contrast to MFs

and MTs IF structures are apolar due to the mode of assembly of proteins into the corresponding filaments. Based on in vitro studies with vimentin, used as a paradigmatic model for the mode of IF assembly, three distinct stages of IF assembly could have been discerned (figure 2). In the first stage of the *in vitro* assembly, vimentin would be reconstituted from 8 M urea into low-salt buffer to form relatively uniform tetrameric complexes of antiparallel, half-staggered coiled-coil dimmers. Subsequently by increasing ionic strength of the buffer, on average eight tetramers associate laterally into unit-length filaments (ULFs). In the following phase ULFs would first longitudinally anneal to form short filaments which could further associate into longer IFs. In the last stage of the IF formation, long filaments would reduce their diameter by radial filament compaction, eventually giving rise to mature IFs.

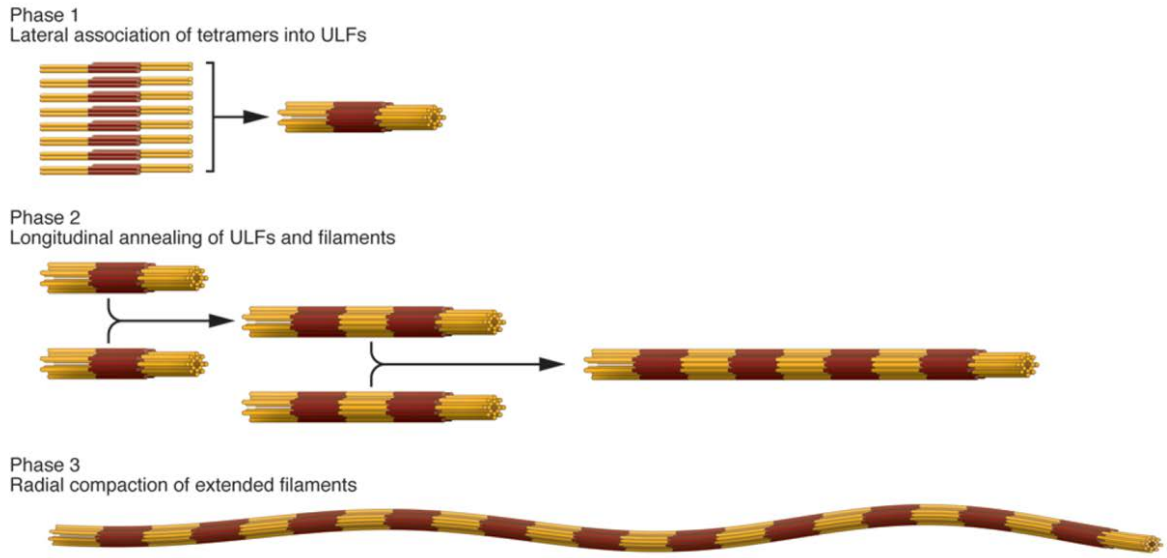

Figure 2. Scheme of the three major phases of the cytoplasmic IF assembly. In the phase 1, eight tetrameric subunits made from two antiparallel, half-staggered coil-coiled dimmers associate laterally to form unit-length filaments (ULFs). In pahse 2, ULFs longitudinally anneal thereby steadily creating longer filaments. In the last phase, filaments would radially compact to yield mature filaments. Each vimentin molecule is represented by a single cylinder; coil 1 is dark red and coil 2 is yellow (adapted from Herrmann et al. 2009).

1.2 Myocytes and IF-associated diseases

1.2.1 IF networks in myocytes

Striated muscle is composed of mature muscle cells, or myotubes, spanned by repeating sections of sarcomeres, which represent their contractile units characterised by a striated distribution of their proteins (Sanger and Sanger 2008). Skeletal myotubes arise by differentiation from myoblasts through the process of cell fusion. They have a complex of

plasma membrane proteins that connect the extra-cellular matrix with the cell cytoskeleton. IFs are the major cytoskeleton component that regulates cellular plasticity and signal transduction from the plasma membrane down to the chromatin. Through Z-discs, sarcomeres are connected to the plasma and nuclear membranes via desmin IFs (figure 3).

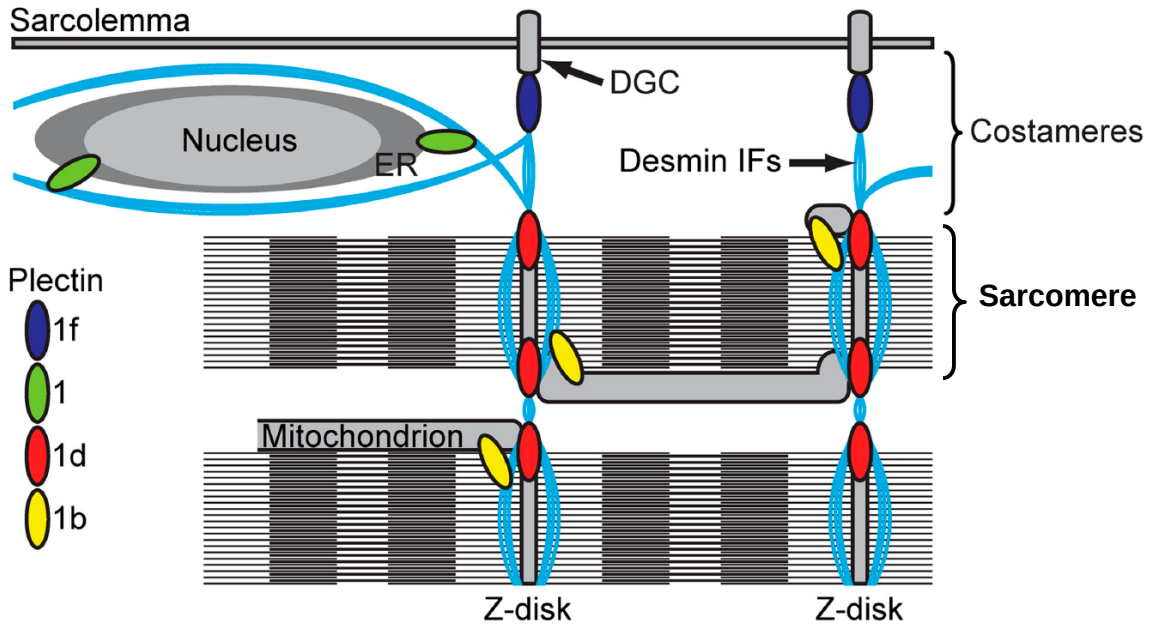

Figure 3. Scheme depicting role of the desmin IFs in maintaining skeletal muscle integrity. Desmin IFs (blue) interact with associated proteins to generate myofibre support. Different plectin isoforms (1, 1b, 1d and 1f) are also depicted to bridge the desmin IF connections to the nucleus, mitochondria, Z-discs and, in subsarcolemmal region (costameres), to dystrophin-glycoprotein complex (DGC). The scheme was adapted from Konieczny et al. 2008.

Desmin (Greek *desmos* denotes a link or a bond) is the key IF protein found in cardiac, skeletal and smooth muscle cells (Lazarides 1980). It is one of the earliest muscle-specific markers that occur during development (Herrmann et al 1989). As they span the entire muscle cell, desmin IFs connect the plasma membrane, sarcomere, mitochondria and nuclei via different plectin isoforms, as well as other bridging proteins such as nestins. In addition, via plectin and different inner and outer nuclear membrane (ONM) proteins, such as SUNs and nesprins, desmin filaments are connected to the nuclear lamins. Therefore, they could be said to further bridge the link from the plasma membrane down to the chromatin (figure 4) and thereby create a uniform and coordinated filamentous network in the myocytes.

Other types of non muscle-specific IFs found in myocytes include synemin and paranemin (Titeux et al. 2001, Schweitzer et al. 2001), both of which are found primarily around the Z

discs (Bellin et al. 2001). Another class of prominent muscle IF proteins are the nuclear lamins, predominantly found adjacent to the INM. In adult mammalian cells, lamins exist in four major isoforms: lamin A and lamin C (A-type lamins), which are coded by the same gene but are generated by alternative splicing; and lamin B1 and B2, which are products of two separate genes (Gruenbaum et al. 2005). In addition, whereas A-type lamins were also found to form speckles throughout the nucleoplasm in myoblasts, they appear to be largely lamina-incorporated upon differentiation (Muralikrishna et al. 2001).

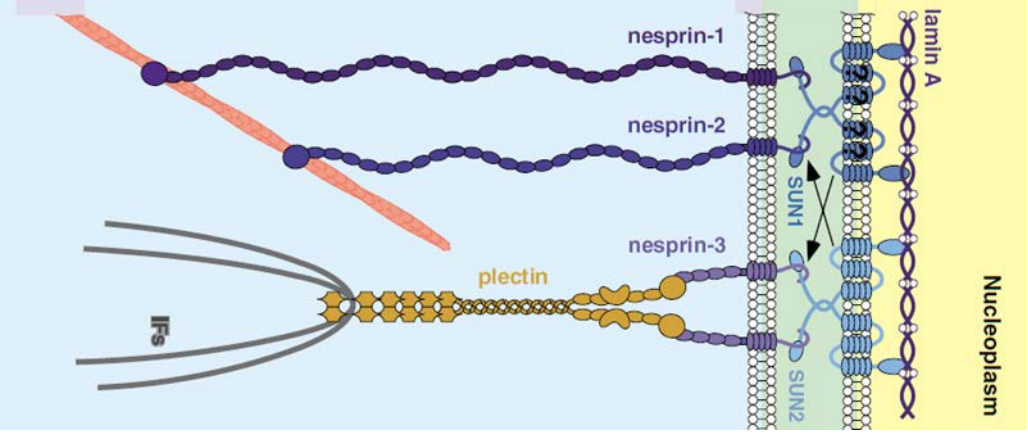

Figure 4. Protein complexes spanning the nuclear envelope of mammalian cells. Through plectin, IFs are bound to nesprin-3, and via its link to SUN2 they are connected to the nuclear lamins (adapted from Wilhelmsen et al. 2006).

1.2.2 Myofibrillar myopathies

Considering the tissue-specific expression of most of the IF proteins, there is a wide range of tissue-specific diseases that could originate due to mutations in various IF proteins (the database of the diseases can be found at http://www.interfil.org/). For example, mutations in various keratins cause skin blistering diseases whereas mutations in GFAP or neurofilament proteins lead to Alexander's disease or Charcot-Marie-Tooth disease, respectively (discussed in Herrmann and Aebi 2000). On the other hand, Hutchinson-Gilbert progeria syndrome (HGPS), a rare premature aging disorder, is caused by mutations in A-type lamins and therefore affects most of the tissues.

One group of diseases, myofibrillar myopathies (MFMs), are caused by mutations in desmin, as well as other sarcomeric and extra-sarcomeric proteins. These proteins include plectin, titin, filamein-C and αB-crystallin, the chaperone associated with desmin filaments, as well as lamin A (Schröder and Schoser 2009). Apart from being caused by mutations in various extra-myofibrillar and myofibrillar proteins, these diseases are clinically quite heterogeneous.

Nevertheless, the most prominent characteristic of these diseases is myofibrillar degeneration. In addition to the high variability in symptoms or degree of progression, most of the MFM patients have an adult onset of the disease, beyond the fourth decade of their lives.

1.2.3 Desminopathies

Desminopathies (synonyms: desmin-related myopathy, desmin myopathy, desmin storage myopathy, Selcen et al. 2004) are a subgroup of MFMs which are caused by mutations in desmin and tend to manifest themselves already in early and middle adulthood. In rare cases, the disease phenotype is already evident in the first decade of life (for example: Goldfarb et al. 1998). Clinically the diseases primarily manifest themselves with distal skeletal muscle dystrophies. Further clinical phenotypes include cardiomyopathies which may precede, coincide with or succeed the skeletal muscle weakness and, in some cases, respiratory insufficiencies (van Spaendonck-Zwarts et al. 2010).

Another prominent characteristic of these diseases is the co-occurrence of desmin-enriched accumulations throughout the myofibres with preserved desmin IF pattern at the level of their Z-discs (figure 5A). In particular, one case analysed in greater detail was the severe desmin arginine (R) 350 to proline (P) (denoted as *Des*R350P) mutation, which is considered to be one of the most frequently found desmin missense mutations in Germany with a founder allele already established (Bär et al. 2005a, Walter et al. 2007). By analysing the muscle biopsies from patients baring that mutation in greater detail, the segregation of desmin deposits from the fully formed myofibre Z-discs was observed (figure 5B). Hence one of the key questions that arose from the studies with desmin disease mutants was to what extent are the mutant and the normal (i.e., wild type, WT) desmin proteins segregated in a cell.

1.3 Objectives

1.3.1 Background of the Study

The large majority of mutations leading to desminopathies have been found in the coil 2B of the α-helical rod domain of desmin (Bär et al. 2006, figure 6A). However, these mutants have also been previously found to vary with respect to the severity of the disease phenotype. In one of the earlier studies by Bär et al. (2005b), some of the known mutations found in coils 2B and 1B were categorised *in vitro* based on the stage at which they affect desmin filament assembly (figure 6B). In case of *in vivo* experiments, the mutants were primarily analysed in

the vimentin- and desmin-free SW13 cell line (e.g. Bär 2005b) or vimentin-possitive but desmin-negative 3T3 fibroblast cells (Bär 2005a). In order to investigate the effects of the mutations in the desminWT background, as well as the address the question of mutant and WT desmin segregation, the analysis of these mutants was done in a cell line stably expressing desmin.

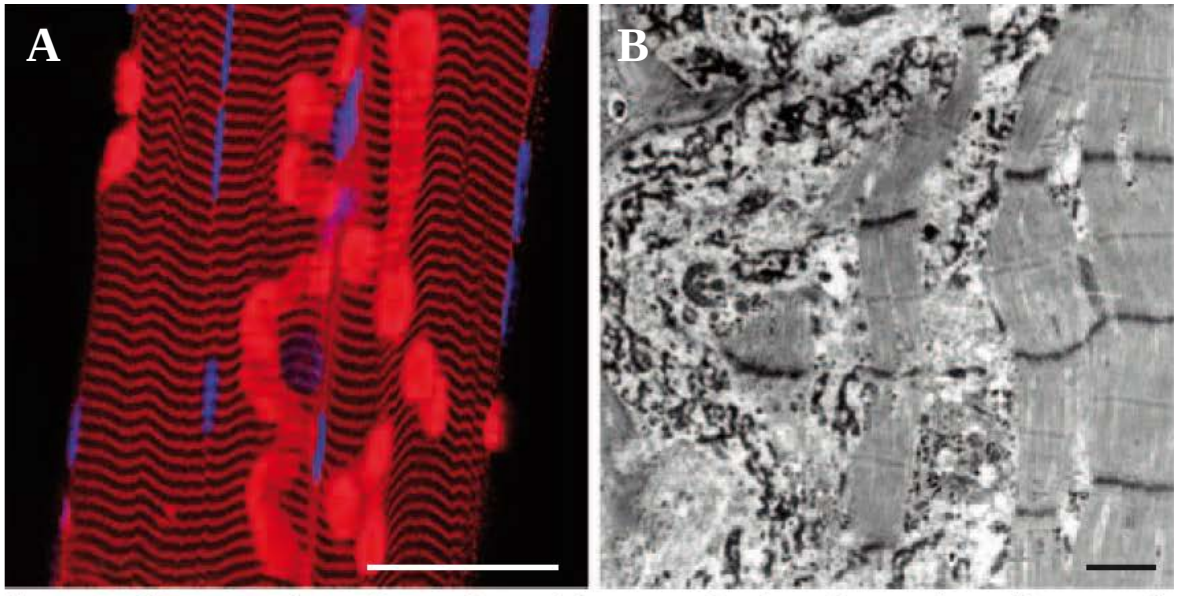

Figure 5. Muscle architecture in desminopathy patients. (A) Immunofluorescence microscopy image of isolated myofibre from a desminopathy patient stained for desmin (red). One can clearly observe the large deposits of desmin accumulates in parallel with a typical staining pattern of preserved desmin filaments intersecting the preserved Z-discs. Scale bar, 50 µm **(B)** Ultrastructural analysis of muscle fibre from desminoapthy patient carrying a *Des*R350P mutation, with pronounced aggregation of filament granules (left side of the image). Scale bar, 0.5 µm. The figures are adapted from Herrmann et al. 2007 and Bär et al. 2005a.

A common cell culture system employed in studies of myocyte biology is the C2C12 murine embryonic myoblast cell line (first isolated and described by Yaffe and Sexel 1977) which could be induced to differentiate by culturing the cells in serum-poor medium. Thereby, in addition the fact that they endogenously express desmin, these cells are a suitable system for the indicated analyses as one could study the effects of the mutants on cell differentiation.

Finally, in order to be able to specifically detect the transfected mutant or WT desmin in the mouse desminWT background we have transfected human desmin (*hDes*) gene variants of the WT and respective mutant proteins into the mouse cells. Human and mouse desmin

sequences differ in 12 out of total 470 amino acids (appendix 2). Therefore, we have also attempted to generate human and mouse desmin (*mDes*)-specific antibodies to able to differentiate the transfected (i.e. WT or mutant) desmin from the endogenous one.

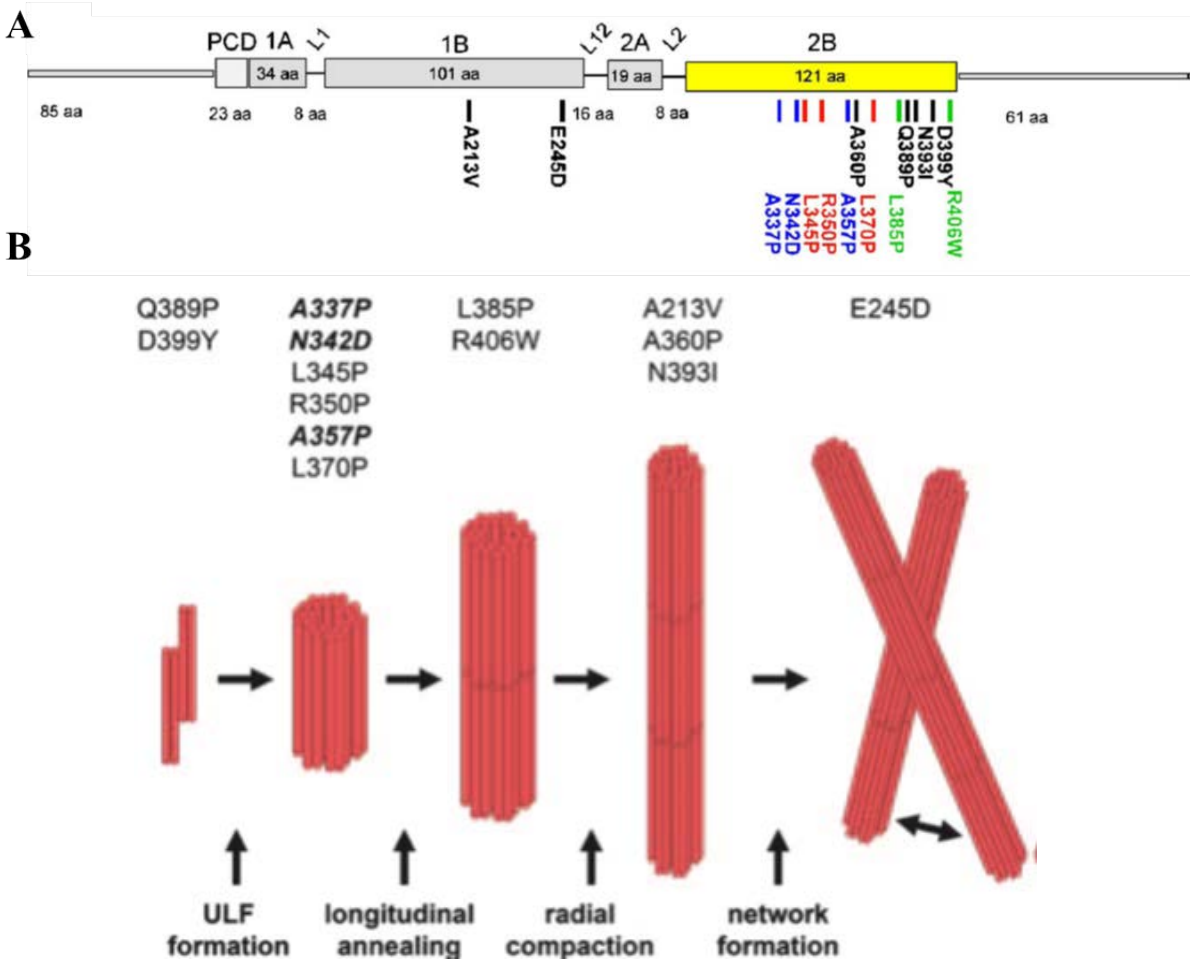

Figure 6. Some of the prominent mutations causing desminopathies. (A) Scheme of the desmin molecule (domain organisation as in figure 1A) with the prominent mutations mainly in coil 2B, as well as 1B, denoted. Lengths of each of the sequence segments are indicated (adapted from Bär et al. 2006). Mutations are colour coded based on the severity of the mutation as indicated in figure 6B. **(B)** Hypothetical scheme of desmin *in vitro* assembly (as in figure 2). The mutations indicated above are ordered with respect to the earliest stage in filament assembly when their effects could be detected *in vitro* (image adapted from Bär et al. 2005b).

1.3.2 Aims of the Work

The aims of the work were to determine the effects of some desmin mutations on myoblasts differentiation and thereby analyse the amounts and distribution of the A-type lamins, as well as that of both transfected and the total desmin. Therefore the following was performed:

1) C2C12 cells cultured in the growth or differentiation medium were characterised with respect to the indicated IF proteins.

2) The same analyses were performed in C2C12 cells stably transfected with *hDes*WT as well as two desmin mutants, *hDes*R350P and *hDes*E245D (figure 6).
3) Further analyses were performed on C2C12 cells stably expressing the respective *hDes* proteins and which were induced to differentiate.
4) In addition, to address the question of desmin mutant segregation from the *Des*WT the immunoprecipitation (IP) of the transfected protein was performed, as well as the analyses of colocalisation of vimentin and either endogenous or transfected desmin.
5) Finally, the scope of the work involved the analyses of the antibodies which were generated, i.e. the *h/mDes*-specific ones, with a focus on examining their specificity.

In order to perform the above indicated analyses the *in vitro* cell fractionation and subsequent Western blotting (WB), as well as immuno-cytochemistry (ICC) experiments were performed on the respective cells.

2. Materials and Methods

2.1 Materials

2.1.1 List of Chemicals

Acrylamide (30%)	Roth
Boric acid, H_3BO_3	Sigma-Aldrich
Chrome-sulphuric acid (H_2SO_4 / CrO_3)	NeoLab
Digitonin	Aldrich
Ethanol (CH_3CH_2OH)	Sigma-Aldrich
Ethylenediaminetetraacetic acid (EDTA)	Sigma
Ethylene glycol tetraacetic acid (EGTA)	Sigma
Gylcine	Sigma
Genetic Technology Grade (GTG) agarose	Biozym
Hydrochloric acid (HCl)	Sigma-Aldrich
Low Electroendosmosis (LE) agarose	Biozym
3-(N-morpholino)propanesulfonic acid (MOPS)	Gerbu
Magnesium sulphate heptahydrate ($MgSO_4$ *7 H_2O)	NeoLab
Nonyl phenoxypolyethoxylethanol (NP40)	Sigma
Phenylmethylsulfonyl fluoride (PMSF)	Serva
Potsssium chloride, KCl	Roth
Potassium dihydrogen phosphate, KH_2PO_4	Roth
Sodium chloride, NaCl	Sigma
Sodium dodecyl sulfate (SDS)	Fluka
Sodium hydroxide (NaOH)	Riedel-de Haën
Sodium phosphate dibasic dihydrate, Na_2HPO_4 x 2 H_2O	Riedel-de Haën
Tris(hydroxymethyl)aminomethane (Tris)	Sigma
Triton X-100	Gerbu
Polysorbate 20 (Tween 20)	Gerbu
Urea	Serva

2.1.2 Primary Antibodies

Below are listed the primary antibodies used in the experimental procedures. The standard dilutions (both in WB and ICC) are also indicated.

Antibody	**Epitope**	**Dilution in ICC**	**Dilution in WB**	**Source**
anti-desmin ms monoAb (D9)	in the tail domain of human desmin	1: 100	1: 2000	Progen, #10519
anti-*hDes* rb polyAb (HD1)	TTRTPSSYGA in head domain of *hDes*	1: 200	1: 10 000	Generated and purified by PSL GmbH, Heidelberg
anti-*mDes* rb polyAb (MD1)	GFGTKGSSSSMTS in head domain of *hDes*	(as indicated)		Generated and purified by PSL GmbH, Heidelberg
anti-*mDes* rb polyAb (MD2)	PGFSLGSP in head domain of *hDes*	(as indicated)		Generated and purified by PSL GmbH, Heidelberg
anti-*Des*WT rb polyAb (HD2)	GGMRQMREL in coil 2B of *hDes*	(as indicated)		Generated and purified by PSL GmbH, Heidelberg
anti-*Des*R350P rb polyAb (HD350P)	GGMRQMPEL in coil 2B of *hDes*	(as indicated)		Generated and purified by PSL GmbH, Heidelberg
laminA/C ms monoAb (LaZ)	L1 subdomain of human LaminA/C	1: 5	1: 10	generated in collaboration with H. Zentgraf, DKFZ
DesminCT Rabbit monoAb	C-terminal tail domain	1: 100	not used	Epitomics Clone Y66
GAPDH ms monoAb (6C5)	unknown	not used	1: 5000	Calbiochem Cat. No. CB1001
mCherry ms monoAb (OmicsLink)	unknown	1: 500	not used	GeneCopoeia, CGAB-RFP-0050
myosin heavy chain monoAb ms (MF20)	unknown	1: 100	1: 500	R&D Systems, MAB4470
Vimentin 3B4 arc2 1-13 ms monoAb	rod domain, coil 2	1: 200	not used	Progen, #65113
VimentinCT rabbit monoAb	C-terminal tail domain	1: 100	not used	Epitomics, EPR3776

2.1.3 Primers

Desmin01_for	GAGAGATCCGGAATGTCCCAGGCCTACTCGTC
Desmin01_rev	AGAGAGCTCGAGTTAGAGCACTTCATGCTGC
DesminE245D_for	CTTAAGAAAGTGCATGACGAGGAGATCCGTGAGTTG
DesminE245D_rev	CAACTCACGGATCTCCTCGTCATGCACTTTCTTAAG

DesminR350P_for	CTGATGAGGCAGATGCCGGAATTGGAGGACCG
DesminR350P_rev	CGGTCCTCCAATTCCGGCATCTGCCTCATCAG

2.1.4 Plasmids (Clones)

pHβAPr-1-neo	vector containing the rat β actin promoter, geneticin resistance (described in Gunning et al. 1987)
p163/7	vector with an MHC promoter, no drug resistance
pIRES_mCherry	contains internal ribosome entry site (IRES) of encephalomyocarditis virus (ECMV) with mCherry cloned in C-terminally to the insert, geneticin resistance
mCherry-C1	vector containing mCherry, geneticin resistance

2.1.5 Cell Lines and Bacterial Strains

BHK21	Baby hamster kidney fibroblast cell line
BHK21-C13	Clone 13 of the BHK21 cells
C2C12	Murine myoblast cell line (C2), as generated by Yaffe and Saxel (1977); clone 12 established by Blau et al. (1983)
C2C12 +*hDes*	C2C12 cells transfected with particular human desmin constructs
RD	Human rhabdomyosarcoma cell line
TG1	Highly competent strain of *E. coli*
$Vim^{-/-}$	Embryonic fibroblasts originating from $vimentin^{-/-}$ mice

2.1.6 Cell Culture Media and Solutions

Bovine Serum	Biochrom
Fetal Calf Serum (FCS)	Biochrom
LB-Medium (Lennox)	Sigma-Aldrich
LB	20g/l LB-Medium, 10mM $MgSO_4$ *7 H_2O, pH7.5
L-glutamine (200mM stock)	Invitrogen
Non-Essential Amino acids	Biochrom
Goat Serum	Invitrogen

DMEM	Dulbecco's Modified Eagle's Medium (Gibco)
MEM	Minimum Essential Medium (Biochrom)
Growth medium (GM)	DMEM, supplemented with 2mM L-glutamine and 10% fetal calf serum
Differentiation medium (DM)	DMEM, supplemented with 2mM L-glutamine and 2% Horse serum
MEM Medium	MEM, supplemented with 2mM L-glutamine, 1% Non-essential amino acids and 10% FCS
EDTA/PBS	0.02% EDTA in 1x PBS
Trypsin	0.25% / 0.05% Trypsin (Invitrogen)

2.1.7 Buffer Solutions

SDS running buffer (10x): 0.25M Tris, 1.92M Gylcine, 1% SDS, pH 8.3

Stacking gel buffer (4x): 0.5M Tris, 0.4% SDS, pH 6.8

Separating gel buffer (4x): 1.5M Tris, 0.4% SDS, pH 8.8

Borate buffer (20x): 0.4M Boric acid, 20mM EDTA, pH set to 8.8

Phosphate buffered saline, PBS (10x): 143 mM NaCl, 26.8 mM KCl, 64.6 mM Na_2HpO_4 x 2 H_2O, 14.7 mM KH_2PO_4; pH 7.4 (autoclaved)

Tris buffered saline with Tween, TBST (10x): 100 mM Tris pH 8.0, 1.5 M NaCl, 0.5% Tween 20

2.1.8 Reagents and enzymes

Lipofectamine LTX	Life Technologies
ECL solutions	Western Lighting
BIX-01294	Sigma
Geneticin (G418)	PAA
Fluoromount-G (with DAPI)	Southern Biotech
Dynabeads M-270 Epoxy	Invitrogen
Pefablock	Serva
T4 ligase	Serva
Bovine serum albumin (BSA)	New England BioLabs
Benzonase nuclease	Novagen
EcoRI, BamHI, SalI, BspEI, XhoI	Roche
Mini-, Midiprep kits, Gel extarction kit	Qiagen

QuikChange XL Site-Directed mutagenesis kit	Stratagene

2.1.9 Laboratory Equipment and Software

Axioskop 40 Microscope with AxioCam MRc	Zeiss
Blotting apparatus	Cti
Cell counter (Vi Cell-XR)	Beckman
CH350 12-bit camera	Photometrics
Olympus IX70 microscope, DeltaVision microscope system	Applied Precision
Petri dishes (10 cm, 6 cm diameters)	Falcon
Pipetboy	Integra
Polyvinyl difluoride (PVDF) membrane	Immobilon-FL
SDS PAGE apparatus	BioRad
Shaker	Stuart Scientific
SoftWorks imaging software	Softworks Inc.
Spectrophotometer	Jenway
Table top centrifuge	Eppendorf
X-ray films	Fujifilm

2.2 Methods

2.2.1 Maintenance of Cell Cultures

All cell lines (except BHK21-C13) were cultured in 10 cm x 2 cm Petri dishes with 10 ml growth medium (GM). In case of 6 cm Petri dishes, half of the volumes indicated below were used. The cells were incubated at 37 ^{o}C (5% CO_2) and passaged every 3 days. In case of C2C12 cell lines, cells were always split when they were underconfluent (about 80% confluence). After two days, additional 30% of culturing medium was added to the cells. To passage the cells, the medium was removed and the cells were washed briefly in 5 ml 0.05% EDTA/PBS and rinsed with 3 ml 0.25% Trypsin. After 1-2min at room temperature (RT), the cells were resuspended in 5 ml GM and split accordingly. In case of C2C12 cells, they were split 1:20 and 1:30, whereas in case of RD cells, they were split 1:10 and 1:12. In case of C2C12 cells transfected with *hDes* constructs, they were split 1:10 and 1:15 and maintained in additional 1.5 mg/ml genaticin (G418). BHK21-C13 and RD cells were cultured in the MEM medium and split 1:10 and 1:15 or 1:8 and 1:12, respectively, every three days.

In case of C2C12 cell differentiation, the cells were cultured up to over 95% confluence. GM was then removed and the same volume of differentiation medium (DM) was added. If BIX-01294 (2.5 mg/ml stock solution) was added, it was diluted 1:1000 in the DM. If geneticin (G418) was added, it was done as above (1.5 mg/ml). After three days additional 20% of DM (with a corresponding amount of either BIX-01294 or G418) was added to the cells. The cells were used for further experiments after 6 days in DM.

2.2.2 Cloning and Mutagenesis

hDes gene sequence was subcloned from p163/7 vector into a pBluescript II KS+ using EcoRI enzyme. To clone into the pJ6Ω vector, the sequence was digested with BamHI (1 h digestion) and SalI (10 min partial digestion) restriction enzymes. After digestions, the products were run on a low melting agarose gel (0.5% LE and 0.5% GTG agarose) after which the corresponding bands were cut out and purified from the gel according to the manual (Qiagen).

In case of cloning *hDes*WT into pIRES_mCherry vector, *hDes*WT was first amplified by polymerase chain reaction (PCR), using Desmin01_for/_rev primers. Subsequently, both the PCR-amplified *hDes*WT DNA and the pIRES_mCherry-LaminA were digested with BspEI and XhoI enzymes and ligated together.

The restriction digestions and ligations with T4 ligase of plasmid and an insert were all performed according to the instruction manuals (Roche Diagnostics). The ligation reaction was then added to 50 µl of TG1 competent *E. coli* cells, which were then incubated 20 min on ice, 2 min heat-shocked at 37 ^{o}C, cooled down 3min on ice following addition of up to 1ml of LB medium and incubation for 1 h at 37 ^{o}C. The bacterial cells were plated (either 1:10 ratio or they were spun down at 4000 g for 5 min and the pellet was resuspended in 200 µl of LB).

Minipreps of the bacterial cultures were performed according to the company instructions (Qiagen). To verify the digestion products, the minipreps were subjected to restriction digestions with the respective enzymes (as above). Site directed mutagenesis (using the QuikChange XL Site-Directed mutagenesis kit) was performed on the *hDes* gene subcloned in pBlueScript II KS+ vector and subsequently transformated into the TG1 *E. coli* (procedure as above). For each of the mutations (*hDes*E245D, *hDes*R350P) a corresponding set of forward (for) and reverse (rev) primers was used (section 2.1.3). After clone verification by restriction

digestion and sequencing (done by GATC Biotech) the mutant sequences were subsequently recloned into the pJ6Ω vector and again verified by restriction digestion and sequencing. Finally, a larger amount of plasmid DNA was generated by using a midiprep procedure (Qiagen).

2.2.3 Cell Transfection

C2C12 (as well as $Vim^{-/-}$ fibroblasts) cells were transfected using Lipofectamine LTX according to the manufacturer's instructions (Invitrogen), using the Plus reagent. Cell transfections were always performed at 50% confluence on 2cm Petri dishes in DMEM only, with an additional medium change to GM 6h after transfection. In case of stable cell lines, geneticin (G418) was added to the medium (to 1.5 mg/ml final concentration) the following day. The cells were left in the dish with occasional (2-3 days) partial (20-50%) medium removal and replacement with the fresh medium. Only once the dish was starting to get confluent were the cells trypsinised and split and always cultured in the medium with G418.

In case of transfections of C2C12 cells with *hDes*R350P cloned into vector p163/7, the vector was cotransfected with the mCherry-C1 vector, which contains the geneticin resistance gene (in ratio 9:1). This was necessary for generating a cell line stably expressing the mutant desmin as the vector p163/7 does not contain any resistance genes.

2.2.4 In situ Cell Fractionation: Preparation of Cytoskeletons

The cells were grown in 10 cm x 2 cm Petri dishes until confluence. In case of differentiation, the procedure was performed after 6 days in DM. The cell dish was first rinsed twice with a solution of 1x PBS (with 25 μm Pefablock and 1 μg/ml PMSF) at RT. 1 ml of digitonin buffer (Dig, 0.5x PBS, 50 mM MOPS pH 7.4, 10 mM $MgCl_2$, 50mg/ml digitonin, 1 mM EGTA with 0.5 mM Pefablock, 0.5 μg PMSF) was then added and the cells were incubated for 1 min on ice. The buffer was collected in an Eppendorf tube and the cells were subsequently incubated with 1 ml Low NP40 buffer (*LIB*, 0.5x PBS, 50 mM MOPS pH 7.4, 10 mM $MgCl_2$, 0.2% NP40, 1 mM EGTA with 0.5 mM Pefablock, 0.5 μg PMSF) for 4 min (on ice). The *LIB* sample was then collected in another Eppendorf tube and then 1 ml of High NP40 buffer (*HIB*, 0.5x PBS, 50 mM MOPS pH 7.4, 10 mM $MgCl_2$ and 1.0% NP40 with 0.5 mM Pefablock, 0.5 μg PMSF and 250 U Benzonase nuclease) was added (incubation on ice). After 5min, 200 μl of pre-cooled 5 M NaCl was added to the buffer and the cells incubated for another 3 min (with occasional rinsing). Finally the cell remnants were collected by scraping

in 1.2 ml buffer and the sample was stored in a fresh Eppendorf tube. After 10 min centrifugation (at 13000 rpm, 4 ^{o}C) 800 µl of supernatant was collected in a separate tube and the rest of supernatant discarded. The pellet was resuspended in 200 µl of UBS (6.7 M Urea in 1x Laemmli sample buffer) and heated at 95 ^{o}C for 3min.

For determination of the protein content in *LIB* the Bradford protein assay was used according to the standard procedure. In short, the Bradford stock reagent was diluted 1: 5 in water. For the blank measurement, 1 ml of the dilution reagent was used. In case of the BSA standard curve, 1, 2, 3, 4, 5 µl each of 1.05 mg/ml bovine serum albumin (BSA) stock solution was dissolved in 1 ml Bradford dilution. For each measurement, 1 µl of the LIB samples was mixed in 1 ml of Bradford dilution. Three separate dilutions were prepared for each measurement. After 5 min of incubation, the light intensity (at 595 nm wave length) was measured. The concentration of the protein was calculated from the standard BSA curve.

2.2.5 SDS-Polyacrylamide Gel Electrophoresis and Western Blotting

All the SDS polyacrylamide gel electrophoresis (PAGE) were performed on 8% separating gels in SDS running buffer (2.6% stacking gels). Samples were mixed with 3x SDS sample buffer (190 mM Tris HCl pH 6.8, 30% glycerol, 6% SDS) and immediately heated at 95 ^{o}C for 5 min. The SDS PAGE was run at 80 V for 15 min and another 75 min at 120 V (maximum amperage).

To perform protein transfer to a PVDF membrane (0.45 µm pore size), the membranes were briefly activated in 100% ethanol and rinsed in the Borate buffer. Subsequently, they were placed on the gels and covered with three layers of Whatman filter paper (and two thin sponges on either side). The cassette was then placed into the blotting chamber so that the membrane faced the positive electrode and blotted for total of 110 min (starting from 100 mA with a 100 mA increase every 5 min to reach 500 mA, at maximum voltage). Protein transfer would be verified by Ponceau staining (for 5 min) and subsequent destaining with ddH_2O and 1x TBST.

To subject the membrane to the antibody reactions it was first blocked in 5% milk (m/v) in 1x TBST (blocking solution) for 1 h at RT (or overnight at 4 ^{o}C). The antibody was then diluted (table in section 2.1.2) in the blocking solution and added to the membrane (incubated for 1 h at RT), following washing in 1x TBST 3 times for 5 min. Secondary antibody (from Jackson

ImmunoResearch, Horse radish peroxidise, HRP-conjugated) was then diluted 1: 5000 (in the blocking solution) and incubated with the membrane for 30 min at RT, on a shaker, followed by washing in 1x TBST, 2 times for 15 min, once for 30 min. Before incubating with the X-ray films, each membrane was incubated (10 s) with the mix of ECL solutions (1 ml each per 9 cm x 6 cm of membrane).

2.2.6 Cell Fixation and Immuno-cytochemistry (ICC)

Cells were initially grown on cover slips (in case of C2C12 differentiation, the cells were differentiated on chrome-sulphuric acid (H_2SO_4 / CrO_3-activated cover slips to prevent cell detachment). In all cases, cover slips with 1.5 mm thickness were used. Prior to ICC, the cover slips were rinsed in 1x PBS with 2 mM $MgCl_2$ and then incubated for 5 min in methanol, following washing in acetone for 30 s and air drying.

In the first part of the ICC procedure, the cells were briefly washed in ICC washing solution (0.002% Triton X100 in 1x PBS) and blocked with blocking solution (1: 10 goat serum diluted in 1x PBS) for 20 min in a humid chamber. In case of ICC with the HD350P and HD2, the cover slip was dipped 3 times into 2M urea following 5 min washing in the ICC washing solution prior the blocking step. Subsequently, the antibodies were diluted in the same blocking solution (20 µl per cover slip, diluted as in the table in section 2.1.2) and added onto the cover slips (1 h incubation, RT). If another primary antibody was used, it was added following the first incubation the same way after removing the previous antibody dilution by slanting the cover slip.

Subsequently, the cover slips were washed in the ICC washing solution (2 times 5 min) and incubated with the secondary antibody (from Jackson ImmunoResearch, either Alexa488 or 568 or Cy3-conjugated), previously diluted 1: 100 in 1x PBS, for 30 min. If more secondary antibodies were used they were added consecutively after removing the previous secondary antibody dilution exactly as above. After washing off the secondary antibody, 2 incubations in the ICC washing solution for 5 min each, the cells were briefly rinsed in ddH_2O followed by a brief rinse with 100% ethanol and then left to air dry. Finally the cover slips were mounted by putting them on top of a 3µl drop of Fluoromount-G (with DAPI) on a glass slide and left 3 h or overnight before using them for microscopy.

2.2.7 Hematoxylin-Eosin (HE) Staining

The cells were grown on square (18 x 18 mm) cover slips, fixed in methanol/acetone (as above) and washed in in ddH_2O. In the subsequent staining procedure the cover slips were placed on a porcelain holder and incubated in Hemalum (8 min) following its washing in a running tap (with calcium) water. Subsequently the cover slips were stained in 1% Eosin for 5 min and shortly rinsed with ddH_2O. Then the cover slips were briefly washed in 70%, 96% and then 100% ethanol and incubated with Xylol for 2 min. The cover slips were then mounted using the Eukitt mounting medium. The HE staining was kindly performed by Michaela Hergt (our group).

2.2.8 Microscopy and Image Processing

All the images were made using the *Deltavision* system using the SoftWoRx software. All the images were acquired in 50 stacks with 0.2 µm distance (1024x1024 image size, 100x magnification) and with the exposure times set for the maximum in the focus. Deconvolution was always performed using the *Enhanced Additive* algorithm with 10 cycles. The images were finally saved in JPEG format.

In the case of staining cytoskeleton with MF20 and HD1, as well as with images from HE staining, the images were made with the Axioskop microscope at 40x or 63x maginification. For MF20 and HD1 statistics, between 250 and 350 MF20-possitive cells were counted in two separate experiments. In case of C2C12 +*hDes*E245D DM +G418 and +bix cells, three different experiments were performed. The total number of cells being 3- to 5-fold higher.

2.2.9 Immunoprecipitation (IP)

The cells were first grown in a 10 cm dish (up to a confluence of over 80%). The cells were then trypsinised (as described in 2.2.1) and collected in 5 ml medium of which 0.5 ml were used for cell counting (Beckman cell counter). The cells were then centrifuged (1000 rpm, 2 min) and the medium was removed. The cells were then incubated with 1ml of RIPA buffer (0.1% SDS, 1% NP40, 150 mM NaCl, 50 mM Tris pH 8.0) for 5min. Subsequently the cells were transferred into an Eppendorf tube and centrifuged at 13000 rpm for 10 min at 4 ^{o}C.

Prior to antibody coupling to the Dynabeads M-270 Epoxy (Invitrogen), the antibody was dialysed against PBS (2 times 30 min). Antibody coupling was performed according to the

product manual. IP was performed according to the Dynabeads Protein G manual (Invitrogen). For sample incubation, the volume of the cells RIPA lysates corresponding to 0.5 million cells (volume set to 250 µl) was incubated for 20 min on a rotator and it was finally eluted in 25 µl 0.1M glycine, pH 2.3. The beads were finally heated in 20 µl 1x Laemmli sample buffer (70 ^{o}C, 10min). For Western blotting half of the collected IP sample was loaded onto an 8% polyacrylamide gel.

2.2.10 Electron Microscopy (EM)

Conventional Epon-embedding-ultrathin sectioning-EM was performed by the division for electron microscopy in DKFZ (head: Dr. Karsten Richter). In short, the cells were fixed in 2% formaldehyde and then 2% glutaraldehyde, following the washing in 2 mM $MgCl_2$ and 66 mM CaCo-buffer pH 7.2, for 1 h at 4 °C. The samples were washed 5 times in 66 mM CaCo 66-buffer and treated with 1% OsO_4 in 40 mM CaCo-buffer for 60 min. Subsequently, the samples were washed in 66 mM CaCo twice and then 3 times with ddH_2O. After subsequent washing in 33% and 50% ethanol, the procedure was continued with a 70 min incubation in Uac1%/ 70% ethanol. The samples were then washed in 70%, 95%, 100% ethanol at RT, 1 h total, and then incubated with Epon without accelerator (2A plus 2B) in 10% ethanol at RT overnight. After inverting the gelatin-capsules onto the cell layer, it was left to polymerase at 60 °C overnight.

3. Results

3.1 Generating desmin antibodies and the analyses of their specificity

In the first step of the indicated analyses, different antibodies were generated and tested with respect to their specificity in both WB and ICC. The analyses were performed on C2C12 (mouse) and RD (human) cells, in case of the ICC. For WB, mouse and human desmin (*m/hDes*) recombinant proteins and extracts from C2C12 or RD cells were used. The antibody used for a standard comparison was a mouse monoclonal D9 antibody. Initially the location the epitope of the antibody was narrowed down and the antibody was analysed with respect to the extent of its specificity for either *m/hDes*. This was performed by applying different dilutions of the antibody on WB membranes containing varied amounts of the two proteins (ranging from 1 to 100 ng). Thereby the specificity of the antibody was reliably determined.

3.1.1 Anti-desmin D9 monoclonal antibody detects mouse and human desmin with equal specificity

In order to narrow down the epitope of the mouse monoclonal antibody (monoAb) D9, recombinant peptides of different fragments of *mDes* were run on the gel and blotted onto a membrane. The recombinant peptides included the full length desmin (positive control), desmin 1st half (peptide of amino acids 1-240) and desmin 2nd half (amino acids 251-470). In addition, headless desmin (ΔHead) and two tailless desmin (ΔTail) fragments were also used in the procedure. 500 ng and 100 ng of each protein was loaded (figure 7). As it can be seen from the blot, the antibody detected only the desminΔhead and desmin(251-470) but not any of the desminΔtail constructs nor desmin(1-240). Therefore, the WB clearly demonstrated that the epitope of the D9 antibody is located on the tail domain. The tail domain of desmin contains 61 amino acids (figure 6A) out of which only one amino acid is different between mouse and human desmin sequences (appendix 2).

In the subsequent steps, varied amounts of *m/hDes* (1/5/10/20/50/100 ng of each) were loaded on the gel and blotted on the PVDF membrane. By applying different D9 dilutions on the blots (1: 2000 / 1: 5000 / 1: 10 000) one could have compared the specificity of the antibody at different concentrations on different amounts of desmin (figure 8). The experiment has demonstrated that with dilution of 1: 2000 one could detect up to 5 ng of either *h/mDes* equally (with traces of 1ng of protein being detected) after 2 min of film exposure to the

membrane. In case of 1: 5000 and 1: 10 000 dilutions, one could detect up to 5 or 10 ng of protein respectively. In all dilutions, the relative amounts of signals of detected in the lanes of either mouse or human desmin were mostly quite similar. This result demonstrates that D9 is equally specific for both mouse and human desmin proteins.

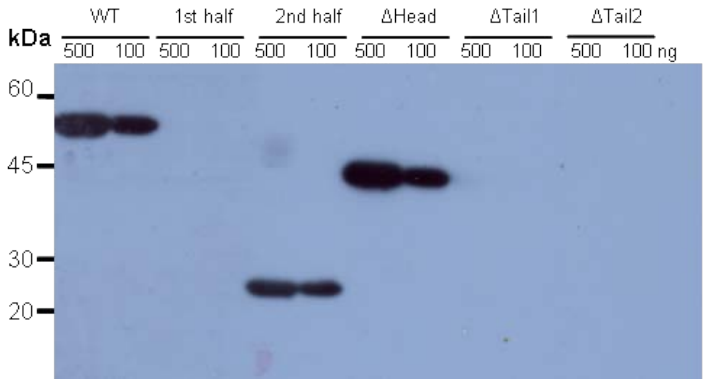

Figure 7. Narrowing down the epitope of D9 antibody. WB on 500 ng / 100 ng of different *Des* constructs: *mDes* complete (WT), desmin 1st half (amino acids 1-240), desmin 2nd half (amino acids 251-470), headless (ΔHead) and two tailless (ΔTail1/2) desmin truncations.

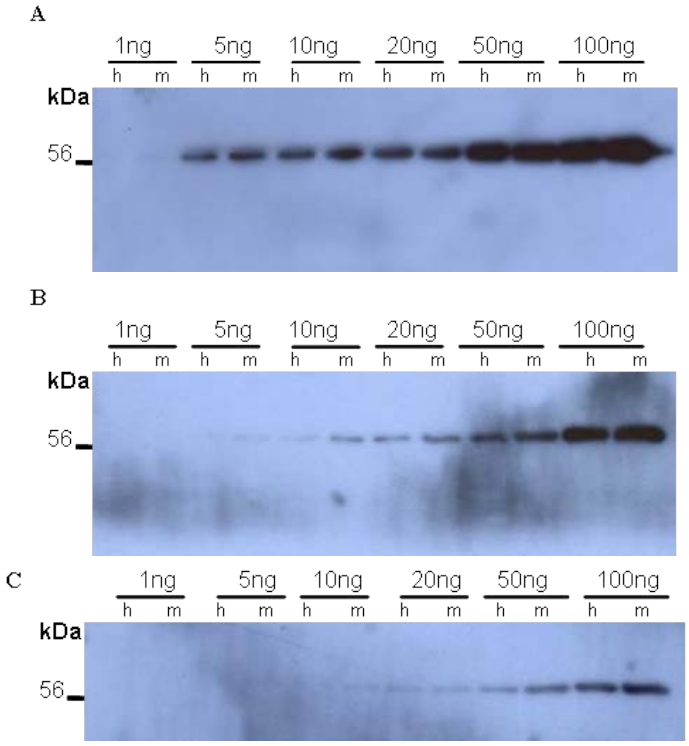

Figure 8. Specificity of D9 antibody on *m/hDes*. Different amounts mouse (m) and human (h) desmin were blotted on the membranes and detected with the D9 antibody diluted **(A)** 1: 2000, **(B)** 1: 5000 and **(C)** 1: 10 000.

3.1.2 Human desmin 1 antibody is highly specific for human desmin

In order to generate an *hDes* specific antibody, we have chosen a 10-amino acid epitope sequence located on the non-α-helical head domain of the *hDes*, which differs at two amino acids positions from mouse desmin (figure 9). The corresponding peptide was initially injected into two guinea pigs, two mice and two rats. Immunisation of mice and rats was done for the purpose of attempting to generate monoclonal antibodies. However, despite the fact that one of the sera from the rats did contain antibodies which could specifically detect *hDes* (data not shown), no *hDes*-specific monoclonal antibodies could have been found in the subsequent screening. In addition, both guinea pigs generated antibodies that also had a high extent of crossreactivity with *mDes* and which stained poorly in ICC (data not shown).

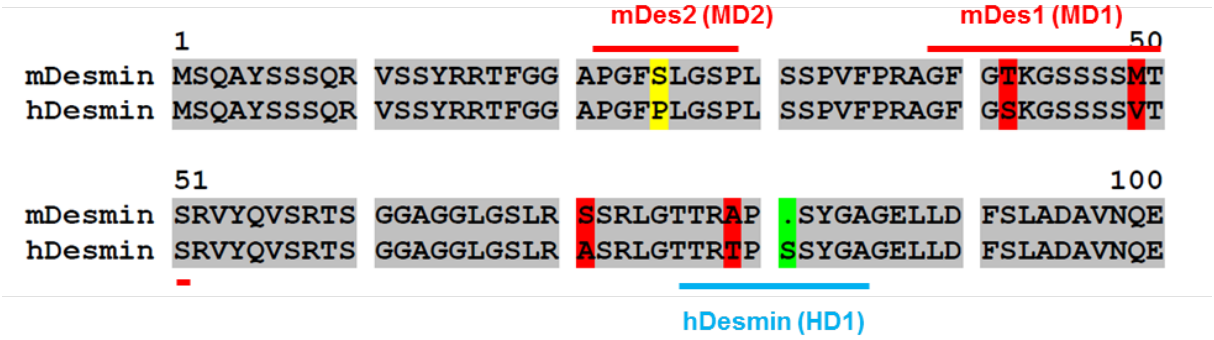

Figure 9. Epitopes of the HD1 and MD1/2 antibodies. Sequence alignment of the first 100 amino acids of human and mouse desmin proteins (colour code: amino acids with a substitution were coloured with yellow or red background; the same amino acids in the two sequences were coloured with grey background; the amino acid lacking in *mDes* has green background). The epitopes of the antibodies are marked: blue for HD1 and red for either MD1 or MD2 antibodies.

In the subsequent steps we have injected the same peptide into two rabbits and again tested the sera. Not only that the blood sera of the two rabbits contained antibodies highly specific for *hDes* but they also had a very high titre (figure 10A). Subsequently the sera were tested by ICC on the two desmin-positive cell lines, mouse C2C12 and human RD. Both sera were negative on murine C2C12 cells but the serum from the first rabbit (human desmin 1, HD1) stained the desmin filaments very strong (figure 10B).

Subsequently, the HD1 antibody was purified from the serum and the eluate with the antibody was collected in the fractions 3 to 6 (all antibody purifications were done by PSL GmbH, Heidelberg). As the antibody generated was polyclonal all of the fractions were tested for the antibody specificity. Namely, as the serum contained all of the antibodies generated by the

immune system of the animal upon injections, the fractions collected after antibody elution could have contained antibodies of different specificities or binding affinities. Nevertheless, all of the HD1 fractions have detected up to 5 ng of *hDes* at dilutions up to 1: 20 000 (fractions 5 and 6) or 1: 10 000 in fractions 3 and 4 (figure 11). Interestingly, although HD1, fraction 6 had lower antibody concentration (0.3 mg/ml) than either fraction 4 or fraction 5, the same or higher dilution of fraction 6 than either of these two antibodies fractions detected up to 1 ng of *hDes* (compared to 5 ng in case of these two antibody fractions). This observation does indicate heterogeneity of the antibody fractions with respect to the antibodies they contain.

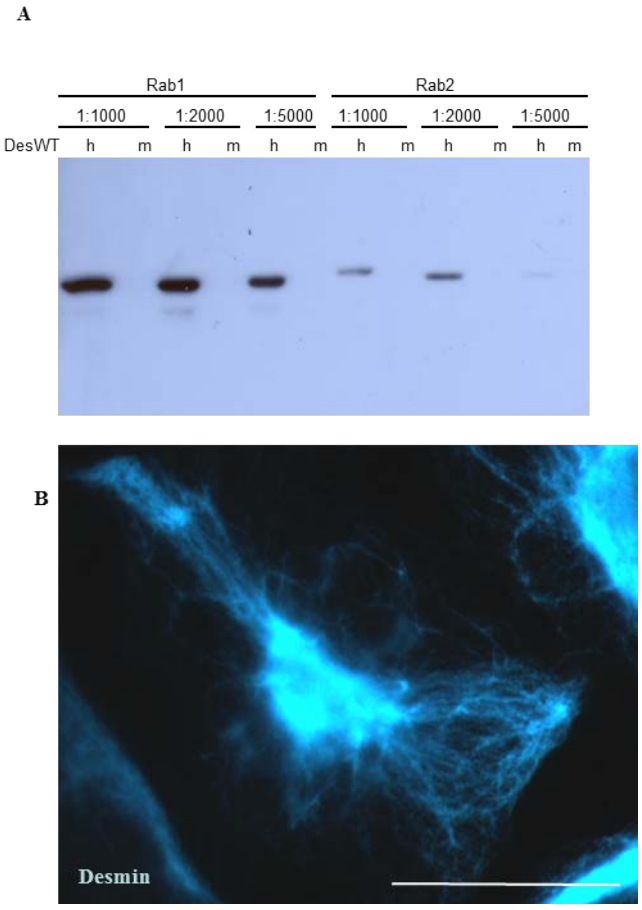

Figure 10. Testing of the sera from rabbits immunised with *hDes*-specific peptide. (A) WB with recombinant mouse (m) and human (h) desmin (100 ng of either per lane) tested with rabbit 1/2 sera (Rab 1/2) diluted 1: 1000, 1: 2000 and 1: 5000. **(B)** ICC on RD cells with rabbit 1 serum (1: 100 diluted). Blue, desmin; scale bar, 20 μm.

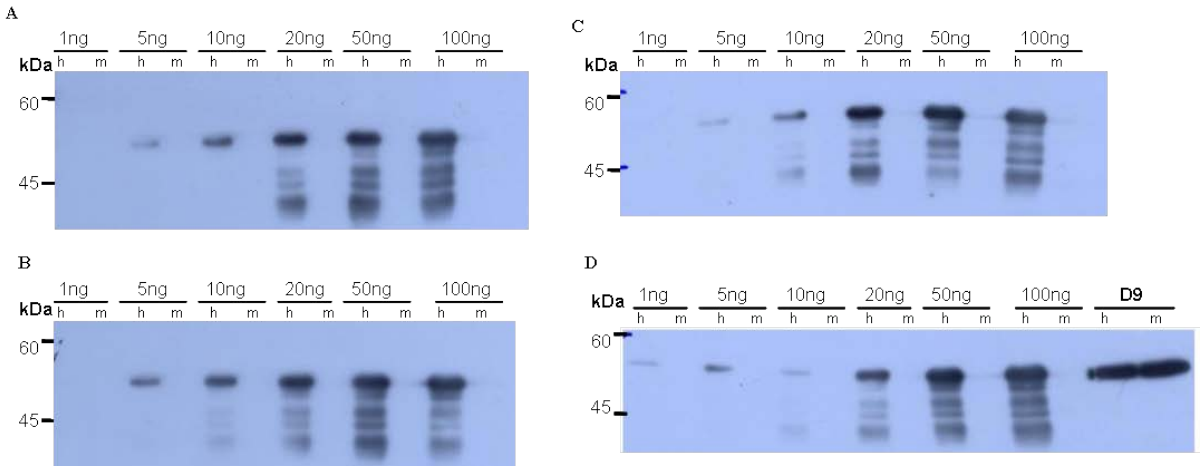

Figure 11. Specificity of different fractions (3 to 6) of the eluted HD1. Different amounts of mouse (m) and human (h) desmin were blotted on the membranes and detected with the HD1 antibody diluted **(A)** 1: 10 000 (fraction 3, 0.2 mg/ml of antibody), **(B)** 1: 10 000 (fraction 4, 0.5 mg/ml conc.), **(C)** 1: 20 000 (fraction 5, 0.4 mg/ml conc.) and **(D)** 1: 20 000 (fraction 6, 0.3 mg/ml conc.), as well as D9 (1: 2000) WB on 100 ng *h/mDes*.

3.1.3 Whereas mouse desmin 1 antibody detects both mouse and human desmin proteins, mouse desmin 2 antibody is specific for mouse desmin on WB

In the subsequent steps we have attempted to generate a *mDes*-specific antibody. The purpose for that was to generate an antibody that could be used for ICC in addition to HD1 to examine the extent of segregation of the transfected and endogenous desmin proteins. Although one would expect that D9 antibody, which detects both mouse and human desmin equally (figure 8), could be used in addition to HD1 the arguments in favour of generating the *mDes*-specific antibody would further be addressed in sections 3.1.5 and 3.3. Thereby, two other epitopes were chosen (8 and 13 amino acids) for the *mDes* antibodies generation (figure 9), for which peptides were synthesized and injected into two rabbits each. Similarly as for HD1, the antibodies were purified from 10ml blood serum from the animals (one for each of the animals injected with the same peptide, with higher specificity and titre of the antibodies) and collected in fractions 3 to 6 (named mouse desmin 1 and 2, MD1 and 2).

The antibodies generating by immunising rabbits with the two peptides vary with respect to their specificity. Namely, whereas MD1 detects both mouse and human desmins (albeit *mDes* with a higher specificity, figure 12A1–5), MD2 appears to be *mDes*-specific but with significantly lower binding affinity (i.e., very low dilution of the antibodies are needed for the protein detection on WB). However, although MD1 detected filaments thoroughly in ICC (figure 13) MD2 appears to stain only sections or points of filaments (data not shown).

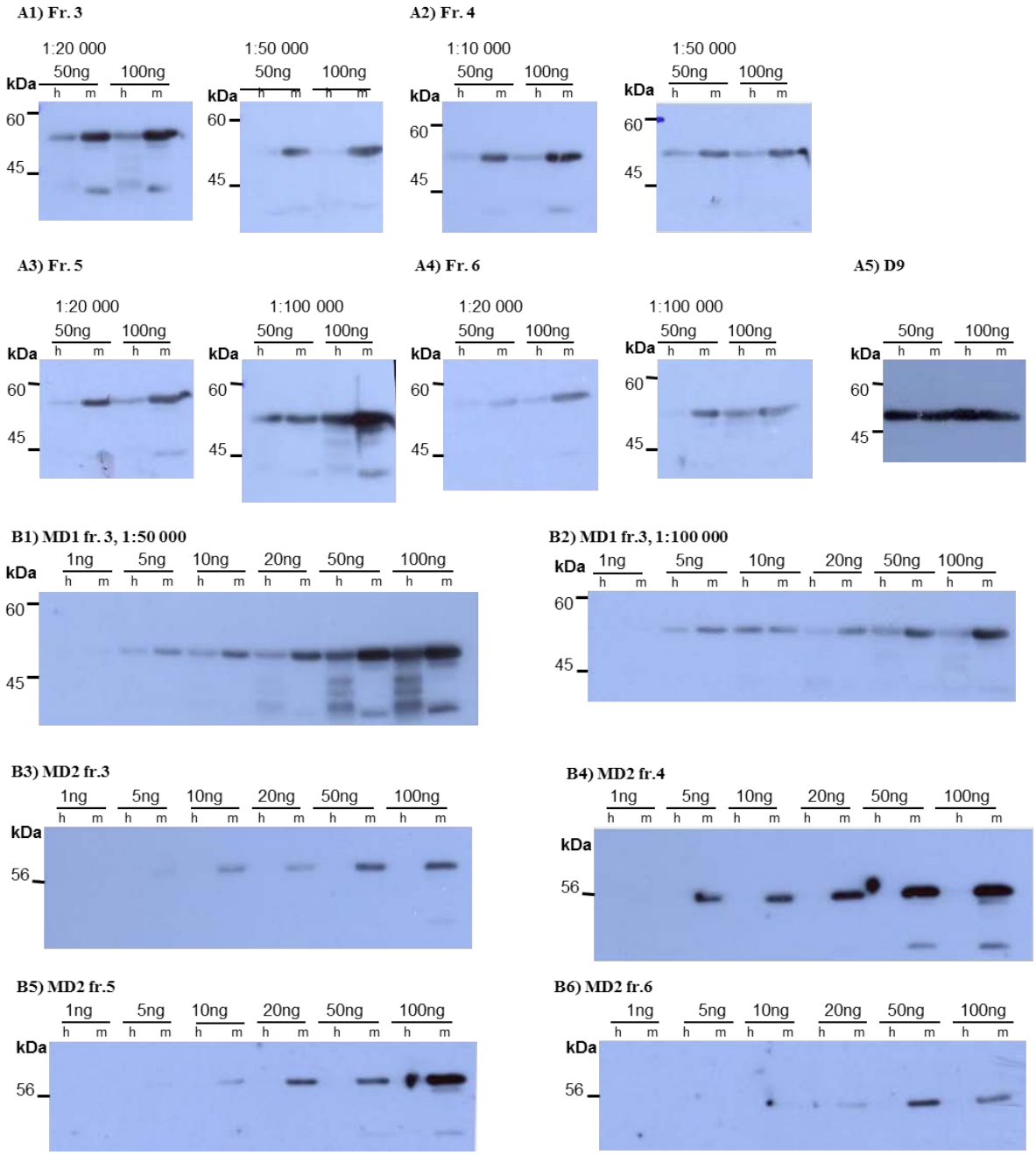

Figure 12. Specificity of different fractions (3 to 6) of the eluted MD1 and MD2 antibodies. (A) Different amounts of mouse (m) and human (h) desmin were blotted on the membranes and detected with the MD1 antibody **(A1)** fraction3, **(A2)** fraction 4, **(A3)** fraction 5, **(A4)** fraction 6 (antibody dilutions are indicated above each blot), as well as **(A5)** D9 (1: 2000). **(B)** Different amounts of mouse (m) and human (h) desmin were detected with MD1, fraction3 **(B1)** 1: 50 000 and **(B2)** 1: 100 000, as well as MD2 antibody **(B3)** fraction3, **(B4)** fraction 4, **(B5)** fraction5 and **(B6)** fraction6, all 1: 500 diluted.

Finally, as the fraction 3 of MD1 still appeared to detect *mDes* with significantly higher specificity than *hDes*, we have attempted different strategies to obtain an antibody highly specific for *mDes*. In the ICC we have washed the antibody with high (up to 2 M) concentrations of NaCl with a rationale that more stringent washing could remove antibodies

weakly bound to the *hDes* epitopes. The procedure was, however, unsuccessful as the antibody affinity to *mDes* appeared not to be sufficiently higher as compared to its binding affinity to the *hDes*. In the second step, we have generated a peptide of the corresponding *hDes* epitope aiming to use it to bind a subset of antibodies from the eluate more specific for *hDes*. The rationale was that there was a possibility, due to the high *mDes*-specificity of the MD1, fraction3, that there could be a significant proportion of antibodies in the eluate specific for *mDes* only. However, as in the previous case, we were unsuccessful in purifying an antibody detecting predominantly *mDes* (data not shown). Namely, there was very little antibody bound to the purification column whereas the unbound antibody was equally specific for desmin in C2C12 (mouse) and RD (human) cells.

*3.1.4 Successful generation of antibodies specific for either Des*WT *or Des*R350P

In the final step of generating antibodies to specifically detect mutant or endogenous WT desmin rabbits were immunised with 9-amino acid peptides from the desmin coil 2B region, surrounding the arginine (R) 350. Hence two rabbits were immunised with the WT version of the peptide and two with *hDes*R350P mutant peptide. The first sera analyses indicated that, whereas both antibody sera specific for the *hDes*R350P-epitope detected the mutant protein specifically on the WB, only one of the antibodies generated against the *Des*WT epitope specifically detected the protein (figure 14).

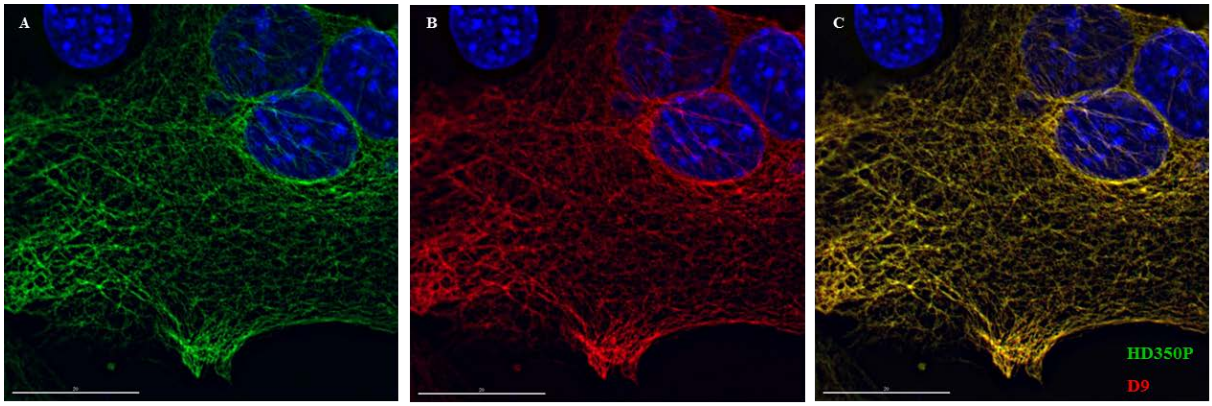

Figure 13. ICC with MD1/2 on C2C12 cells. (A) The MD1 antibody serum (green), diluted 1:50, stained filaments thoroughly **(B)** as did the D9 antibody (red). **(C)** Merge; blue, DAPI; scale bars, 20 μm.

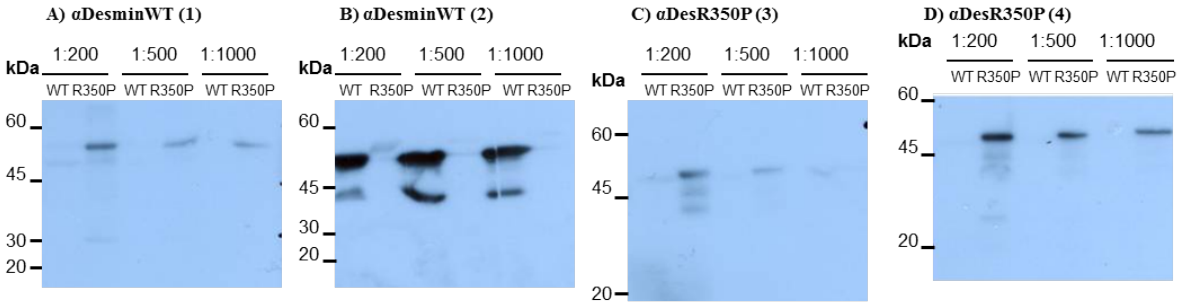

Figure 14. Testing of the rabbit sera detected against *Des*R350 epitope. 100 ng of *hDes*WT and *hDes*R350P was detected with 1: 200, 1: 500 and 1: 1000 dilutions of **(A)** anti-*Des*WT (1), **(B)** anti-*Des*WT (2)**, (C)** anti-*Des*R350P (3) and **(A)** anti-*Des*R350P (4). Note that anti-*Des*WT (1) antibody specifically reacts with *Des*R350P.

Therefore sera 2 of the *Des*WT (human desmin 2, HD2), as well as the *hDes*R350P (human desmin *hDes*R350P, HD350P)-immunised rabbits, were used for the standard antibody purification procedure to obtain 4 fractions of each of the antibodies. Fraction 4 of each of the antibodies was then tested in higher dilutions on the WB with respect to their specificity to the *hDes*WT and *hDes*R350P proteins (figure 15). Whereas HD350P was found to detect 10 ng *hDes*R350P at 1: 20 000 dilution, HD2 detected the same amount of *hDes*WT at 1: 10 000.

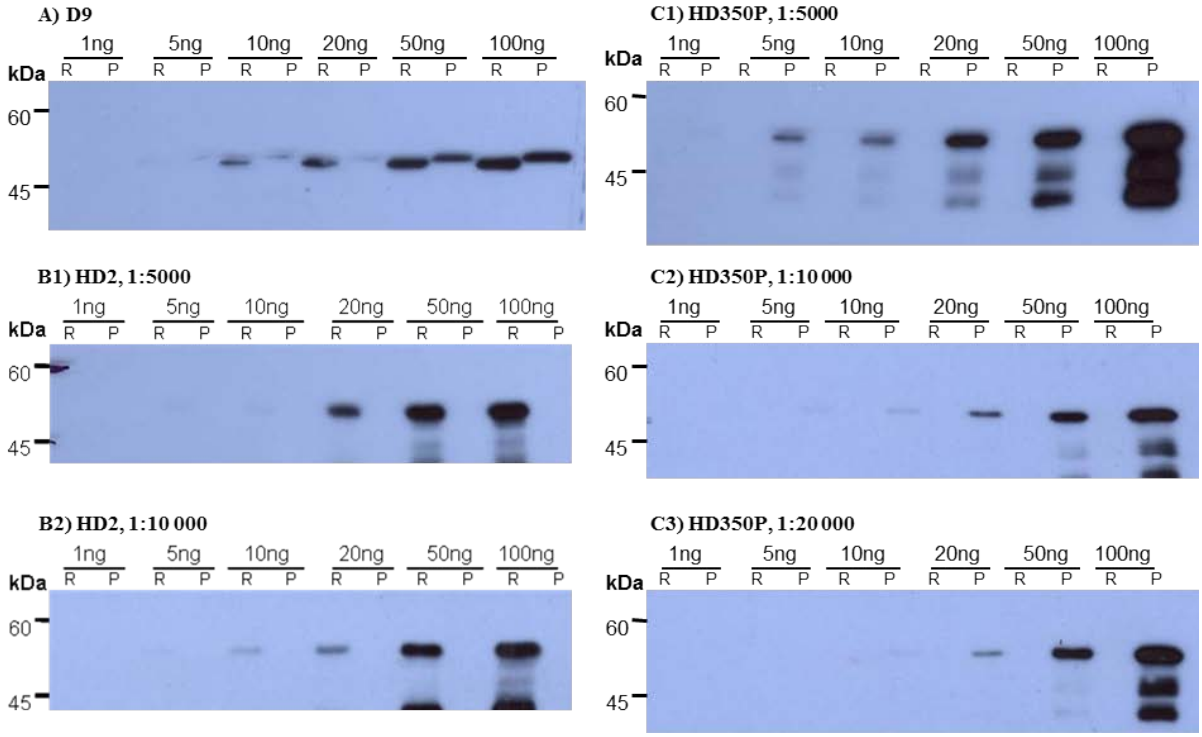

Figure 15. Specificity testing of the HD2 and HD350P. Different amounts of *hDes*WT (R) and *hDes*R350P (P) were detected on the WB with **(A)** D9, **(B)** HD2 fraction 4: **(B1)** 1: 5000 and **(B)** 1: 10 000 and **(C)** HD350P fraction 4: **(C1)** 1: 5000, **(C2)** 1: 10 000 and **(C3)** 1: 20 000. Note that in figure (A) *hDes*R350P runs somewhat higher than the *hDes*WT.

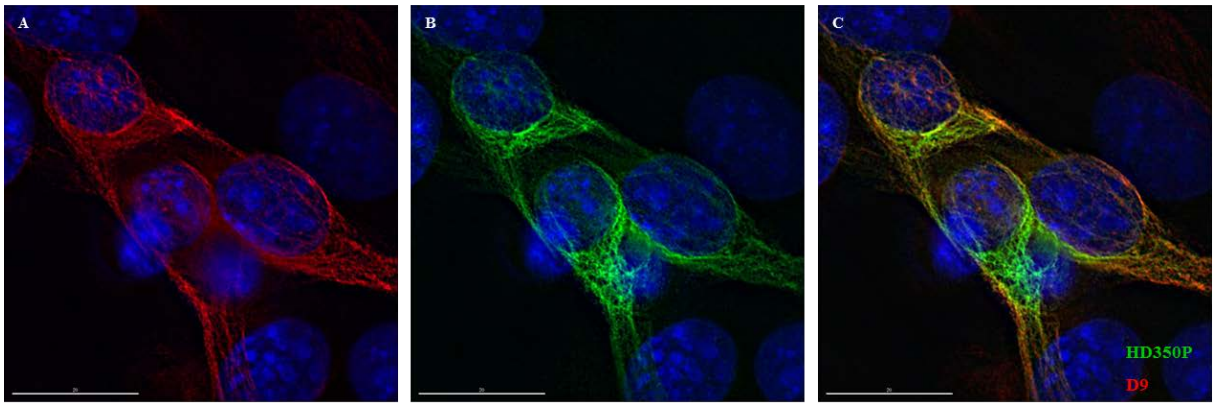

Figure 16. ICC of C2C12 +*hDes*R350P with HD350P. After treatment with 2 M urea, the cells expressing the *hDes*R350P desmin mutant were detected using the HD350P antibody (fraction4, 1: 100). The **(B)** HD350P (green) signals were found to largely colocalise with **(A)** D9 (red), which can detect both endogenous and transfected desmin proteins. **(C)** Merge. Blue, DAPI; scale bars, 20 μm.

The initial ICC procedure previously used for D9, HD1 and other desmin detection, was unsuccessful using these purified antibodies. Therefore, in order to make the epitope more accessible (discussed in section 4.1.1) the cover slips were briefly treated with 2 M urea (the procedure as described in the methods section, 2.2.6). Although only few cells were successfully stained by this method the staining on the cells positive with the HD350P was similar to that of the HD1 (figure 16). Further (i.e., longer) treatment of cells with 2 M urea did not significantly improve the staining efficiency with HD350P but appeared to affect the overall cell architecture (data not shown).

3.1.5 Antibodies binding to different epitopes of IF proteins could have a different staining pattern in ICC

As generation of *mDes*-specific antibody that would be suitable for use in the ICC was unsuccessful we analysed the potential of the available antibodies to be implemented in the study. One of the possibilities would be to use the D9 antibody which recognises both *h/mDes* (figure 8). The obstacle of using this antibody in the current studies is further addressed in section 3.3.1. As it has been previously indicated, desmin and vimentin were previously found to form heterodimers (Quinlan and Franke 1982) in hamster kidney cells. Therefore we employed a clone of the same cell line, BHK21-C13 to investigate the possibility for specific detection of the endogenous (in this case, vimentin/desmin) IF network in parallel with the transfected desmin. Thereby, we have proceeded with staining the cells with D9, made in mouse, and VimCT, a rabbit antibody.

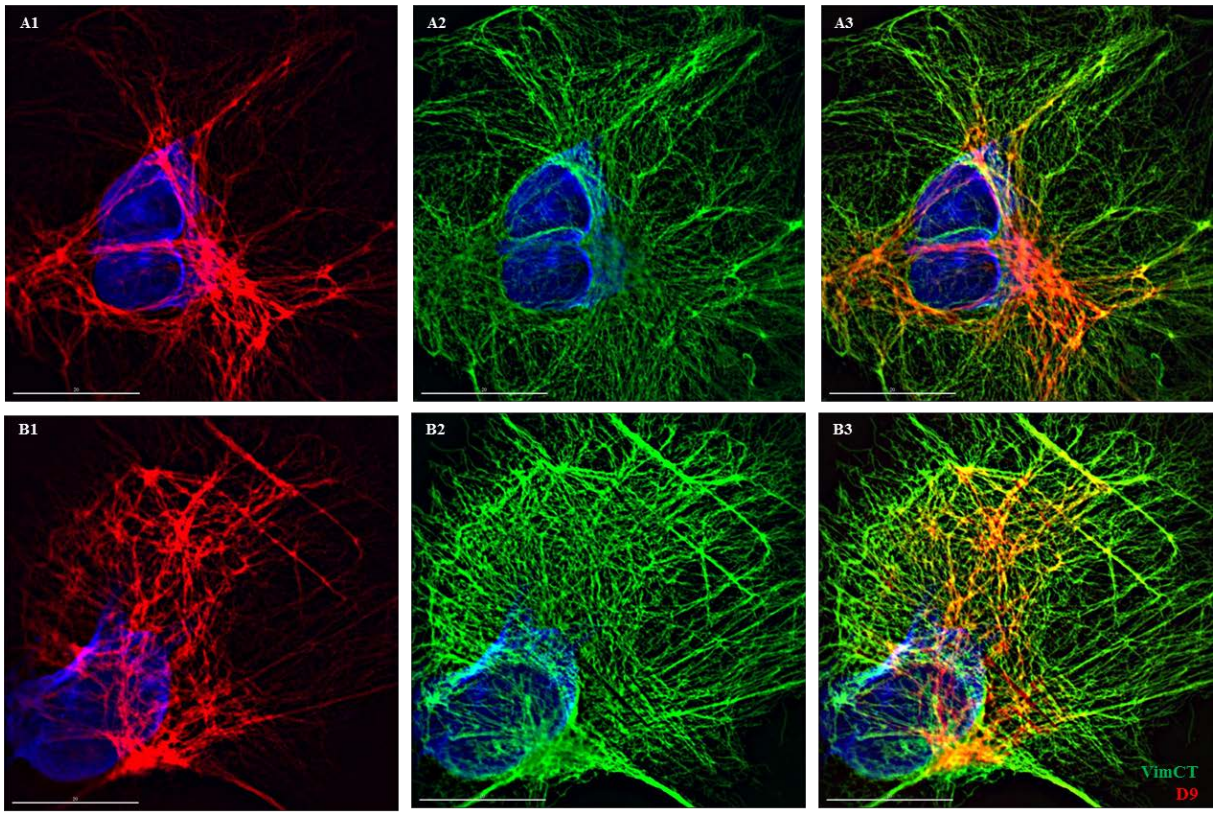

Figure 17. ICC of BHK21-C13 with C-terminal vimentin and desmin antibodies. Two examples of cells stained with D9 desmin antibody, red **(A1, B1)** and VimCT vimentin antibody, green **(A2, B2)**. **(A3, B3)** Merge. Blue, DAPI; scale bars, 20 μm.

As it can be seen on figure 17 the two IF systems, vimentin (figure 17A,B2) and desmin (17A,B1), both stained with antibodies generated against epitopes on their tail domains, colocalise to a significant extent (17A,B3). However, what one repeatedly notices is that, whereas the vimentin antibodies appeared to spread rather uniformly throughout the cytosol desmin IFs appeared to form bundles. Such bundles appeared to have been more specifically and thereby disproportionally stained by the D9 antibody and were most commonly located in the perinuclear region (such as in image 17A).

To resolve if such disproportional staining of the desmin and vimentin antibody could reflect the different distribution of the desmin or vimentin IFs, the staining was repeated on the BHK21 cells with two antibodies binding to different epitopes on vimentin (figure 18). Whereas the epitope of VimCT antibody is located at the tail domain of vimentin the epitope of the Vim3B4 mouse antibody is located at the coil 2 in the rod domain of the protein. It can be seen in figure 18a that the Vim3B4 signals colocalised with the VimCT ones to a very high degree. However, there were some filaments stained only or predominantly with the VimCT antibody. Do note in figure 18a1 that there is a significant area in the periphery of the cell that

is only weakly stained with the Vim3B4 antibody. However, another frequent observation, depicted by example on figure 18B, was that there was a significant portion of single filaments stained with only one of the antibodies (either VimCT or Vim3B4). Hence in interpretation of the ICC on IFs one should also take into consideration the epitopes of the particular antibodies.

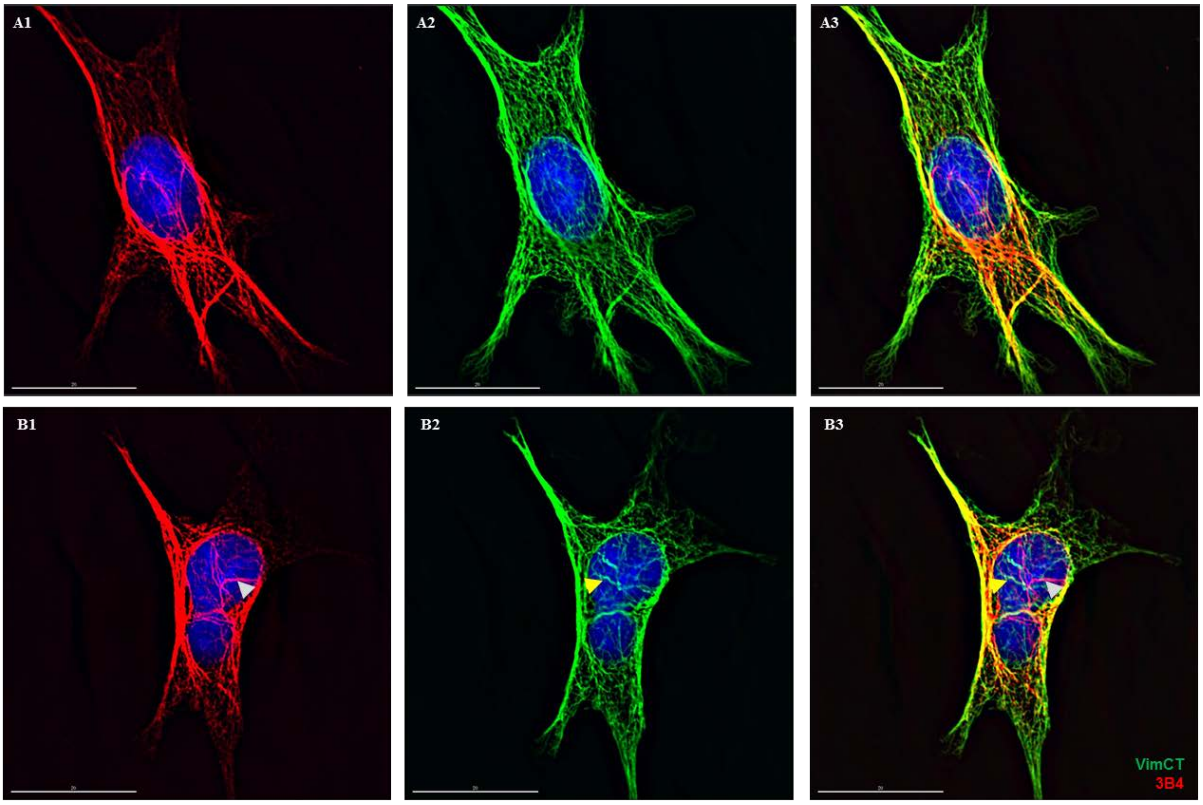

Figure 18. ICC of BHK21 with VimCT and Vim3B4 antibodies. Two examples of cells stained with Vim3B4, red **(A1, B1)** and VimCT, green **(A2, B2)**, both vimentin antibodies. **(A3, B3)** Merge. The arrows in **(B)** point to the filaments stained either with Vim3B4 (grey) or VimCT (yellow arrow). Blue, DAPI; scale bars, 20 μm.

3.2 Analyses of the IF proteins in C2C12 cells

Before performing any analyses on the C2C12 cells transfected with either WT or mutant desmin proteins, the cell line was first characterised with respect to the key IF proteins studied, namely the nuclear A-type lamins as well as desmin and vimentin. All of the analyses were performed both in cells grown in GM as well as those incubated in the DM for 6 days.

3.2.1 A-type lamins are differently distributed in C2C12 cultured in growth or differentiation medium

Distribution of A-type lamins was compared in the C2C12 (GM) and (DM) cells. As it was briefly indicated in the introduction, distribution of A-type lamins was found to differ in cells in GM and of those cultured in DM (Muralikrishna et al. 2001). As these observations were made in ICC we wanted to examine if the same conclusion could be drawn from A-type lamins distribution in different fractions upon cell fractionation. Therefore, the cells were first treated with a buffer containing digitonin (Dig fraction), which principally permeablises the plasma membrane; subsequently, the cells were treated with low concentration of NP40 detergent and salt (LIB fraction), following the harsh treatment with higher concentration of NP40 and NaCl and subsequent centrifugation (yielding supernatant and pellet fractions). Using this procedure, we could separate the cytosolic (i.e., mitotic) lamins (Dig), from soluble (LIB) and filament-incorporated lamins, probably as single, shorter filaments (Sup. fraction) or longer filaments and filament networks (Pel. fraction).

As it can be seen in figure 19, C2C12 (DM) had a higher amount of A-type lamins (detected with LaZ antibody) most of which was found in the pellet fraction (i.e., insoluble). In contrast to that, A-type lamins in C2C12 (GM) were found in both supernatant and the LIB. This result indicates that, similarly to the previous observations by ICC, A-type lamins are also found in nucleoplasm (i.e., part of them remained soluble) in the undifferentiated cells, in contrast to C2C12 (DM) where almost all of A-type lamins were lamina-incorporated.

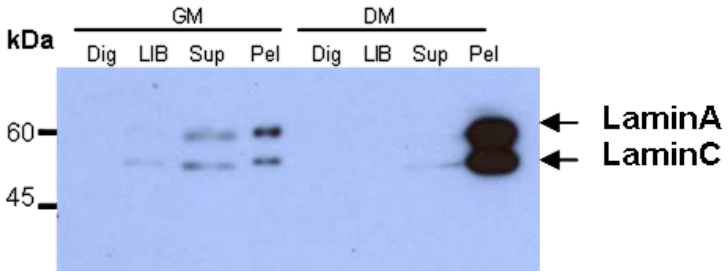

Figure 19. WB with an A-type lamin antibody (LaZ) on fractions of C2C12 (GM) and (DM) cells. Different fractions of C2C12 (GM) and (DM) cells: Dig, LIB, Sup and Pel (diluted 1:2), as described above. Loading scaled to 10 µg of protein in LIB fractions.

In a further step, A-type lamins distribution in the C2C12 (GM) and (DM) was compared to that in RD cells. This has been performed as an additional control of the system as RD cells would have been expected to have a similar A-type lamins distribution as C2C12 (GM). Although A-type lamins content in RD cells was appeared to be lower than in C2C12 cells

(figure 20A) their fraction distribution was similar to that of C2C12 (GM). Note that the exposure of the film to the membrane was prolonged to attempt to detect the weak signals in the LIB and Sup fractions of the C2C12 (DM). Therefore, the amount of lamins in C2C12 (GM) and (DM) pellet fractions appeared similar. Furthermore, WB was also performed with an antibody against Glyceraldehyde-3-Phosphate Dehydrogenase (GAPDH), a common positive control for extraction of the cell cytoplasm (figure 20B). Such control was necessary to confirm that the A-type lamins extracted in the LIB fraction do represent the nucleoplasmic lamins and not the mitotic ones. As GAPDH was extracted first in the digitonin fraction, the extraction of the soluble cytosolic material was concluded to be successful. Note that GAPDH is extracted also in the other fractions indicating the protein might not be found entirely free in the cell cytosol. Therefore the A-type lamins extracted in the LIB fraction did indeed appear to represent the nucleoplasmic and not cytosolic (i.e., mitotic) ones.

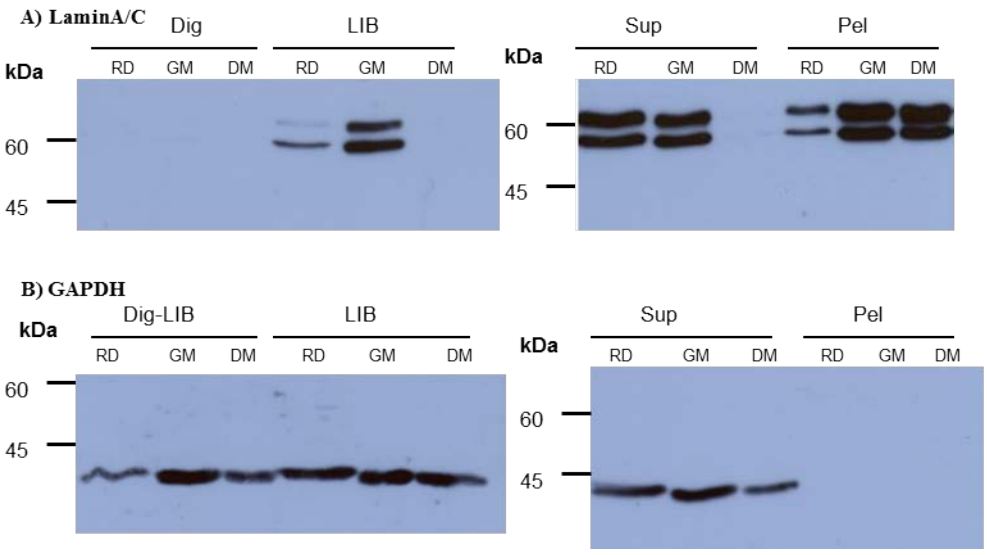

Figure 20. WB with LaZ on fracions of RD, C2C12 (GM) and (DM) cells. Different fractions of RD, C2C12 (GM) and (DM) cells: Dig, LIB, Sup and Pel (diluted 1:2), as described above. Loading scaled to the equal amounts of protein in each of the LIB fractions. The blots were stained with antibodies against **(A)** LaminA/C and **(B)** GAPDH.

3.2.2 Desmin expression increases in C2C12 cells upon differentiation

The C2C12 fractions (both GM and DM) were also used on a WB with a D9 antibody. The purpose was to examine the distribution of desmin in the fractionation procedure before and after the cells have been induced to differentiate. As it can be seen in figure 21, the amount of desmin was several fold higher in C2C12 (DM) compared to the (GM) cells. Note also that only a very small amount of desmin was extracted in the Sup fraction of the C2C12 (DM)

cells. After overexposure of the film to the membrane traces of signals were also detected in the C2C12 (GM) Sup lane (data not shown).

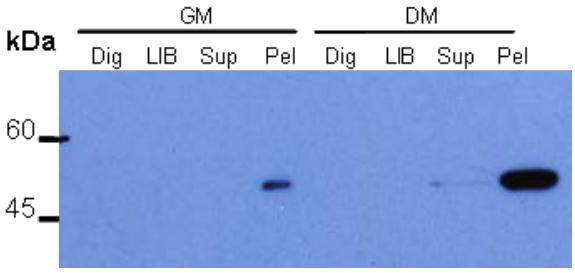

Figure 21. *Des* expression in C2C12 (GM) and (DM) cells. WB with D9 desmin antibody on the fractions: Dig, LIB, Sup and Pel (diluted 1:2) of the C2C12 (GM) and (DM) cells. Loading scaled to 10 µg of protein in LIB fractions.

In the subsequent steps we have performed ICC on these cells (both GM and DM) using the same (D9) antibody. As it can be seen on figure 22, the amount of desmin filament networks in C2C12 (DM) cells appeared significantly higher (the filament network was more dense) compared to the cells in GM. Furthermore, there was a significant number of multinucleated myotubes (figure 22B) after the cells were grown for 6 days in DM. However, no multinucleated cells containing more than 6 to 8 nuclei have been observed.

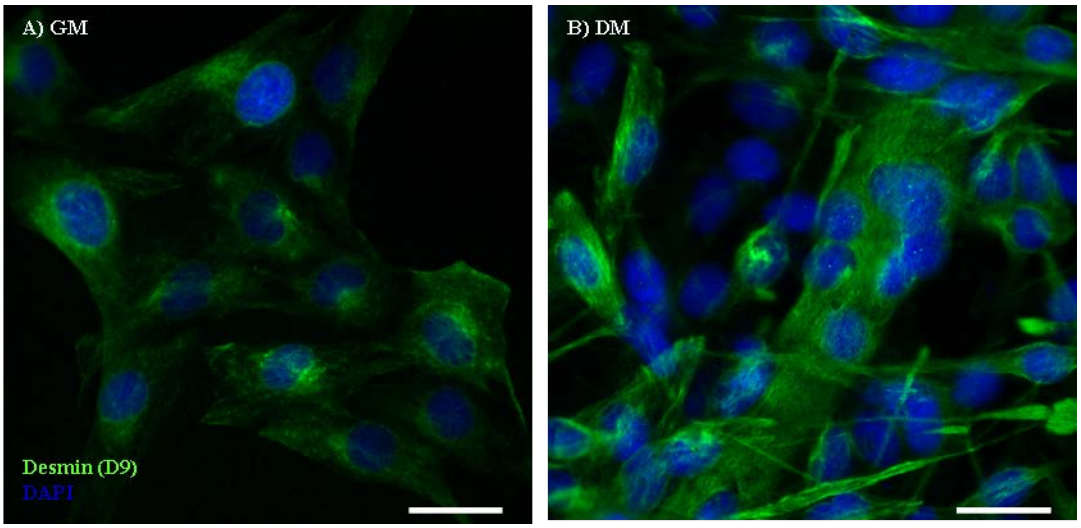

Figure 22. ICC with desmin antibody on differentiating C2C12 cells. C2C12 **(A)** (GM) and **(B)** (DM) cells stained with a desmin (D9) antibody (green). Blue, DAPI; scale bars, 20 µm.

In order to attempt to further optimise the differentiation procedure and to enhance the cell fusion during differentiation the standard protocol was somewhat optimised. Namely, previously the cells were always allowed to get over 95% confluent before changing the

medium to DM. The optimisation of the procedure included growth of cells to over 95% confluence and their subsequent splitting 1:5 using the 0.05% trypsin. The use of lower concentration of trypsin allowed for the cells to detach from the bottom of the dish with most of them still attached to several neighbouring cells. Hence the cells were split upon the initiation of the fusion which could further enhance their fusion potential.

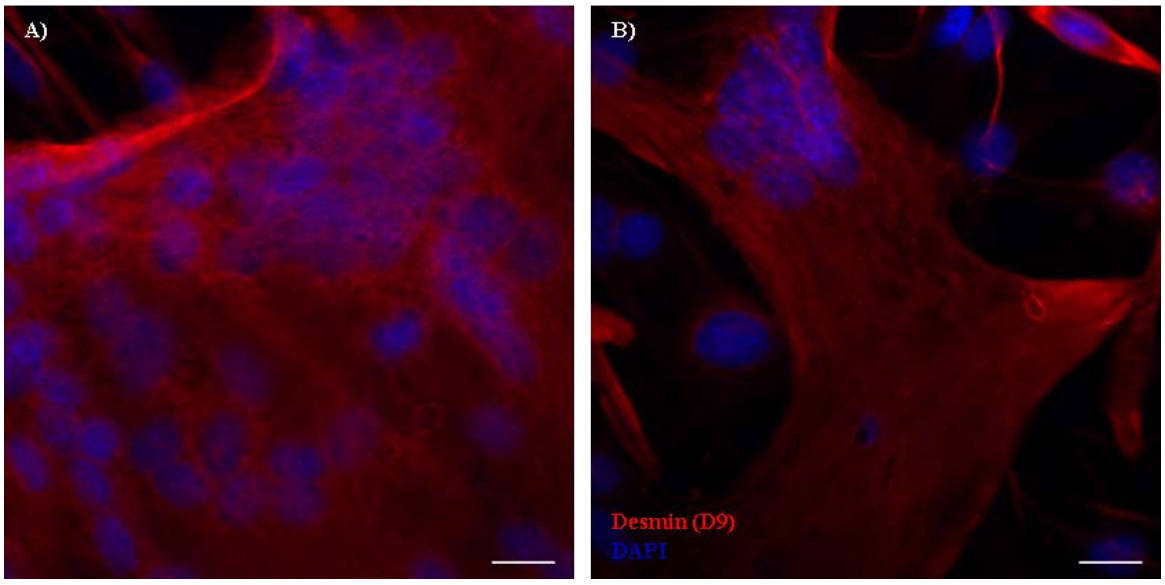

Figure 23. ICC on C2C12 (DM) cells. (A, B) The cells were detached with 0.05% trypsin (1 to 2 days) prior to differentiation induction. Red, desmin (D9); blue, DAPI; scale bars: 20 μm.

The examples of multinucleated myotubes generated by the above described procedure are shown in figure 23. Thereby, the application of the procedure for cell fusion enhancement appeared to have been quite successful, whereby it led to generation of cells consisting out of more than 50 nuclei. However, even though the cells were grown on chrome-sulphuric acid-activated cover slips, or different methods to maintain their attachment to the cover slips were used, they have predominantly detached from the cover slips. The images that were made were of the myotubes located on the edges of the cover slips. Therefore, as the sufficient generation of multinucleated myotubes on cover slips by this method was obstructed by the large amount of cells detaching from the glass surface this procedure was not used any further.

3.2.3 Whereas undifferentiated C2C12 cells are basophilic, they become eosinophilic upon differentiation

In the subsequent analyses of the C2C12 (GM) and (DM) cells, they were subjected to hematoxylin-eosin (HE) staining. This staining method is widely used in histological analyses

to differentiate some particular basophilic (hemalum-stained, blue or purple) and eosinophilic, commonly basic parts of the cell such as cytoplasm (pink or orange structures). The procedure was done on both C2C12 (GM) and (DM) cells and it was kindly performed by Michaela Hergt (our group).

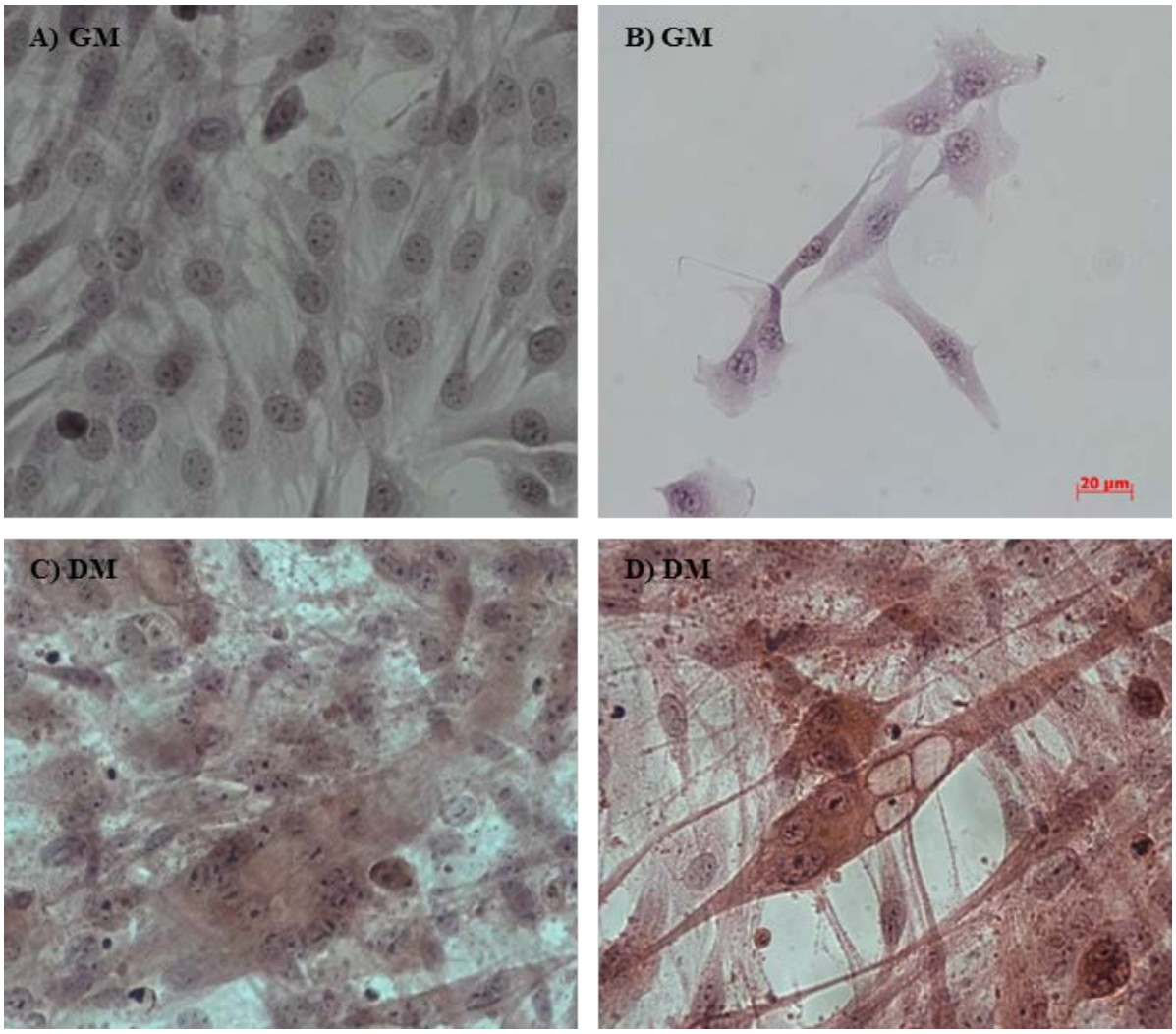

Figure 24. Hematoxylin-eosin staining of C2C12 cells. Whereas C2C12 (GM) cells are only **(A)** or predominantly **(B)** basophilic, the (DM) cells are largely **(C)** or exclusively **(D)** eosinophilic. Scale bar, 20 µm.

As depicted in figure 24A and B, the C2C12 (GM) cells were predominantly stained by hemalum. This result indicates that the undifferentiated C2C12 cells have largely basophilic cytosol. On the other hand, C2C12 (DM) cells were largely eosinophilic, which is a common feature of protein rich structures both in cytosol and extracellular space (figure 24C and D). Thereby, the HE staining results indicate that the cell differentiation in case of C2C12 cells is also accompanied by a change of the chemical composition of the cytoplasm.

3.2.4 Electron Microscopy of C2C12 (GM) and (DM) cells revealed distinct patterns of their IFs

In the last step of analyses on the C2C12 cells cultured in GM versus DM desmin networks were observed under the electron microscope (EM) using the conventional Epon-embedding-ultrathin sectioning-EM procedure for the sample preparation (figure 25). The imbedding as well as sample imaging was kindly performed by the team of the Core facility of electron microscopy in the DKFZ, headed by Dr. Karsten Richter. The aim of the procedure was to reflect on the observations in the ICC performed and compare them with the imaging on higher resolution.

As it can be seen on figure 25A1 and A2, the IFs in the C2C12 (GM) appeared uniformly distributed throughout the cytosol. Detection of the thin layer of the nuclear lamina was somewhat hindered by the dense chromatin material located at the edges of the INM. In case of C2C12 (DM) cells (figure 25, B1 and B2), the cytosolic IFs appeared more densely distributed throughout the cytoplasm. Furthermore, they also appeared more elongated and predominantly aligned in parallel. In some cases, dense bundles of IFs were found adjacent to the plasma membrane (figure 25B1). In case of cell protrusions (figure 25B2), they were more densely packed in filament bundles lining the plasma membrane. Such cellular protrusions were also commonly observed in the ICC as the very narrow pointed extensions of the cells which were stained strongly with the desmin antibodies (such as in figures 22b and 23b).

3.3 Effects of transfection of human desmin in C2C12 myoblasts

In the subsequent set of experiments, different *hDes* constructs, i.e., the *hDes*WT, *hDes*E245D and *hDes*R350P mutants cloned into pHβAPr-1-neo vector were used for cDNA-transfection of C2C12 cells. The vector contains a geniticin (G418) residence gene thereby allowing transfected cells to be selected for. The minimal concentration of G418 necessary for selection was determined to be 1.5 mg/ml. Therefore, in the subsequent experiments cells were always incubated in the GM containing G418 in order to maintain a culture of cells stably expressing the *hDes* constructs.

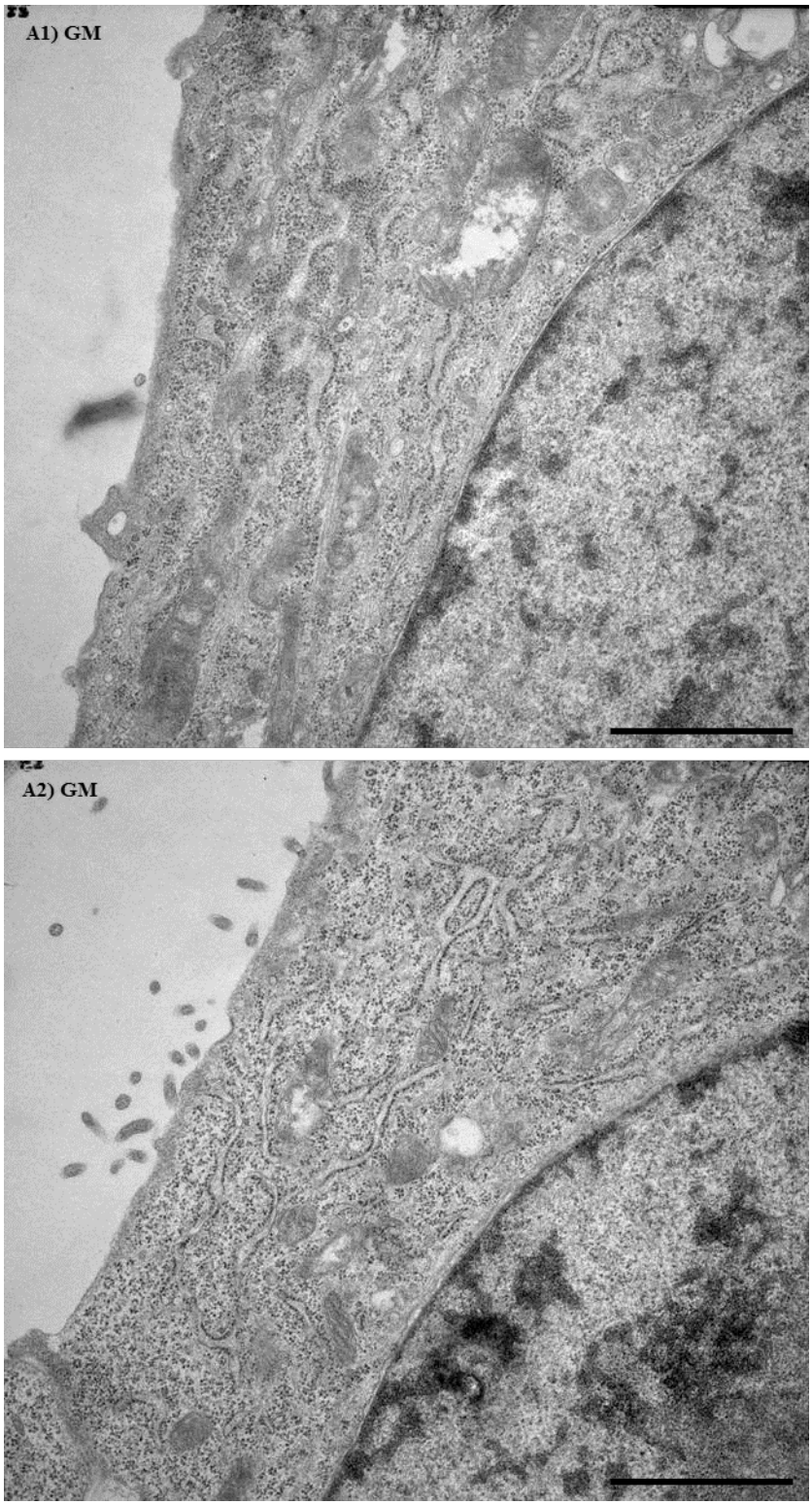

Figure 25. C2C12 cells under EM. (A1, A2) C2C12 (GM) cells prepared with conventional Epon-embedding-ultrathin sectioning and imaged on the EM; scale bars: 1000 nm. Images **(B1, B2)** are found on the following page.

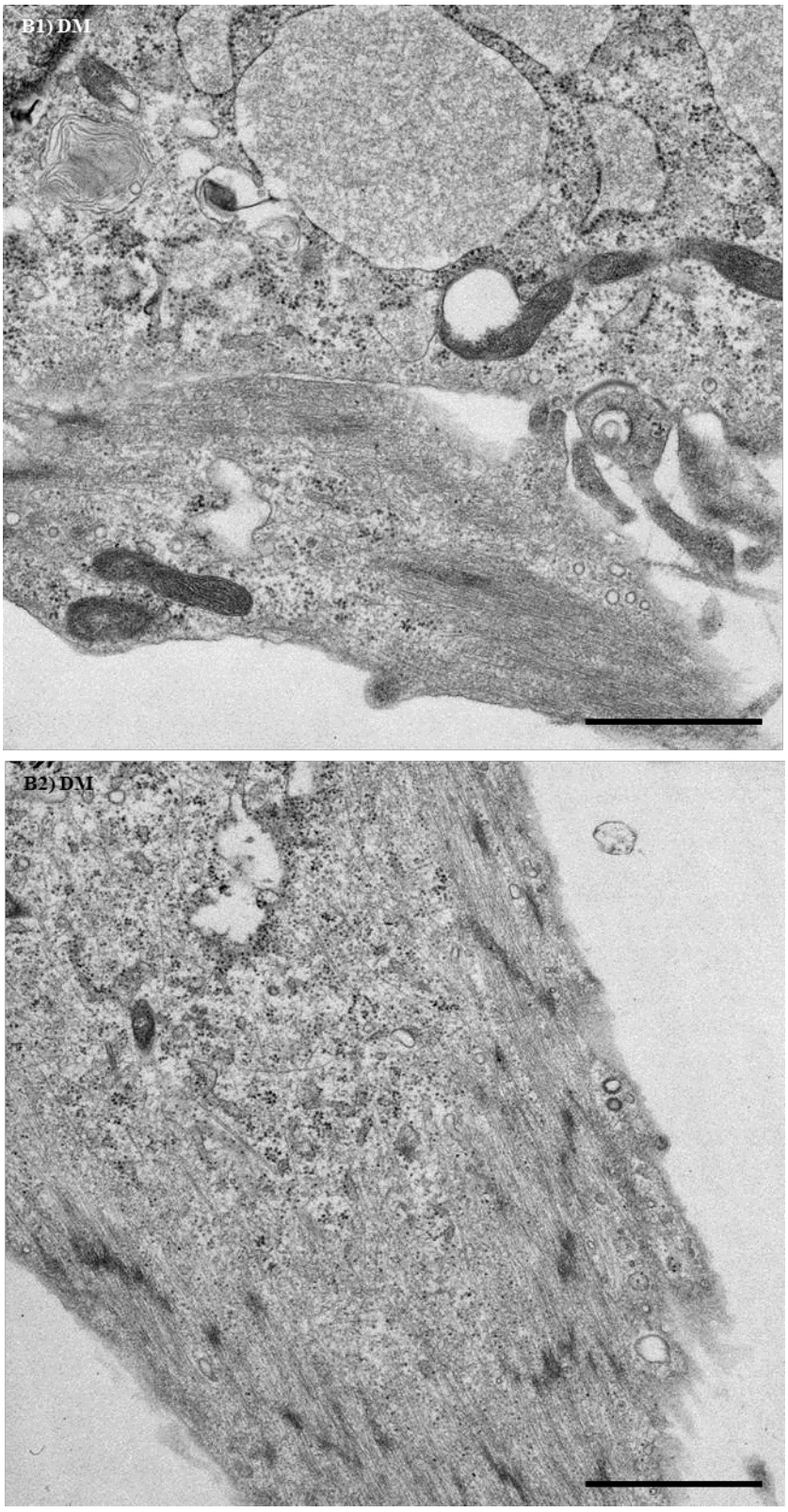

Figure 25. C2C12 cells under EM (continuation from the previous page). (B1, B2) C2C12 (DM) cells prepared with conventional Epon-embedding-ultrathin sectioning and imaged on the EM; scale bar: 1000 nm.

*3.3.1 hDes*WT *is readily incorporated into the pre-existing mouse desmin filament network*

In the first step of the analyses of the effects of the transfected proteins an ICC with both HD1 and D9 antibodies was performed on C2C12 cells expressing *hDes*WT (C2C12 +*hDes*WT). If not otherwise explicitly noted, HD1 staining was always done prior to incubation of cells with the D9 antibody. In figure 26, an example of a cell stained thoroughly with both D9 and HD1 antibodies is shown, demonstrating that *hDes*WT is expressed and integrated into the endogenous filaments. *hDes*WT expression and integration persisted for more than 20 passages after the initial transfection (data not shown). Although there has been some heterogeneity in the cell population with respect to the amount of *hDes*WT being expressed, a large majority (over 70%) of cells expressed the protein to a significantly high extent (i.e., HD1 staining reflected the D9 staining to a significant extent).

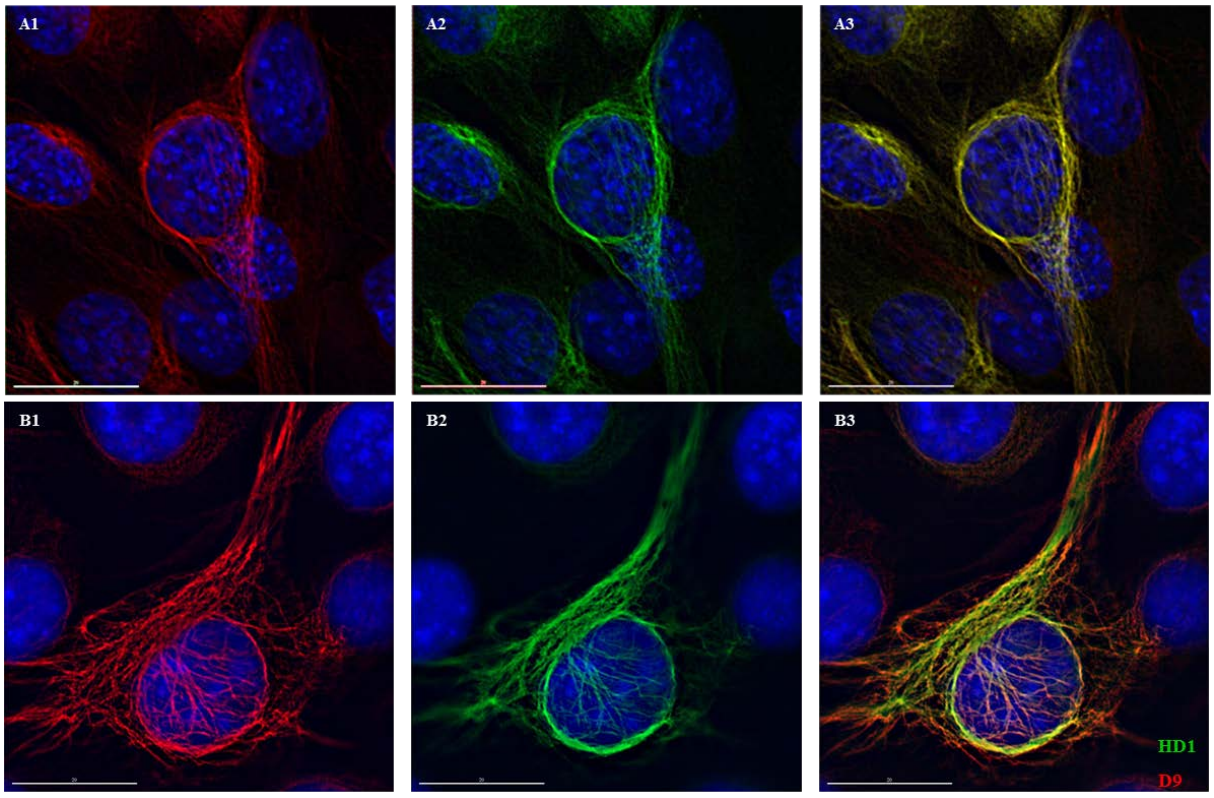

Figure 26. C2C12 +*hDes*WT cell stained with HD1 and D9. Two examples **(A and B)** of C2C12 +*hDes*WT cells stained with both **(A1, B1)** D9, red and **(A2, B2)** HD1 green. **(A3, B3)** Merge. Blue, DAPI; scale bars, 20 μm.

However, HD1 signals did not always appear to fully colocalise with D9 ones. Namely, as D9 antibody detects both human and mouse desmin whereas HD1 detected only human desmin, one would expect the HD1 signals to fully colocalise with the D9 ones. As it can be seen in figure 26B3, a significant amount of HD1 (green) signals was not fully colocalised with the D9 (red) ones. The same type of observation was also made when the cells were initially

incubated with the D9 antibody and subsequently stained with the HD1 (data not shown). In consideration of this effect one should also take into an account that the epitopes of the two antibodies, HD1 and D9, are located in head and tail domains, respectively. Such difference in the position of the epitope could affect the geometry of the antibody binding to the protein (the problem is further discussed in section 4.1.2).

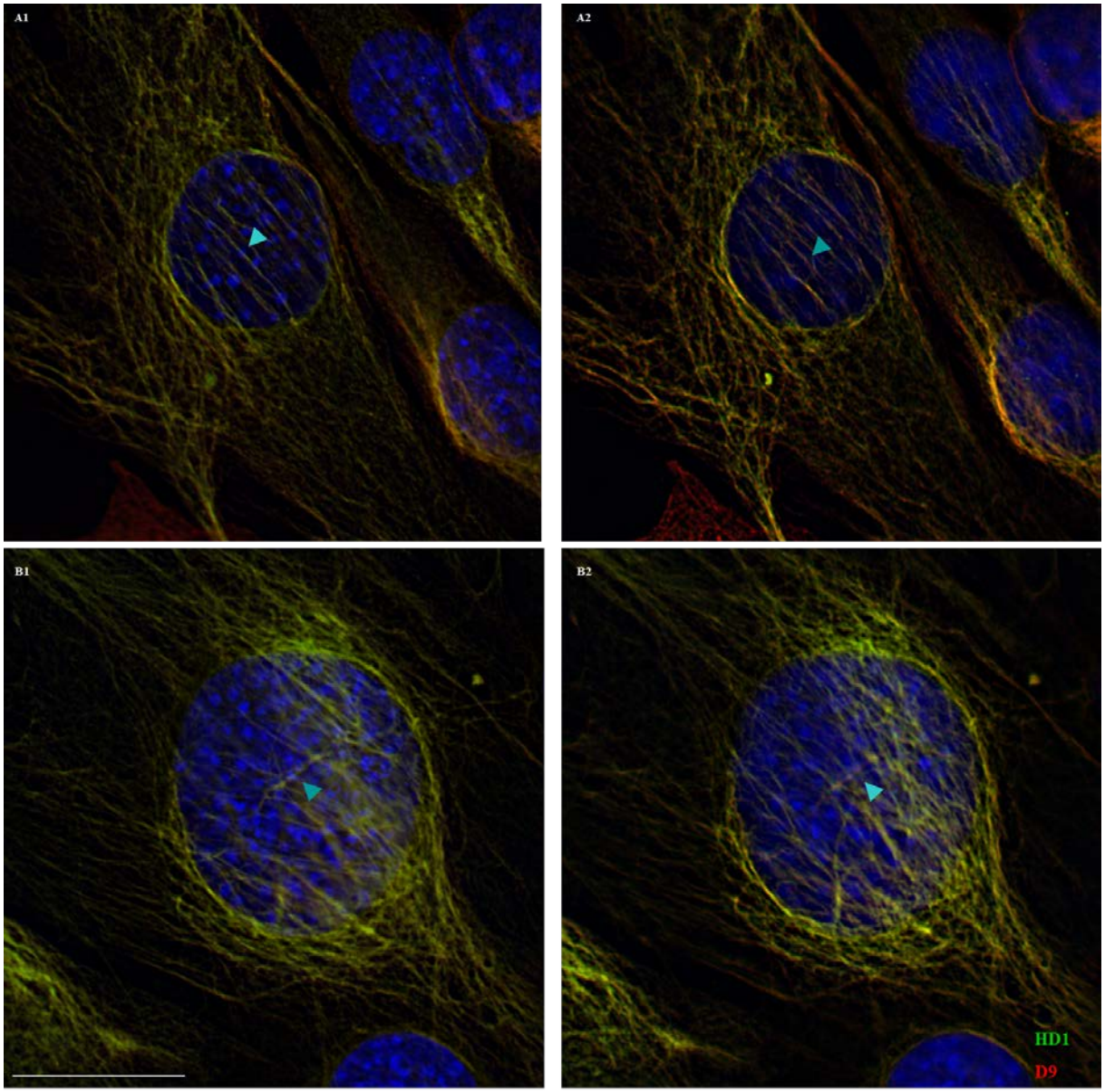

Figure 27. C2C12 +*hDes*WT cells images taken at different Z-height. Images of two cells **(A, B)** were taken at different Z-heights (200 nm distance) of the image stack. **(A1, B1)** An arrow points at the green (i.e., HD1-stained) filament; **(A2, B2)** the arrow points at the apparently corresponding red filament (i.e., D9-stained). Blue, DAPI; scale bar, 20 μm.

In the subsequent steps the images obtained by wide field microscopy in a stack of slides were analysed by comparing neighbouring images in a stack. Namely, in figure 27 two examples

were given (A and B, two images of each) with the apparently same filaments stained predominantly with HD1 (green signals, arrows in A1 and B1) or D9 (red signals, arrows in A2 and B2). One should also point out that, though the D9 epitope is located in the tail domain (figure 7), and the HD1 epitope is located in the head domain (figure 9). The problem is further discussed in more detail in section 4.1.2.

*3.3.2 hDes*E245D *is largely integrated into the endogenous desmin filaments*

In the following experiments, the same type of analyses was performed on C2C12 +*hDes*E245D cells. As it can be seen on figure 28A (1-3), *hDes*E245D was predominantly integrated into the endogenous filaments. The rate of transfection and expression of *hDes*E245D was similar to that of the *hDes*WT (over 70%). Nevertheless, unlike the *hDes*WT, in several instances, predominantly in *hDes*E245D-trainsiently transfected C2C12 cells one could see a very bright, diffuse desmin staining (both with HD1 and D9, figure 28B 1-3). Such result indicates that, although the previous *in vitro* and *in vivo* studies have found *Des*E245D to have no effects on the filament formation in SW13 cells (Bär et al., 2005b) it might still negatively affect the desmin IF network on a rare occasion in special cell systems.

In addition to the analyses of the effects of the mutant desmin on the endogenous desmin IF network, the vimentin IF system in C2C12 +*hDes*E245D cells was also analysed by ICC. As it can be seen in figure 28C (1-3), endogenous vimentin (stained with Vim3B4 antibody) colocalised well with the transfected (i.e., HD1-stained) *hDes*E245D protein. The staining and colocalisation pattern of HD1 and Vim3B4 in these cells resembled that of HD1 and D9. Thereby, one could finally conclude that the effects in C2C12 cells stably expressing *hDes*E245D largely reflect those in vimentin- and desmin-free SW13 cells.

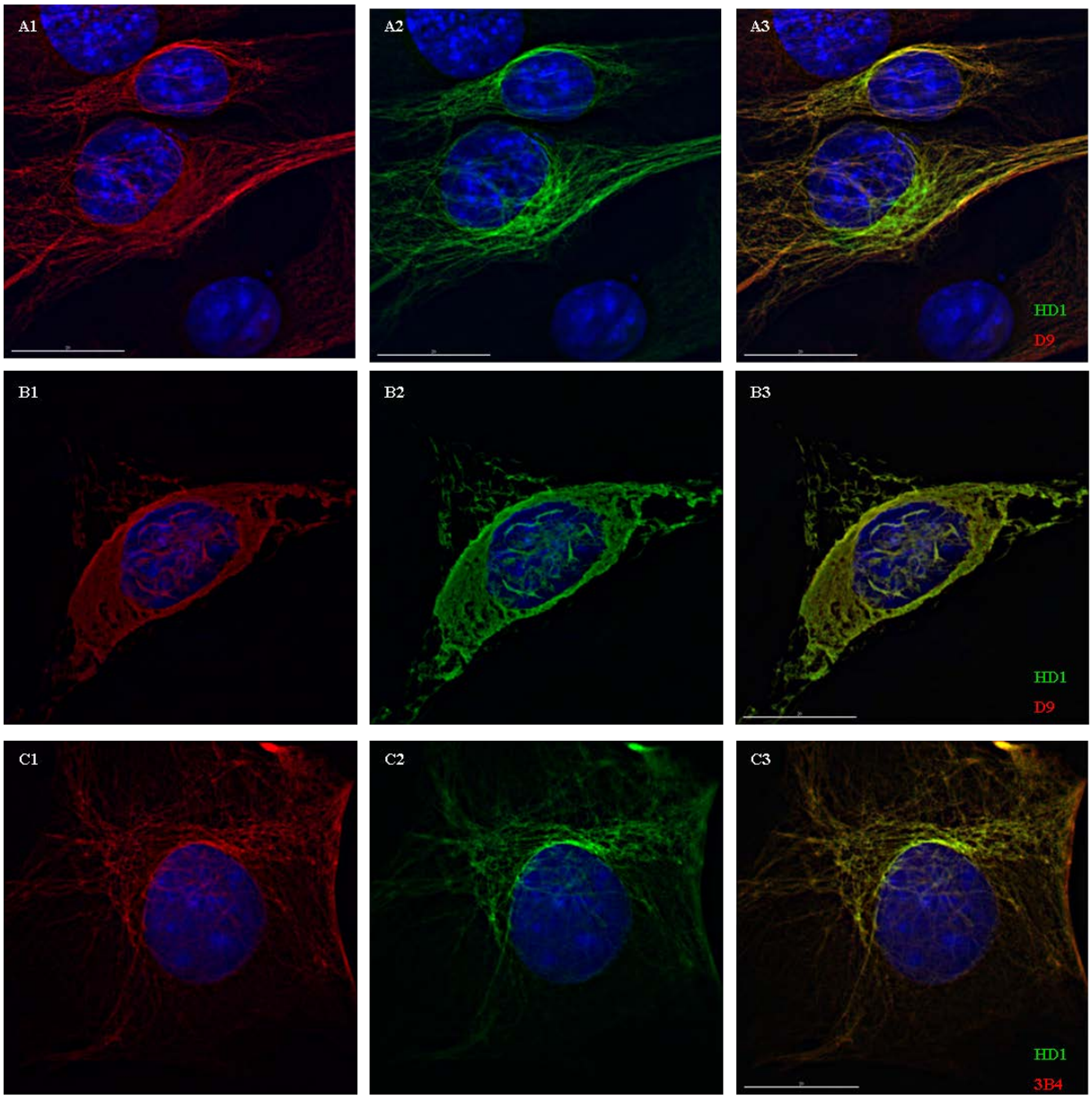

Figure 28. C2C12 +*hDes*E245D cells stained with HD1, Vim3B4 and D9 antibodies. *hDes*E245D-transfected cells stained with HD1 (green, **A2, B2 and C2**) and D9 (red, **A1 and B1**) or Vim3B4 (red, **C1**). **(A3–C3)** Merge. Blue, DAPI; scale bars, 20 μm.

3.3.3 hDesR350P is asymmetrically distributed in C2C12 cells

The second desmin mutation analysed, i.e., R350P, had a much more complex phenotype in cells transfected with the constructs containing this desmin mutation. Namely, the observations made in various cells varied significantly with respect to the amount of the protein expressed or its distribution among small groups of cells or large populations. Therefore, as no rigorous complete statistical analysis could be made (which is discussed at greater length in section 4.2.2), I do outline this observation by presenting some examples of cells encountered under these conditions.

In the initial experiments with *hDes*R350P-transfected cells, the p163/7 vector was used. As the vector contained no resistance gene against any selection marker, it was cotransfected with a plasmid containing geniticin resistance (described in section 2.2.3). Already in the initial experiments, a large heterogeneity with respect to the amount of *hDes*R350P that the cells expressed was observed. A large majority contained weak, diffuse traces of HD1 staining throughout the cytosol (figure 29A) or local accumulations of the HD1 signals (figure 29b). Considering the previously described phenotype of the mutant in SW13 cells (Bär et al. 2005a), one could have expected such a result. However, a fraction of cells contained HD1-stained filaments (i.e., *hDes*R350P) which fully or largely colocalised with the endogenous desmin filaments (figure 29C). As a matter of fact, in a few rare cases, as shown on figure 29C, the HD1-stained filaments were almost indistinguishable from those in *hDes*WT-transfected cells. Namely, the structure and pattern of those filaments in some cases resembled that of HD1 staining in C2C12 cells transfected with the *hDes*WT construct (compare with figure 26).

The same observations was made with C2C12 cells stably expressing *hDes*R350P (cloned in the pHβAPr-1-neo vector, figure 30). However, in this case we frequently observed HD1-possitive cells with a completely collapsed desmin IF network, mainly around the cell nucleus (figure 30A). Another frequent observation was that pairs of neighbouring cells, one expressed distinctly different amounts of *hDes*R350P than the other. In some cases, the cell expressing a higher amount of *hDes*R350P (B2, HD1-stained) seemed to have a similar or even higher amount of total desmin (figure 30B1, D9-stained). Both of the cells that contained higher and lower amounts of *hDes*R350P had a punctuated HD1 (but also to some extent D9) staining patterns. However, in some cases the *hDes*R350P appeared to have been largely integrated into the endogenous IFs of one of the cells (figure 30C) whereas the other one contained a predominantly weak, punctuated HD1-staining pattern. Interestingly, as shown in figure 30c, the cell containing higher amounts of (apparently IF-incorporated) *hDes*R350P also had a lower amount of total (i.e., D9-stained) desmin.

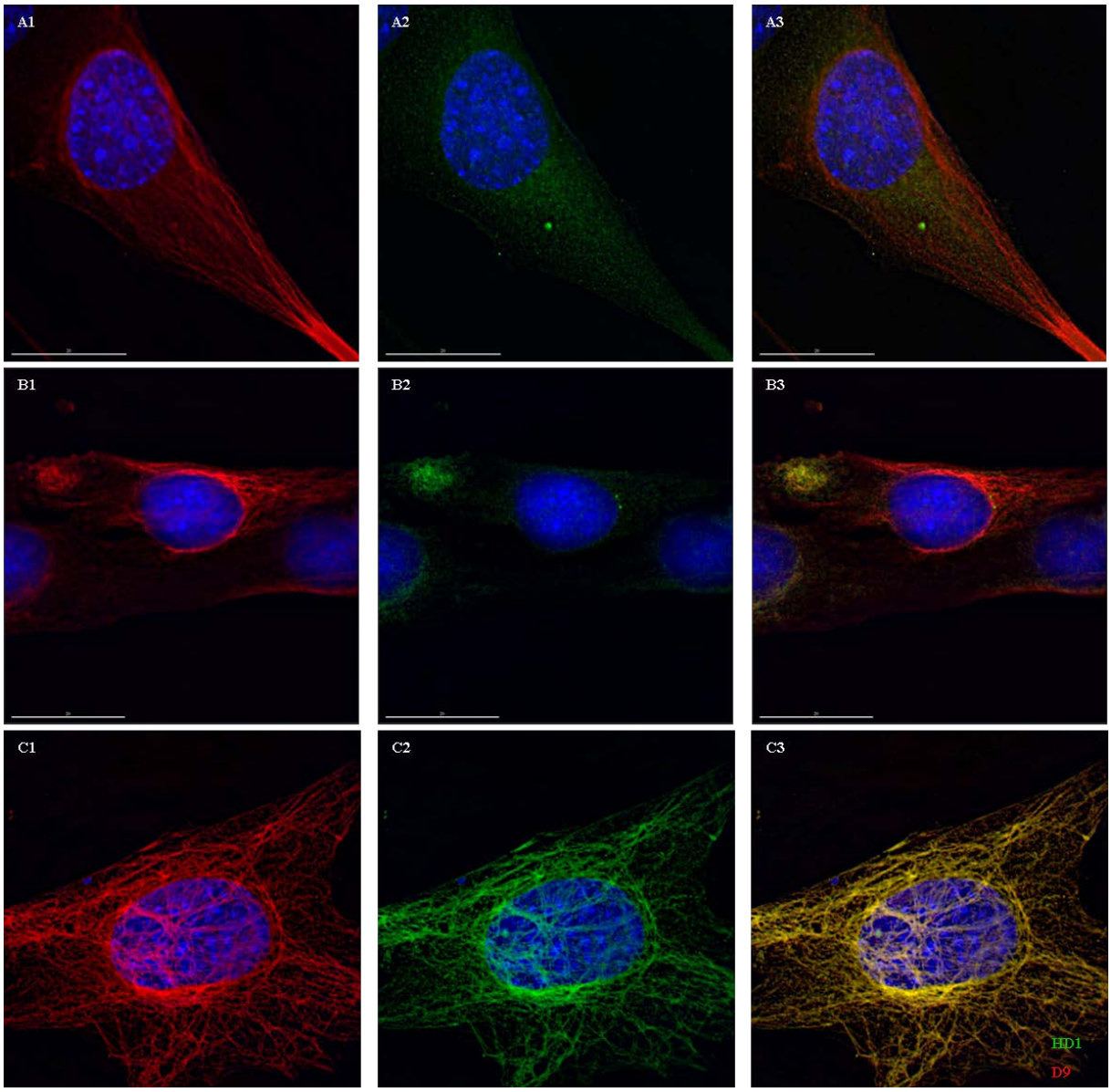

Figure 29. C2C12 +*hDes*R350P (p163/7) cells stained with HD1 and D9. Three examples of cells which have **(A)** which contained large amounts of diffuse *hDes*R350P throughout the cytosol, **(B)** cells where *hDes*R350P is largely accumulated in one part of the cell, or **(C)** cells with *hDes*R350P appeared to be integrated into their endogenous desmin filaments. **(A1-C1)**: red, D9; **(A2-C2)**: green, HD1; **(A3-C3)**: merge; blue, DAPI; scale bars, 20 μm.

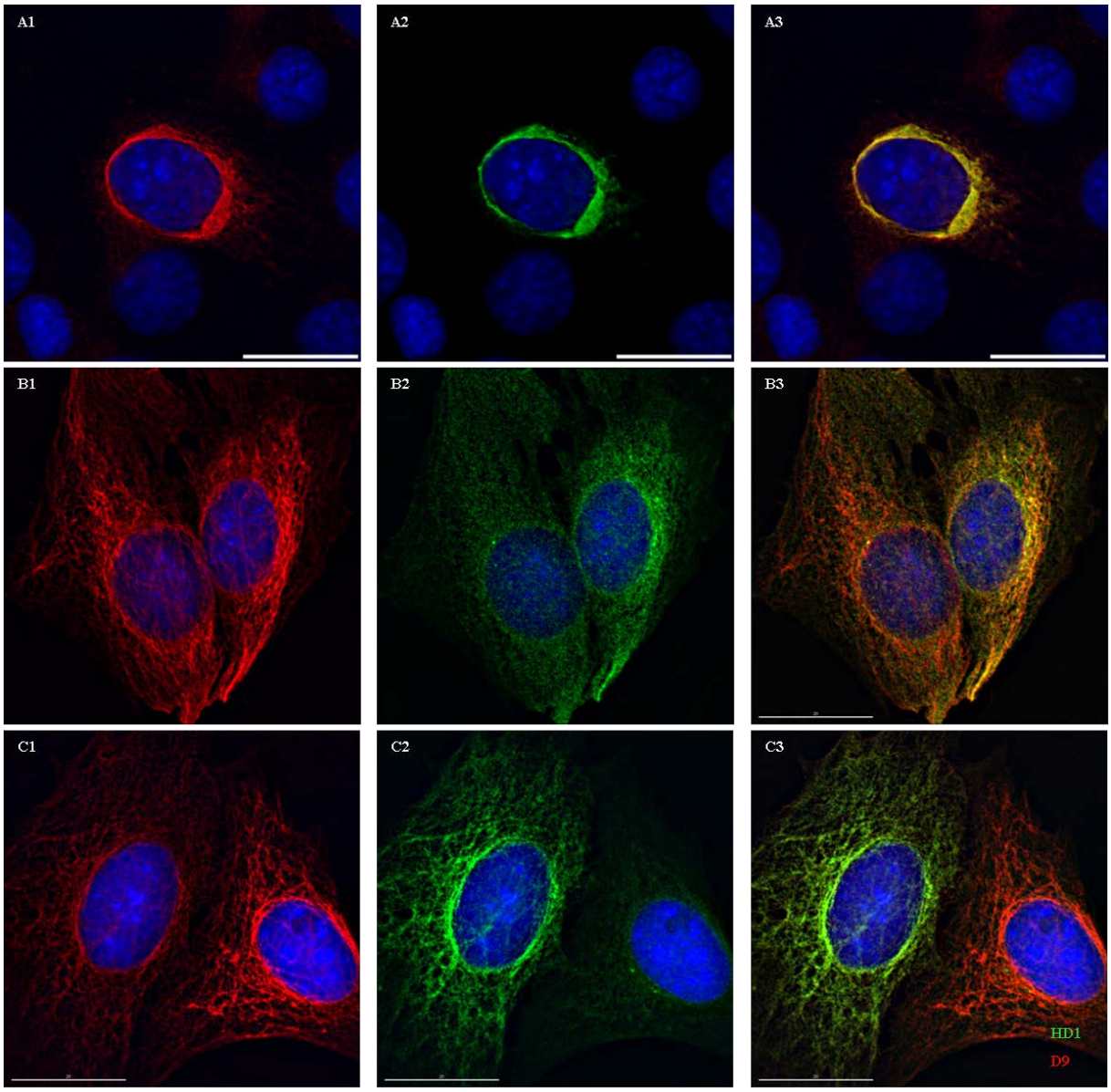

Figure 30. C2C12 +*hDes*R350P cells stained with HD1 and D9. Examples of cells with **(A)** an apparent collapse of the desmin IF network around the nucleus and somewhat **(B)** asymmetrical distribution of *hDes*R350P in close neighbouring cells. In some cases **(C)** the asymmetry in *hDes*R350P between neighbouring cells was far more apparent **(A1-C1)**: red, D9; **(A2-C2)**: green, HD1; **(A3-C3)**: merge; blue, DAPI; scale bars, 20 μm.

In the subsequent analyses, the vimentin network has been looked at in C2C12 +*hDes* *hDes*R350P cells (figure 31). Similarly to the previous observations one could find pairs of cells with distinctly different *hDes*R350P expression (figure 31A, from the cells transfected using the p163/7 vector). In this particular case, vimentin distribution was also found to be different in cells expressing different amounts of *hDes*R350P. Once the analyses were repeated on cells stably expressing *hDes*R350P (transfected using the pHβAPr-1-neo vector) *hDes*R350P was found to be fully incorporated into the endogenous filaments (figure 31B), as well as asymmetrically distributed in pairs of neighbouring cells (in case of figure 31c where

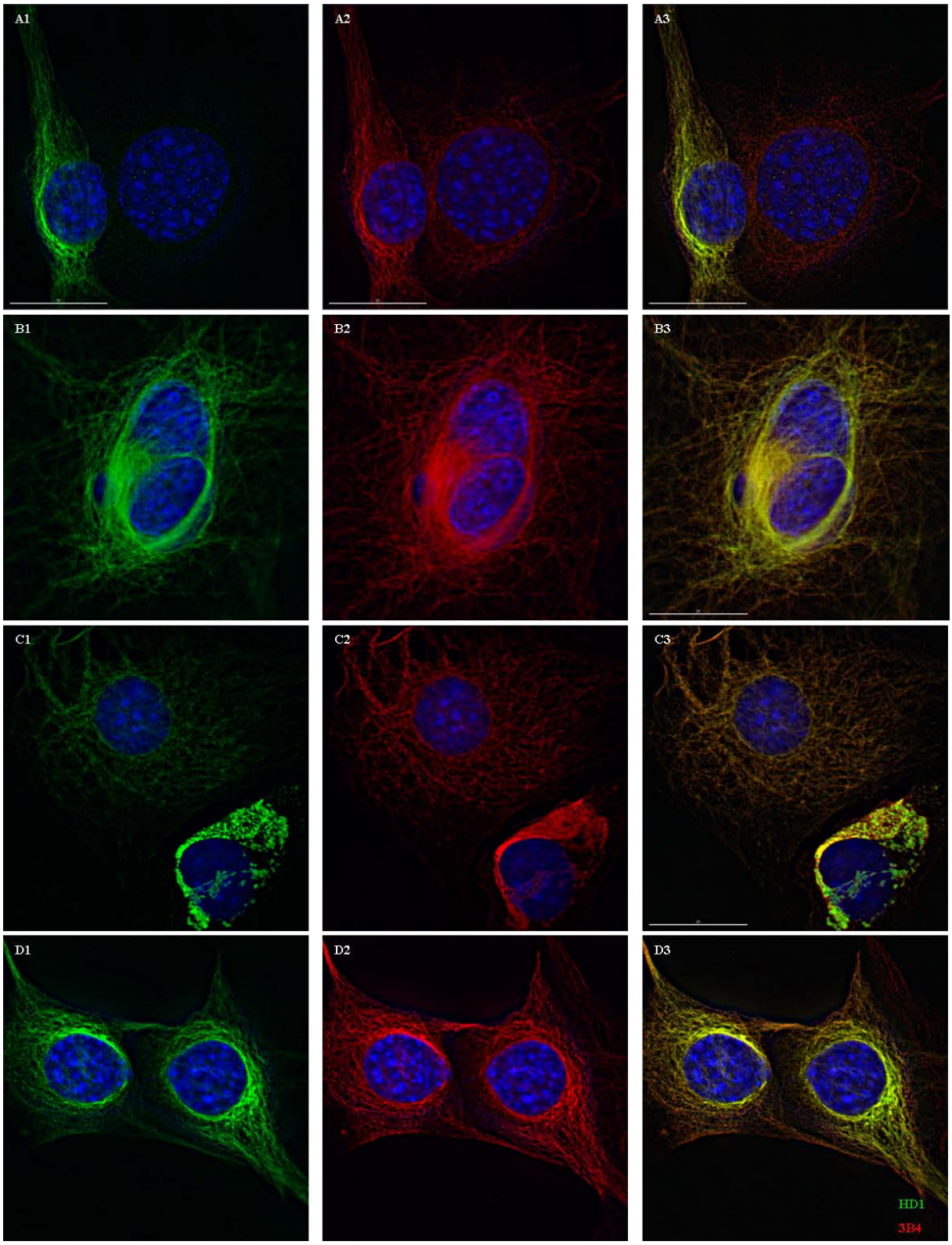

Figure 31. C2C12 +*hDes*R350P cells stained with HD1 and Vim3B4. C2C12 cells transfected with *hDes*R350P, either cloned in **(A)** p163/7 or **(B-D)** pHβAPr-1-neo. Examples of cells with asymmetric (A and C) or a similar (D) distribution of *hDes*R350P. Example (B) depicts a cell with a very efficiently integrated *hDes*R350P into the endogenous IF network. **(A1-D1)**: red, desmin (D9); **(A2-D2)**: green, HD1; **(A3-D3)**: merge; blue, DAPI; scale bars, 20 μm.

in one of the cells there was a complete collapse of the vimentin IFs). Finally, on a rare occasion pairs of neighbouring cells with a quite similar distribution of *hDes*R350P, as well as vimentin (figure 31D) were also observed.

Although the observation of asymmetrical distribution of *hDes*R350P in neighbouring cells was so far indicated only in the cases of pairs of neighbouring cells, such observation was also somewhat frequent in groups of cells. Namely, in cases when multiple cells were observed in a group there was also a high extent of heterogeneity with respect to the distribution of *hDes*R350P. For example, in some cases of groups (4 or more) of cells only one of them which contained some *hDes*R350P incorporated into the endogenous filaments was found (figure 32A and B). In some other cases, however, there were two cells per group which had such a phenotype (figure 32C). However, in several instances one could have also seen that several cells in a group had *hDes*R350P integrated into the desmin IFs (figure 32D).

In all the experiments discussed so far the double immunostaining ICC was performed by incubation with HD1 antibody following the same procedure with D9 or Vim3B4 antibodies. Therefore, to address the issue of possible epitope hindrance of one antibody by the other (discussed in section 4.1.1), the experiment was repeated on *hDes*R350P-transfected C2C12 cells by antibody incubation in a different order. This was done as in several instances previously the cells which had a stronger HD1-staining (such as in figure 30c or, to some extent, 30b) had a lower amount of D9 staining. However, once the ICCs in different order were performed, no significant effect of the antibody staining patterns with respect to the order that the incubations were performed was observed. In some cases, cells that had HD1-stained filaments (figure 33A), also had a stronger D9 staining compared to those around them which had no HD1-stained filaments, even though it was done after the incubation with the HD1 antibody. Therefore, in cases where D9 antibody incubation was done first, no clear epitope competition was observed as both antibodies appeared to stain the transfected and the endogenous desmin thoroughly (figure 33b and c).

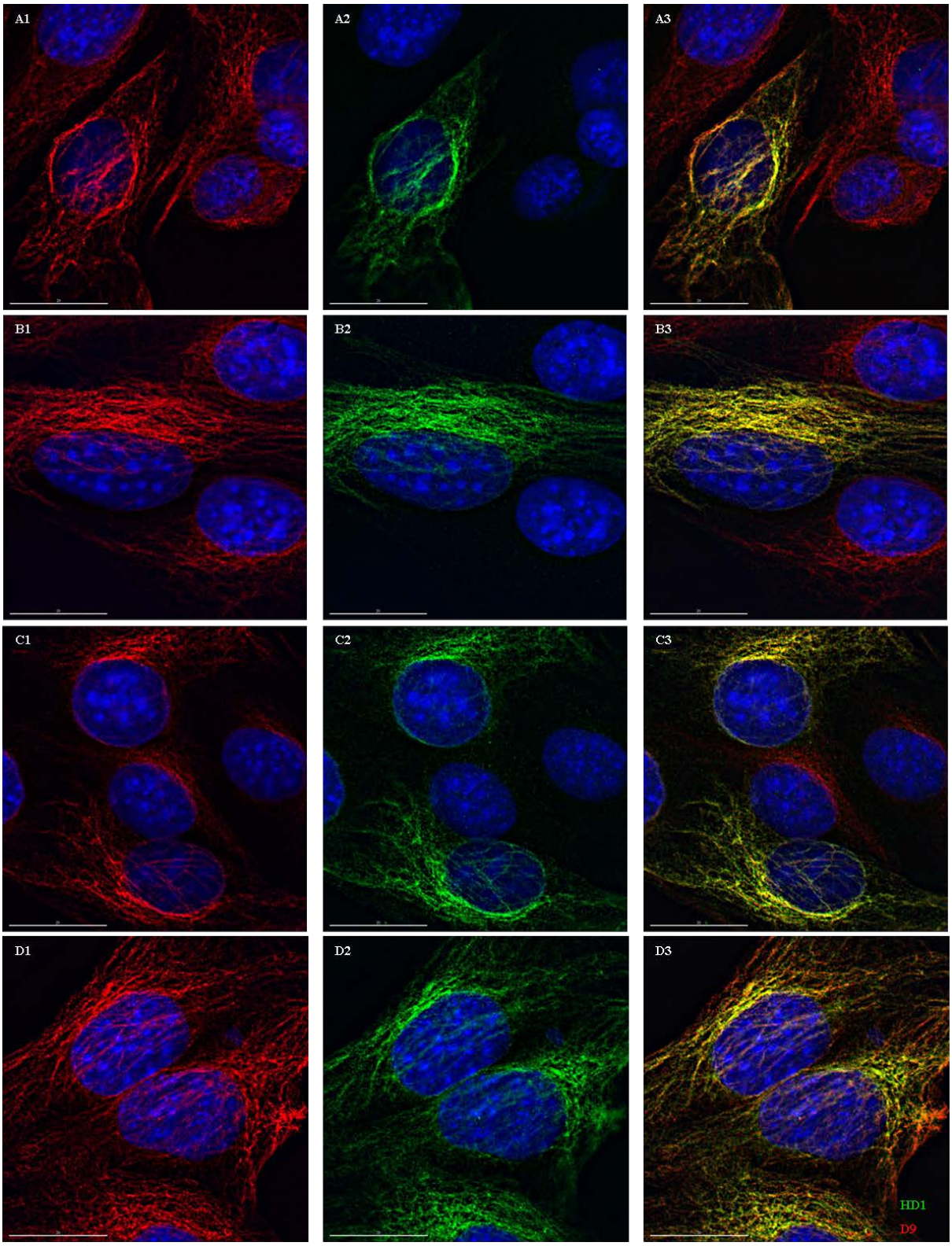

Figure 32. Groups of C2C12 +*hDes*R350P cells stained with HD1 and D9. Groups of C2C12 +*hDes*R350P cells: **(A, B)** examples of single cells with HD1-stained filaments in a group of 4 or 5 cells; **(C)** an example of two cells in a group with *hDes*R350P integrated into the endogenous filaments; **(D)** several cells in a group positive for filamentous HD1 staining. **(A1-D1)**: red, D9; **(A2-D2)**: green, HD1; **(A3-D3)**: merge; blue, DAPI; scale bars, 20 μm.

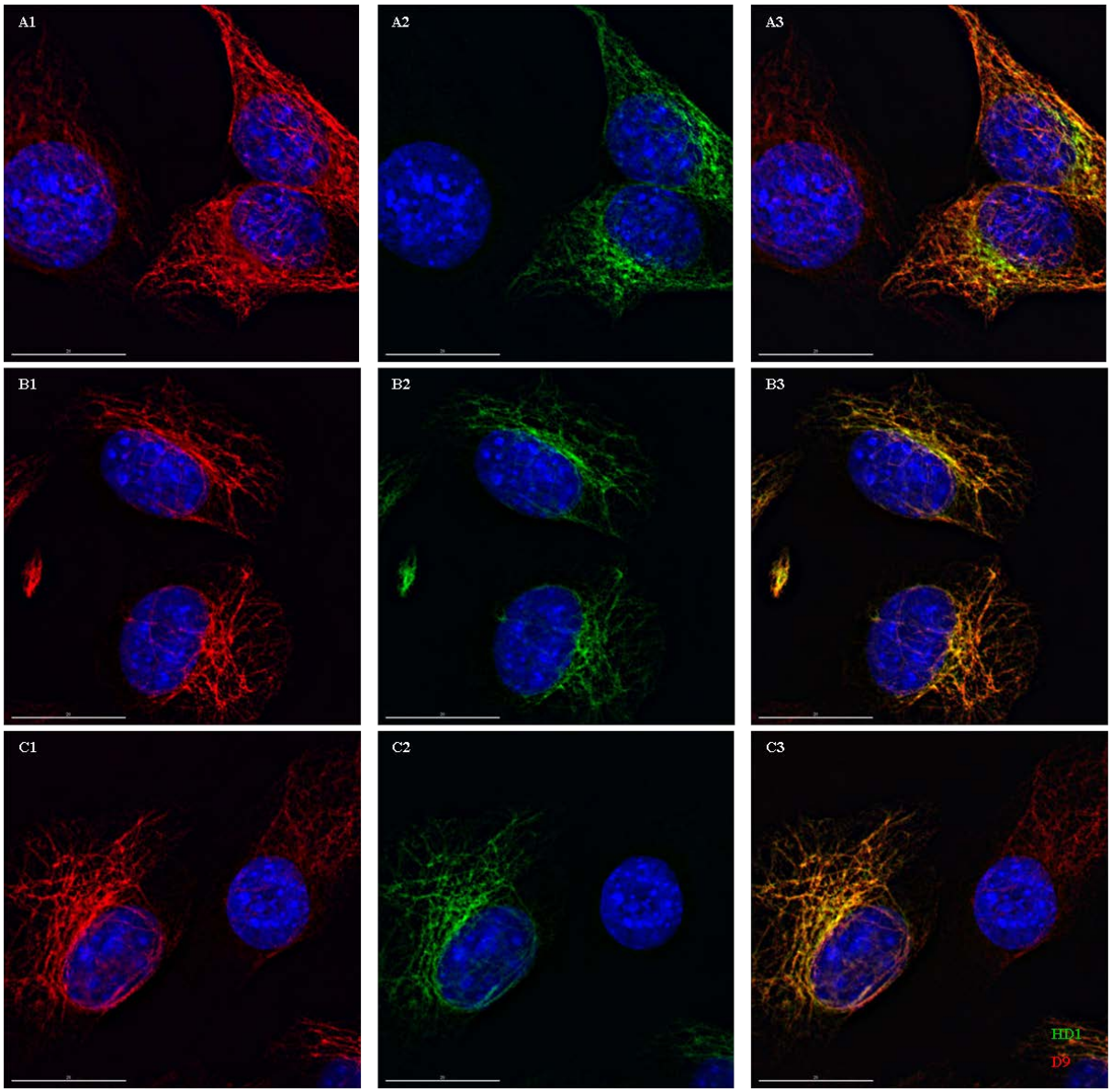

Figure 33. Images of C2C12 +*hDes*R350P cells stained with HD1 and D9 in a different order. Cells stained with a different order of antibody incubation. **(A)** HD1 incubation first, following D9 incubation; **(B, C)** First D9 and subsequently HD1 incubation was performed. **(A1-C1)**: red, desmin (D9); **(A2-C2)**: green, HD1; **(A3-C3)**: merge; blue, DAPI; scale bars, 20 μm.

3.3.4 Western blotting of the cell extracts revealed that the amount of hDesR350P in C2C12 transfected cells decreases during subsequent passages

So far the analyses of the C2C12 cells transfected with either *hDes*WT or mutant desmin proteins have been discussed with respect to the observations in the ICC. Such approach allowed for analyses of individual cells with respect to the expression level of the transfected protein as well as topological issues. In case of *hDes*R350P transfected cells such analysis was shown to be important as it allowed the delineation of the variable phenotypes that different cells exhibited. However, this approach lacks conclusive quantitative information on

how the mutant protein is expressed. Thereby, WB of the cell fractions (as in section 3.2.1) of all three *hDes*-transfected cell lines was performed with respect to their total and transfected desmin content in different fractions.

The results of the WB are shown in figure 34. In case of *hDes*WT- or *hDes*E245D-transfected cells, the amounts of both total (A) and transfected (B) desmin appeared similar between the two cell lines. C2C12 +*hDes*R350P cells, however, had somewhat lower amount of total desmin (a) and a significant amount of reduction in *hDes*R350P (figure 34B, compared to either *hDes*WT or *hDes*E245D). Such observation has been more pronounced with subsequent cell passaging, whereby by passage 10 or 12 the cells would contain only traces of *hDes*R350P (observations by microscopy, data not shown). Furthermore, this progressive reduction in the amount of *hDes*R350P expressed in these cells was also reflected in the WB whereby in higher passages (passage 8 after transfection) one could detect only traces of *hDes*R350P extracted in these cells (further described in section 3.4.1). Both *hDes*WT and *hDes*E245D on the other hand were stably expressed to a similar extent even after passage 10 as determed by WB (figure 34B).

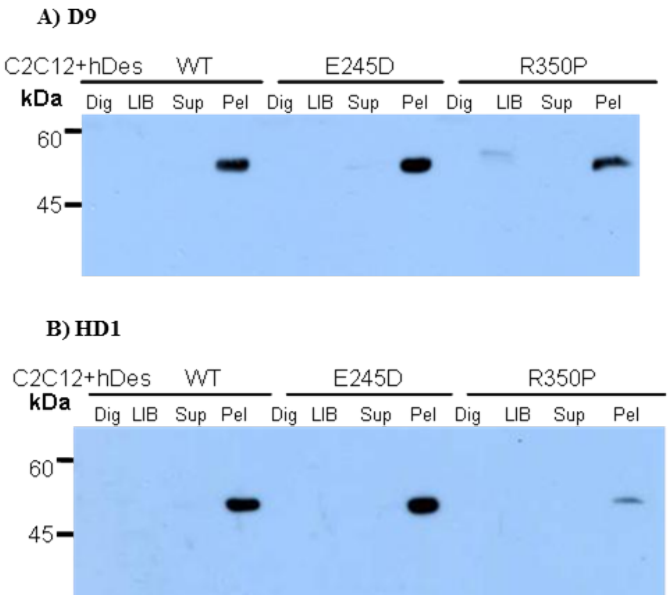

Figure 34. WB on C2C12 +*hDes*WT, *hDes*E245D and *hDes*R350P cell lines fractions with D9 and HD1. The total amount of desmin (A), as well as the amounts of transfected desmin (B) were analysed in fractions (Dig, LIB, Sup, Pel 1:2) of different C2C12 +*hDes* cell lines. Loading was scaled to 10 µg of protein in LIB of each sample.

3.3.5 mCherry-tagged hDesR350P is degraded by the C2C12 cells

In order to attempt to follow up on the observation of asymmetrical distribution of *hDes*R350P in different cells *in vivo*, we have cloned the gene into a vector with an mCherry located upstream (N-terminally) from the desmin insert site. Initially *hDes*WT has been cloned in the vector to analyse the effects of the mCherry tag on the IF protein itself. The initial observation (figure 35A) was that the mCherry-*hDes*WT gets fully integrated into the endogenous desmin filaments. However, a few cells contained what appeared to be small aggregates of the transfected mCherry-tagged desmin (figure 35B). After the subsequent cell passaging the amount of cells containing such desmin accumulations was increasing whereby 10 passages after transfection almost all cells would contain predominantly such mCherry accumulations (data not shown).

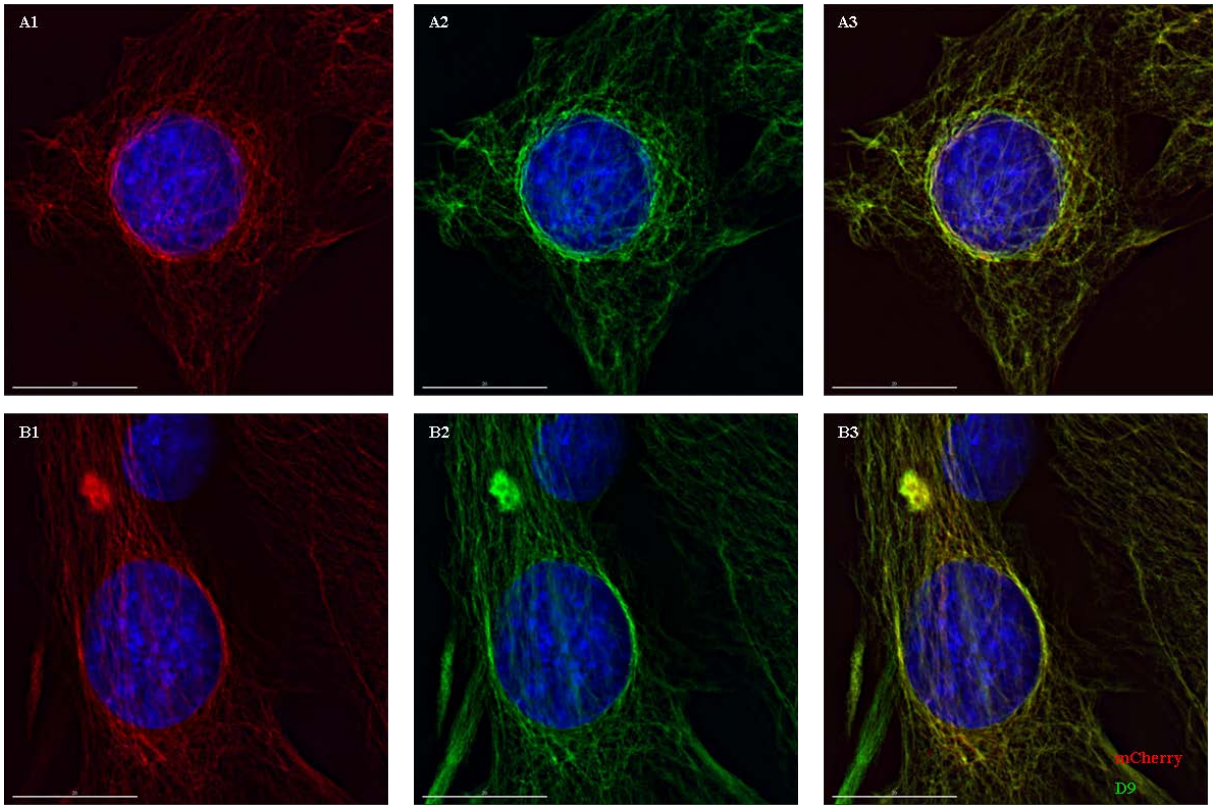

Figure 35. C2C12 +mCherry-*hDes*WT cells stained with D9. (A) mCherry-*hDes*WT is fully integrated into the endogenous desmin IFs; **(B)** an example of a cell where, even though the mCherry-*hDes*WT is predominantly integrated into the endogenous desmin filaments, an accumulation of it at one site could have been observed. **(A1, B1)**: red, mCherry-*hDes*WT; **(A2, B2)**: green, D9; **(A3, B3)**: merge; blue, DAPI; scale bars, 20 μm.

In a next step, we generated an mCherry-tagged *hDes*R350P plasmid in order transfect cells for live cell imaging. In each transfection experiment, some cells were found to express the mCherry-tagged *hDes*R350P, which appeared to be integrated into the endogenous filaments.

However, in all cases the cells either did not divide or most probably degraded the mCherry-tagged desminR350P as the signal was lost after several hours of live cell imaging (data not shown). In order to try to determine what is causing the problem, cells stably expressing mCherry-*hDes*R350P were collected and fractionated. As it can be seen on the WB of their pellet fractions (figure 36), the mCherry-*hDes*WT appears to be degraded whereby only one band in blot stained with an mCherry antibody is detected. The band also corresponds to one band in either D9 or HD1 blots. In case of the mCherry-tagged *hDes*R350P, no signal was detected with the mCherry antibody and only one band, of approximate size of the *Des*R350P, was detected with D9 but not HD1 antibody. Note that the amount of the transfected, mCherry-tagged *hDes* (the top lane in all three blots) was considerably higher than the amount of the endogenous desmin (the smallest band located above the 56kDa band).

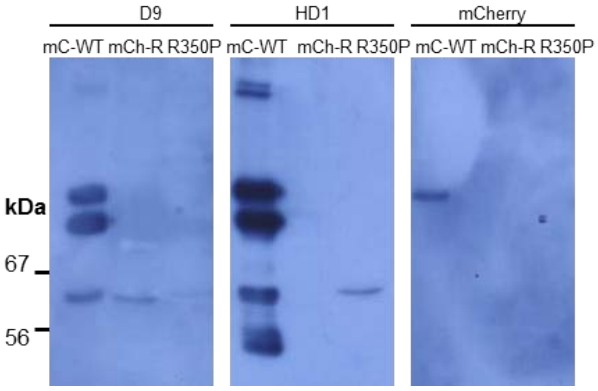

Figure 36. WB on pellets of C2C12 +mCherry-*hDes*WT and *hDes*R350P. Loading: pellets of the C2C12 +mCherry-*hDes*WT (mC-WT) or +mCherry-*hDes*R350P (mCh-R), as well as recombinant desminR350P (R350P). Antibodies: D9, HD1, α-mCherry.

*3.3.6 Whereas hDes*WT *forms irregular filaments in Vim$^{-/-}$ fibroblasts, hDesR350P forms aggregates*

In addition to transfections of the *hDes*WT and desmin mutant genes into C2C12 cells, one additional transfection control has been performed. Namely, the observed results, especially concerning the integration of *hDes*R350P into endogenous IFs, did not correspond to some previous observations (Bär et al. 2005a). Thereby the transfections with *hDes*WT and *hDes*R350P were performed in a cell line fully devoid of any IF proteins, such as Vim$^{-/-}$. These fibroblasts do not contain any desmin or vimentin IF proteins thereby being similar to the SW13 cells in which the previous experiments have been performed. However, in contrast to SW13 cells, which do not support the establishment of a well-spread desmin cytoskeleton, Vim$^{-/-}$ fibroblasts are suitable for generating an optimal desmin system (such as in Sharma et al. 2009). The test would have also demonstrated to what extent is the observed heterogeneity

of *hDes*R350P filament integration cell type- or vector- specific (previous experiments have been done using the p163/7 vector).

As it can be seen on image 37A, *hDes*WT was able to form short filaments in the Vim$^{-/-}$ fibroblasts but they were highly irregular (compare with C2C12 cells, figure 26). Such result indicates that the endogenous IFs (constituted of either vimentin or desmin) might be crucial for formation of a proper IF network in a cell transfected with *hDes*WT. However, in case of *hDes*R350P, all of the HD1- and D9-possitive cells contained only aggregates of the signal as well as some punctuate structures in the background. No case of filament formation was observed thereby being in agreement with the previous *in vitro* data (Bär et al. 2005b) indicating that *hDes*R350P alone is not able to form IFs.

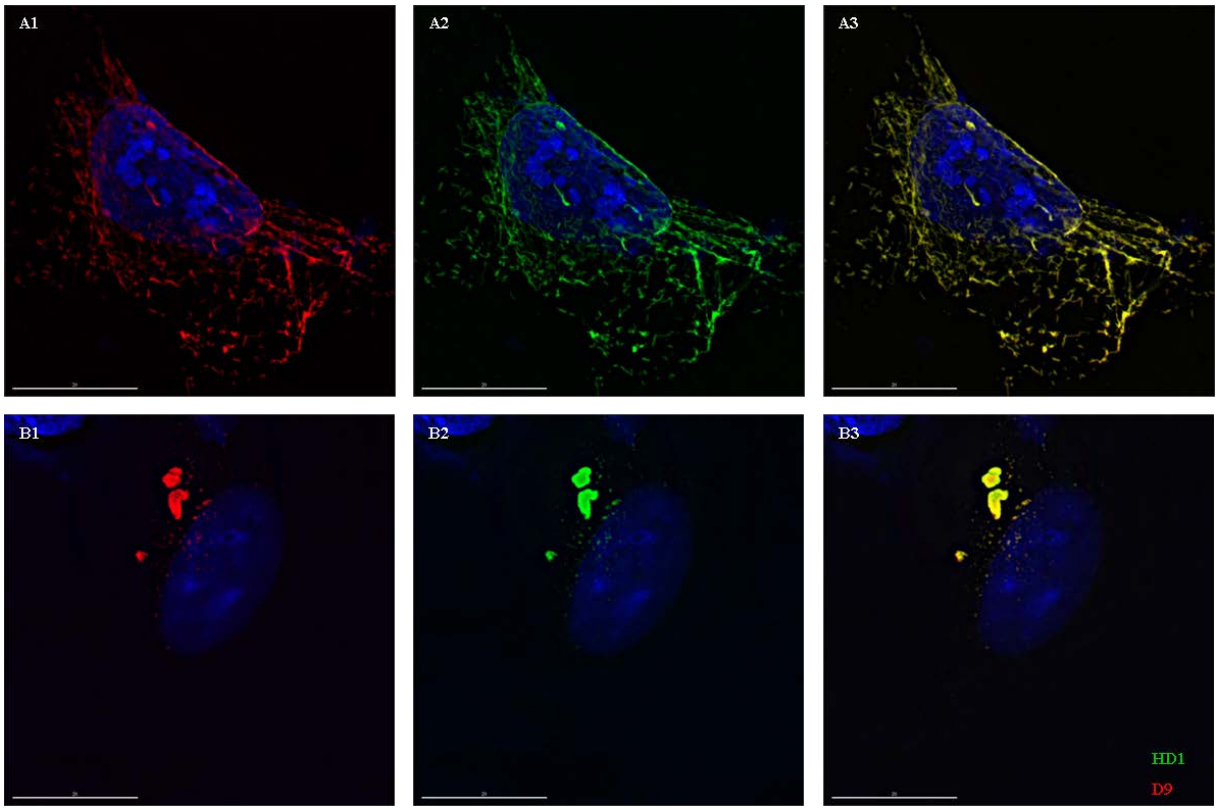

Figure 37. Vim$^{-/-}$ fibroblasts transfected with (A) *hDes*WT and (B) and *hDes*R350P. The cells were stained with both D9, red **(A1, B1)** and HD1, green **(A2, B2)**. **(A3, B3)** Merge; blue, DAPI; scale bars, 20 μm.

*3.3.7 mDes*WT *does not co-immunoprecipitate with the hDes*

In the final stage of the analyses of the *hDes*-transfected C2C12 cell lines, *hDes* variants were immuneprecipitated (IPed) from the transfected cells and analysed if the endogenous *mDes* would have coimmunoprecipitated with the WT or mutant desmin protein. The cells have been fully lysed with a RIPA buffer and subsequently the IPs were analysed on WB with HD1

but also mouse desmin-specific antibody, MD2 (as described in section 2.2.9). The WB with HD1 antibody (figure 38A) has demonstrated that the IP of the *hDes* was successful in case of *hDes*WT and *hDes*E245D. Do note that, due to the very low amount of the *hDes* in case of these cells, the HD1 WB was performed with a higher concentration (1: 2000 dilution) of the antibody. However, no *hDes*R350P was detected in the corresponding IP sample. Whereas the amounts of the *hDes*WT and *hDes*E245D were similar in the RIPA samples the amount of *hDes*R350P was significantly lower. No protein was immunoprecipitated in case of the untransfected C2C12 cells (data not shown).

However, the endogenous *mDes* was coimmunoprecipitated from either of the samples (figure 38B) including the C2C12 +*hDes*WT cell extract. This result indicates that although m- and *hDes* do appear to form heteropolymers (figure 26) once the cells are extracted in RIPA buffer the two desmin-species are not found in the same structures.

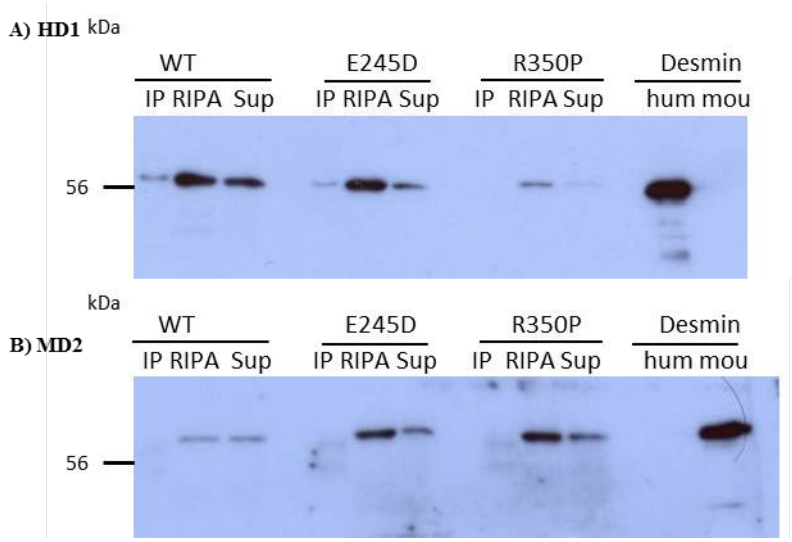

Figure 38. WB of the *hDes* IP in C2C12 +*hDes*WT, *hDes*E245D and *hDes*R350P cells. In all cases a sample of the input was loaded (RIPA) corresponding to 20 000 cells, the eluted sample (IP, 5-fold concentrated) as well as the unbound material (Sup, also corresponding to the volume of 20 000 cells). Recombinant *Des* (human and mouse, 20 ng each) were loaded in addition. The membranes with samples were stained with **(A)** HD1 (1: 2000) and **(B)** MD2 (1: 200) antibodies.

3.4 Differentiation of the human desmin transfected C2C12 cells

*3.4.1 The amount of transfected desmin*R350P *reduces upon differentiation of C2C12 cells*

A major aim of the study was the analysis of the effects of the two mutants on myoblast differentiation. Therefore C2C12 cells were employed as they are an often used cell system

for investigation of muscle cells differentiation. As it has been previously shown (section 3.2), these cells could be successfully induced to differentiate by culturing them in a medium containing a low amount of serum (but without the selection maker in this case, which is further discussed in the section 4.3.1). However, there have been previous reports of some lamin A mutants responsible for one type of myofibrillar myopathy to inhibit C2C12 differentiation (Favreau et al. 2004). Therefore, as there was a possibility that expression of the desmin mutants would delay differentiation in these cells, we have also done the experiments with BIX-01294 (bix) in DM in parallel. This compound is an inhibitor of G9a methyltransferase (Kubicek et al. 2007) which is an enzyme that has been previously shown to methylate MyoD and thereby prevents myoblast differentiation (Ling et al. 2012a). Thereby, in addition to the experiments with DM, C2C12 cells were also differentiated using BIX-01294 in addition to the DM (DM +bix).

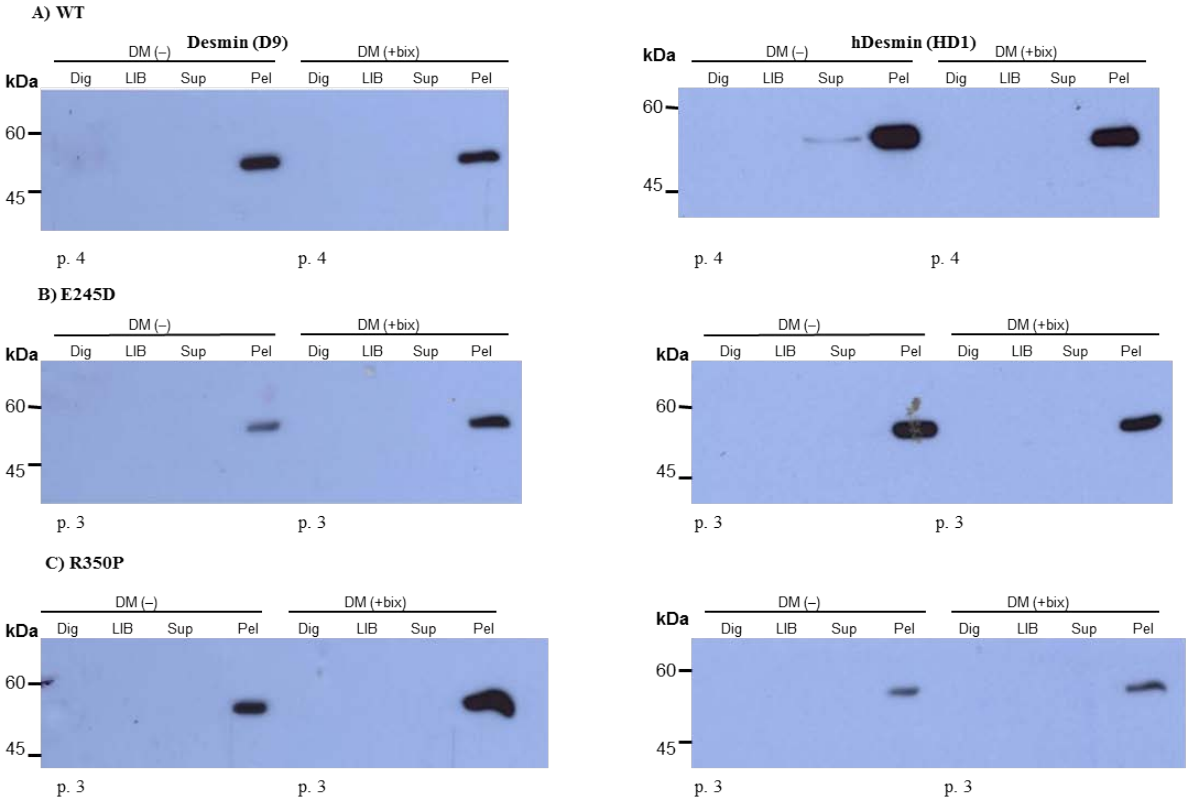

Figure 39. WB with D9 and HD1 on cell fractions of C2C12 +*hDes* variants (DM) in early passages. Cell fractions (Dig, LIB, Sup, Pel 1:2) of C2C12 cultured in DM only or with BIX-01294 of +*hDes* **(A)** WT passage 4; **(B)** *hDes*E245D passage 3; and **(C)** *hDes*R350P passage 3. Loading: 8 µg of protein per LIB.

In the first experiments with three cell lines C2C12 +*hDes*WT, E245D and R350P the cells were differentiated (in DM only, DM (-), or +bix) several passages after transfection they

were subjected to the fractionation procedure. The samples obtained were then loaded on gels and used for a WB with D9 and HD1 antibodies (figure 39). In case of *hDes*WT-transfected cells (figure 39A), the amounts of both total (D9) and *hDes*WT (HD1) desmin were higher in DM (-) than in DM (+bix) samples. Note that under the same incubation time with the film the HD1 signals were more intense than the D9 ones. In case of *hDes*E245D, the total amount of desmin (D9) was higher in (+bix) than DM (-) samples (figure 39B), whereas the amount of the transfected protein (HD1 blot) was again higher in (+bix) compared to the DM (-) cells. The same analysis was made for the C2C12 +*hDes*R350P cells (figure 39C). The most interesting observation was that the amount of transfected desmin was distinctly lower in case of these cells, as compared to either of the two other cell lines. Nevertheless, the total amount of desmin in +*hDes*R350P cells appeared the same or higher as compared to the case with the other cell lines (+*hDes*WT and *hDes*E245D, respectively).

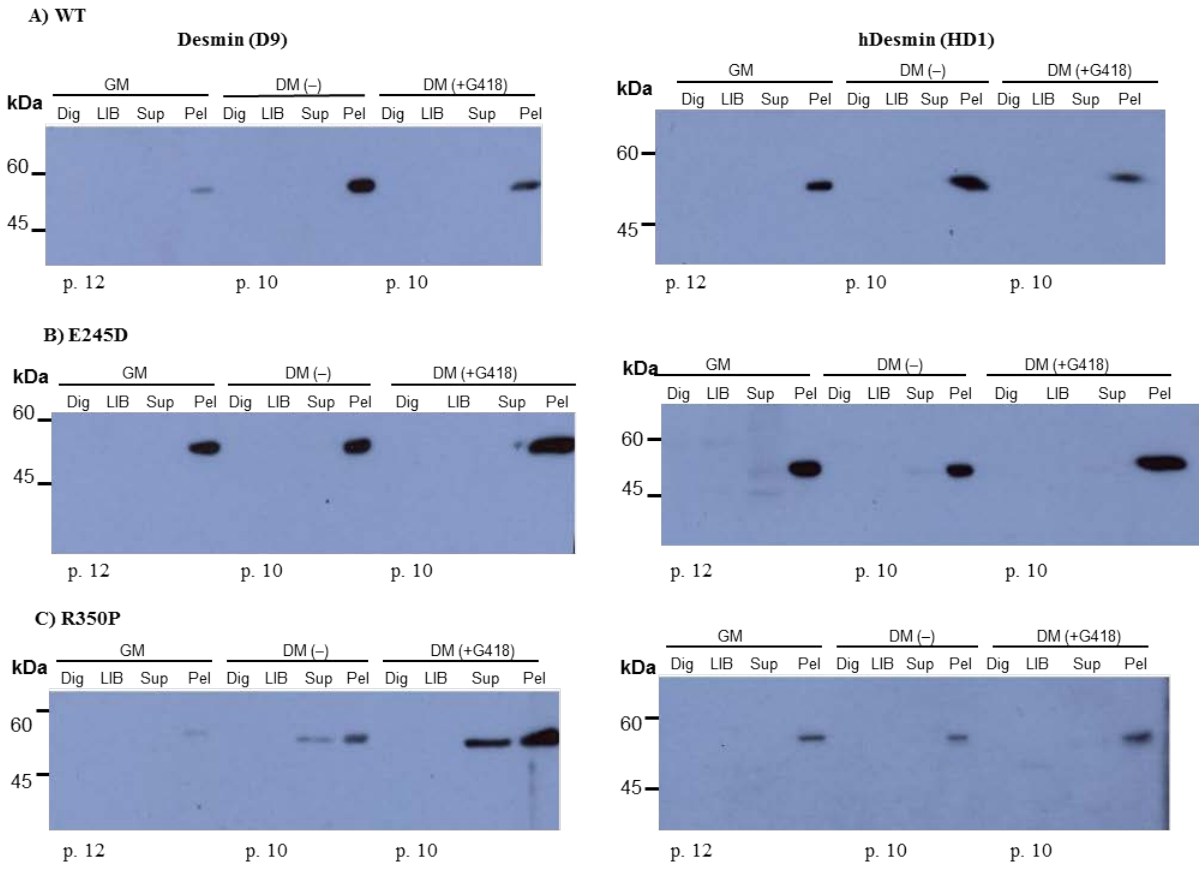

Figure 40. WB with D9 and HD1 on cell fractions of C2C12 +*hDes* (GM, DM) cells in later passages. Cell fractions (Dig, LIB, Sup, Pel 1:2) of C2C12 cultured in GM, DM (-) or with G418 of +*hDes* **(A)** WT, **(B)** *hDes*E245D and **(C)** *hDes*R350P. Loading: 10 µg of protein per LIB.

To determine if these effects persist in subsequent passages the cells were again differentiated and fractionated after passage 10. However, the cells in this case were also differentiated with G418 selection marker in DM in order to attempt to prevent the apparent loss of *hDes*R350P from the cells during the differentiation procedure. The WBs were again performed with the fractions of cells cultured in DM only or with G418, as well as in a standard GM (figure 40). The total amount of desmin in C2C12 +*hDes*WT cells has drastically increased upon differentiation but it was lower in DM (+G418) than in cells incubated in DM only (figure 40A). Interestingly, this was also the case with *hDes*WT (HD1 blot). In case of +*hDes*E245D cells, the total amount of desmin as well as the amount of the transfected protein was similar between GM and DM cells and significantly higher in DM (+G418) cells (figure 40B). Finally, the amount of *hDes*R350P was lower in all three cases (GM, DM only or with G418). The total amount of desmin (D9) was higher in DM (-) than in GM cells and the highest in DM (+G418) cells (figure 40c).

3.4.2 C2C12 cells expressing desmin mutants largely fail to fuse

The WB data so far reflected the distribution of the total amount of desmin protein in the whole population of cells per dish. Although such analysis does aid in our understanding of the distribution of total and the mutant desmin proteins it falls short in clarifying the actual state of the filaments in different cells in a population. In order not to overstate the outcome of these analyses they needed to be correlated to the observations on individual cells. Thereby, in the follow-up experiments the cells were analysed by ICC by staining the differentiated cells with HD1 and D9.

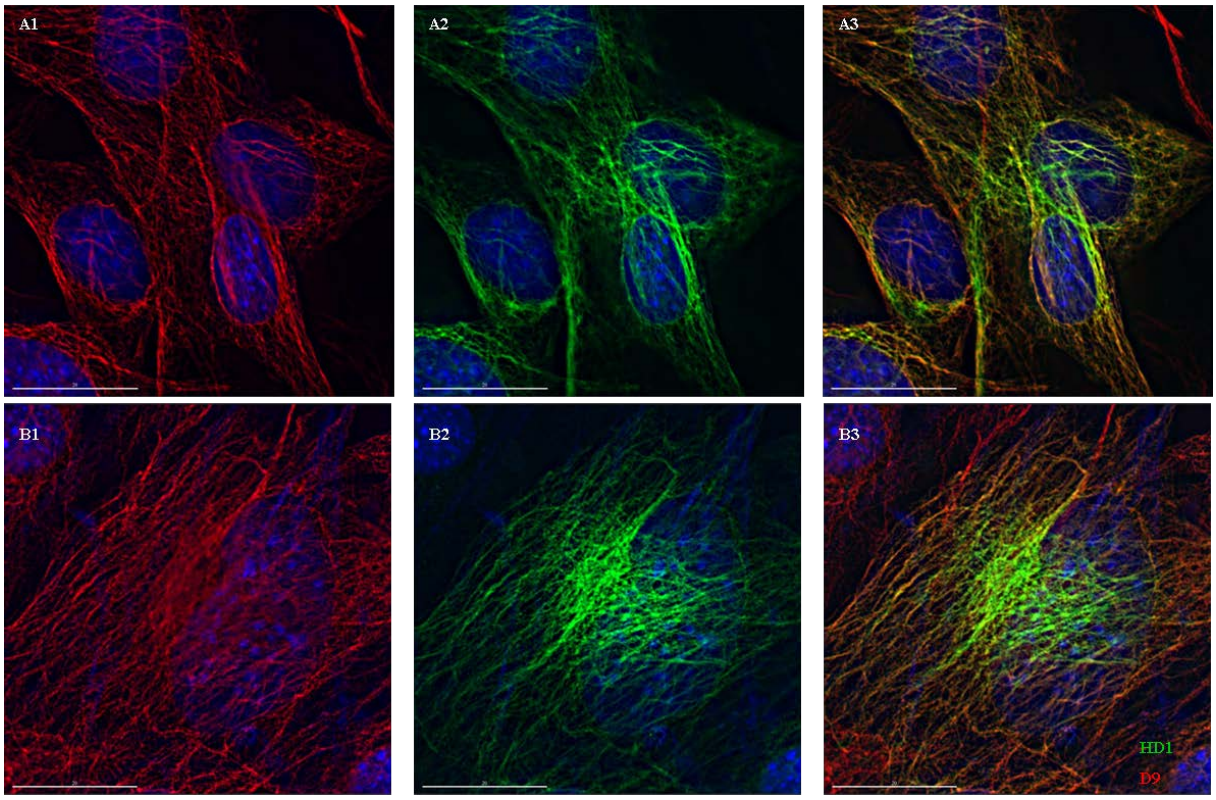

Figure 41. C2C12 +*hDes*WT (DM) stained with HD1 and D9. The cells differentiated with **(A)** BIX-01294 or **(B)** G418. The cells were stained with both D9, red **(A1, B1)** and HD1, green **(A2, B2)**. **(A3, B3)** Merge; blue, DAPI; scale bars, 20 µm.

Some examples of C2C12 +*hDes*WT (DM) are given in the figure 41. When cells are differentiated in DM only or DM with BIX-01294 (figure 41A) the cells undergoing fusion still predominantly retained the *hDes*WT. Similarly, if the cells were differentiated in presence of G418 (figure 41B) most of the multinucleated cells still expressed the *hDes*WT.

Once C2C12 +*hDes*E245D cells were induced to differentiate the situation was somewhat different. Both cell lines differentiated with G418 or in DM alone (figure 42a) had apparently similar amount of multinucleated cells in which *hDes*E245D was integrated into filaments. For +*hDes*E245D cells differentiated in the presence of BIX-01294 (figure 42B), the number of fused cells that were positive for HD1-stained filaments appeared lower.

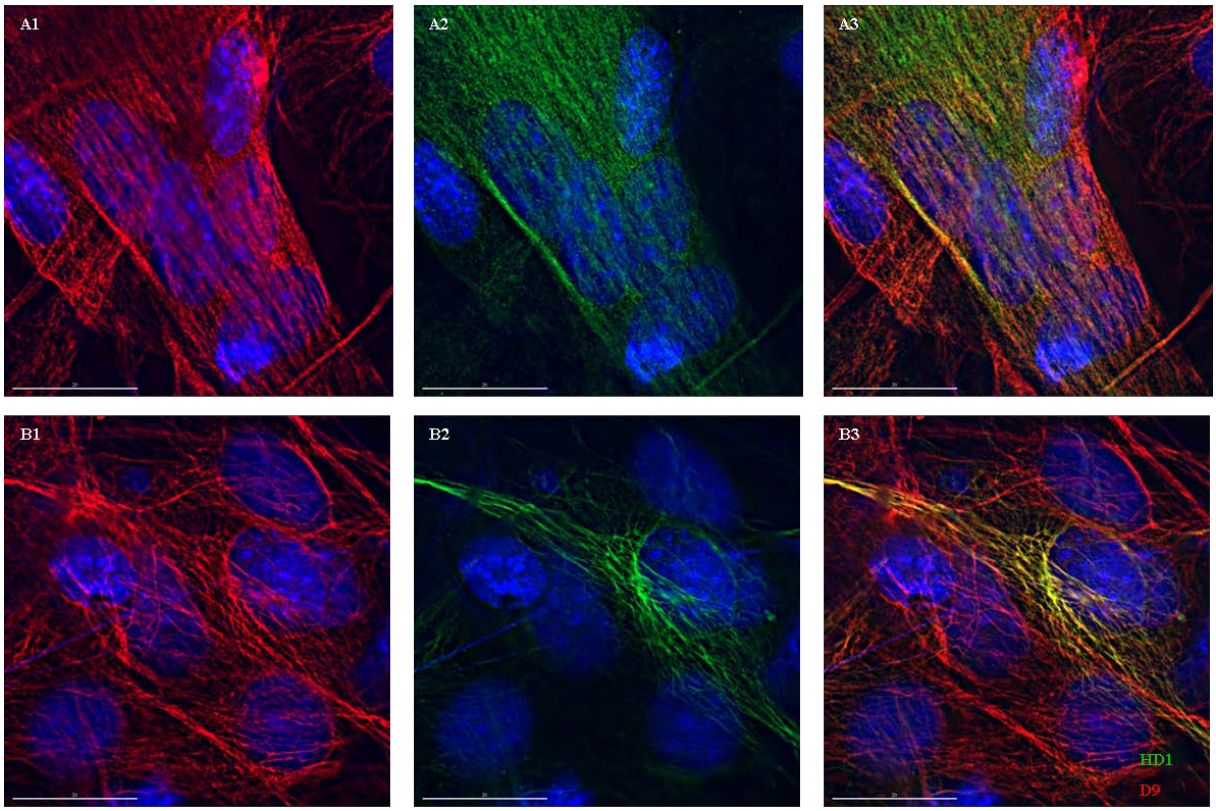

Figure 42. C2C12 +*hDes*E245D (DM) stained with HD1 and D9. The cells were incubated **(A)** in DM only or **(B)** with BIX-01294. The cells were stained with both D9, red **(A1, B1)** and HD1, green **(A2, B2)**. **(A3, B3)** Merge; blue, DAPI; scale bars, 20 μm.

Finally, the same type of analyses was performed on C2C12 +*hDes*R350P cells (figure 43). In case of cells cultured in DM alone (figure 43A), no multinucleated cell with *hDes*R350P expression was observed. The same was the case for cells differentiated in the presence of the BIX-01294 inhibitor (figure 43B), where the majority of the cells, which was HD1-possitive, was unfused. The situation was the same in the case of the cells differentiated in the presence of G418 (figure 43C). Although in most experiments with *hDes*R350P-transfected cells some fused or even multinucleated cells were observed they were almost all negative for any IF-like HD1 staining. An example on figure 43B further describes a common observation in any of these cells: whereas there were still some cells, which appeared to contain *hDes*R350P integrated into filaments, they were predominantly myoblasts-like (single nucleated, round). On the other hand, the multinucleated cells, which did contain some *hDes*R350P, had only scattered, punctuated HD1-staining (figure 43B).

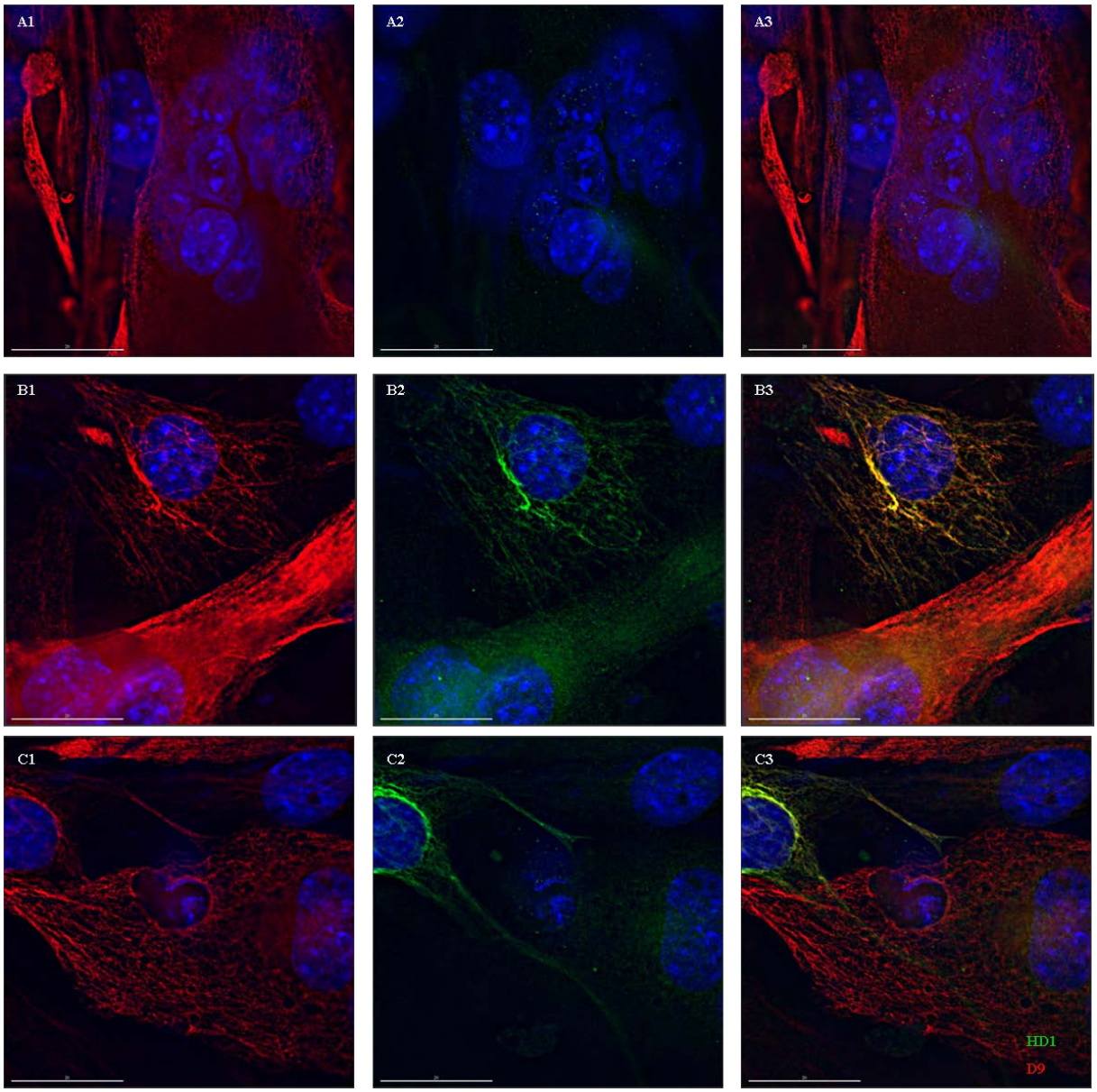

Figure 43. C2C12 +*hDes*R350P (DM) stained with HD1 and D9. The cells were incubated **(A)** in DM only, **(B)** DM with BIX-01294 or **(C)** with G418. The cells were stained with both D9, red **(A1, B1, C1)** and HD1, green **(A2, B2, C2)**. **(A3, B3, C3)** Merge; blue, DAPI; scale bars, 20 μm.

3.4.3 Distribution of A-type lamins in C2C12 cells transfected with desminR350P remains myoblast-like after induction of differentiation

The analyses so far have indicated that either the expression of *hDes*R350P is significantly reduced upon the initiation of differentiation in the transfected C2C12 cells or that the mutant protein is being degraded. That was not the case with either *hDes*WT or *hDes*E245D-expressing cells indicating that this particular mutant might be somewhat toxic to the cells. Therefore what remained open was the mechanism that the cells use to reduce the amount of this particular mutant. For instance, the cells could be rapidly degrading the mutant protein.

Another alternative would involve increasing the rate of proliferation whereby only a subset of the offspring cells could be accumulating the mutant protein. Such hypothesis was drawn from the apparently asymmetrical *hDes*R350P distribution in neighbouring cells (section 3.3.3, depicted on figures 29 to 33). Considering the observation that the mutant protein was still present in the cells, but was largely excluded from the multinucleated ones, we have further analysed the cell cycle state of the cells transfected with the different *hDes* variants.

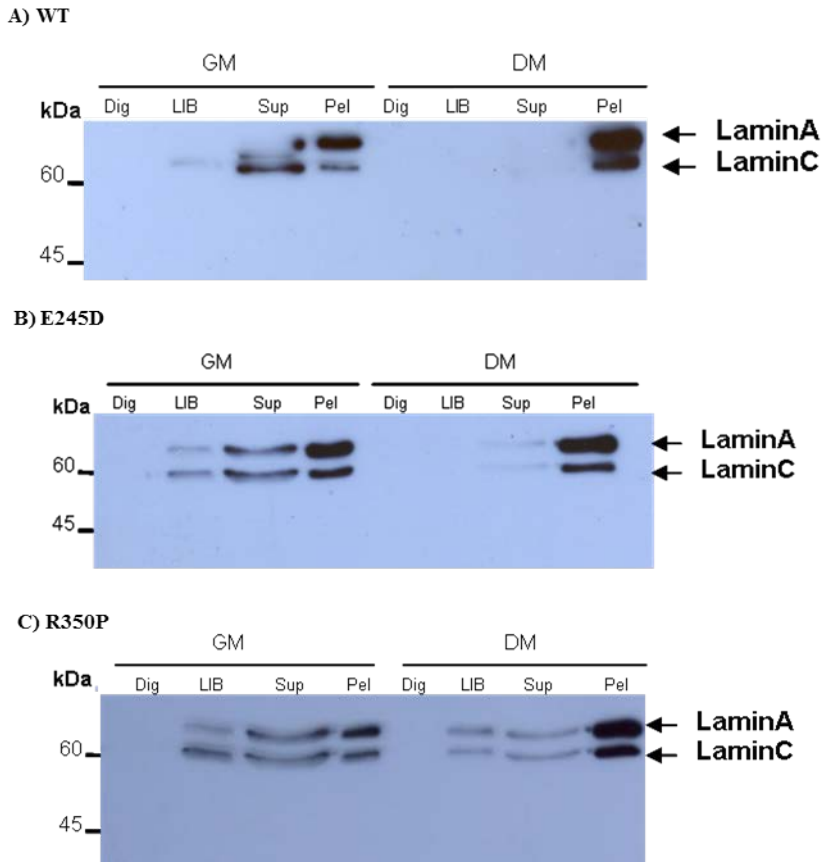

Figure 44. WB of LaminA/C (LaZ antibody) on fractions of C2C12 +*hDes* (GM, DM) cells. Cell fractions (Dig, LIB, Sup, Pel 1:2) of cells cultured in GM or DM of C2C12 +*hDes* **(A)** WT, **(B)** *hDes*E245D and **(C)** *hDes*R350P. Loading scaled to the equal amounts of protein in each of the LIB fractions.

As observed previously (figures 19 and 20A) A-type lamins distribution differs considerably between the undifferentiated and differentiating C2C12 cells. Namely, the undifferentiated myoblasts were shown to contain a considerable amount of A-type lamins in their soluble state, extractable in LIB and Sup fractions. Differentiated C2C12 cells, on the other hand, contained predominantly laminA/C extracted in the pellet fraction of the cell fractionation procedure. When this result was compared to the *hDes*WT and *hDes*E245D-transfected cells (figure 44A and B) it was observed that these cells also undergo differentiation successfully.

On the contrary, A-type lamins distribution in C2C12 +*hDes*R350P (DM) cells resembles that of the corresponding undifferentiated (GM) cells, indicating that a significant amount of those cells fails to enter the differentiation process. Yet one should also note that the amount of soluble, predominantly found in LIB but also in Sup fractions, laminsA/C in +*hDes*R350P (DM) cells is still lower than that in (GM) cells.

3.4.4 C2C12 cells transfected with either of the mutant desmins express a higher amount of differentiation marker compared to those expressing wild type desmin

Another way to analyse the differentiation of respective C2C12 cell lines was to compare the expression of myosin heavy chain (MHC) among them. MHC has been previously successfully used as a differentiation marker in C2C12 cells, as it is expressed already after three days of cell differentiation (for example, as used in the analyses reported in Ling et al. 2012a). Therefore, we have initially cultured untransfected as well as *hDes*WT, *hDes*E245D and *hDes*R350P-transfected cells in DM only or with BIX-01294 and analysed their fractions with a MHC antibody, MF20 (figure 45).

In all cases MHC was only detected in the Sup fractions. Interestingly, in case of both untransfected and *hDes*WT-transfected C2C12 cells the amount of MHC was lower in samples differentiated in the presence of BIX-01294. Furthermore, all *hDes*-transfected cell lines had a higher amount of MHC in their Sup fractions as compared to the untransfected cells. In contrast to what the A-type lamins distribution would suggest (figure 44C) the amount of MHC was the highest in *hDes*R350P cells. However, one should note once again that the fractionation distribution analyses reflect the sum of the protein amount in a cell population and thereby neglect any possible heterogeneity among the cells with respect to the distribution of a particular protein.

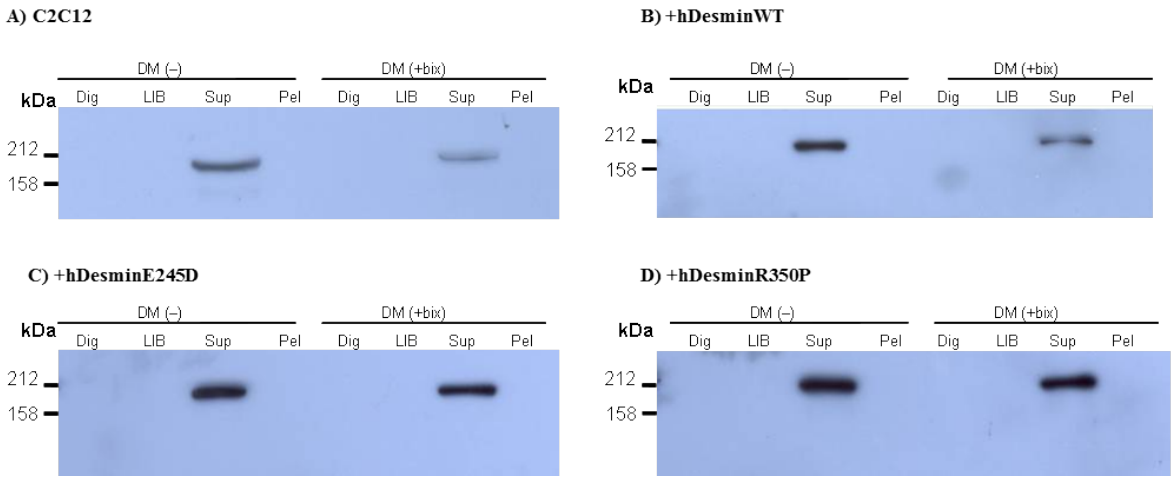

Figure 45. WB with MF20 on fractions of C2C12 +*hDes* (DM) cells. Cell fractions (Dig, LIB, Sup, Pel 1:2) of cells cultured in DM only or with BIX-01294 of **(A)** C2C12 cells, as well as +*hDes* **(B)** WT, **(C)** *hDes*E245D and **(D)** *hDes*R350P cells. Loading: 10 µg protein per LIB fraction.

3.4.5 C2C12 cells expressing hDesR350P delay their differentiation

In a final step to attempt to correlate the presence of a particular desmin variant in a cell with its success in differentiation the cells were stained with the MF20 and HD1 antibodies three days after initiation of differentiation. Although differentiating cells already express MHC at that stage very few of them have started fusing which allows for the analyses of individual cells with respect to their *hDes* content. Therefore, different cells lines (C2C12 +*hDes*WT, *hDes*E245D and *hDes*R350P) were induced to differentiate in DM only, or with either BIX-01294 or G418 and the ICC with MF20 and HD1 was performed after 3 days of differentiation. In total, over 250 HD1-possitive cells of each sample were counted.

As it can be seen on figure 46, C2C12 +*hDes*WT (DM with or without BIX-01294) and +*hDes*E245D (DM) cells have a similar percentage (between 66 to 73%) of MF20-possitive cells which also contained HD1-stained filaments. On the other hand, +*hDes*WT (DM +G418) cell line had a higher percentage (89%) of such cells, whereas *hDes*E245D (DM +bix) had a slightly lower portion (62%) of such cells. Interestingly, in case of +*hDes*E245D cells cultured in DM containing BIX-01294, the percentage of double-positive cells was significantly lower (43%). Note that the degree of variation was also higher in the last two cases.

Finally, with respect to the C2C12 +*hDes*R350P MF20-possitive cells, which also contained HD1-stained filaments, the proportion of cells was significantly lower. Namely 10% of cells

cultured in DM and 5% of those cultured in DM +bix of all MF20-possitive cells contained HD1-stained filaments. Furthermore, only less than 1% (a single cell) of MF20-possitive C2C12 +*hDes*R350P cells cultured in DM +G418 contained HD1-stained filaments. Therefore, although the addition of G418 to DM had a positive effect in *hDes*WT-transfected cell line, the treatment did not help retaining the desmin mutant in the differentiating C2C12 +*hDes*R350P cells.

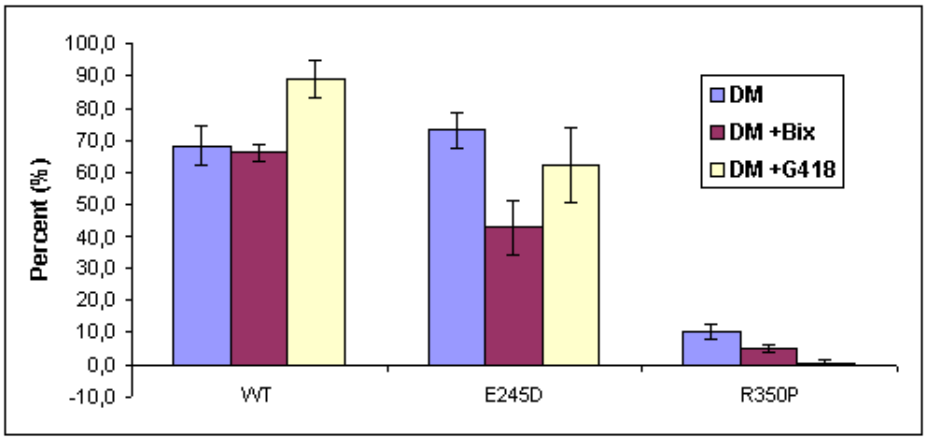

Figure 46. The percentage of MF20-possitive cells which contained HD1-stained filaments. The graph represents the percent of all MF20-possitive cells which also contained *hDes* filaments (HD1-stained) among C2C12 +*hDes*WT, *hDes*E245D and *hDes*R350P cells. The analyses were done after 3 days in DM only, with BIX-01294 or with G418.

In addition, the same ICC was performed on the *hDes*WT, *hDes*E245D and *hDes*R350P cell lines six days after incubation in DM without or with BIX-01294. The observations made are largely in agreement with the above statistical analysis. In case of C2C12 +*hDes*E245D (DM +bix) cells, we observe a considerable number of cells, which contained HD1-positive filaments, that were not fused (figure 47A). In case of *hDes*R350P-transfected cells, almost no MF20- and HD1-double positive cell were found, i.e., MF20-positive cells were largely devoid of HD1-filaments staining (figure 47B). Thereby the outcome from analysis of MHC expression after six days of incubation with DM supported the conclusions made by statistical analyses of cells that were cultured for three days in DM.

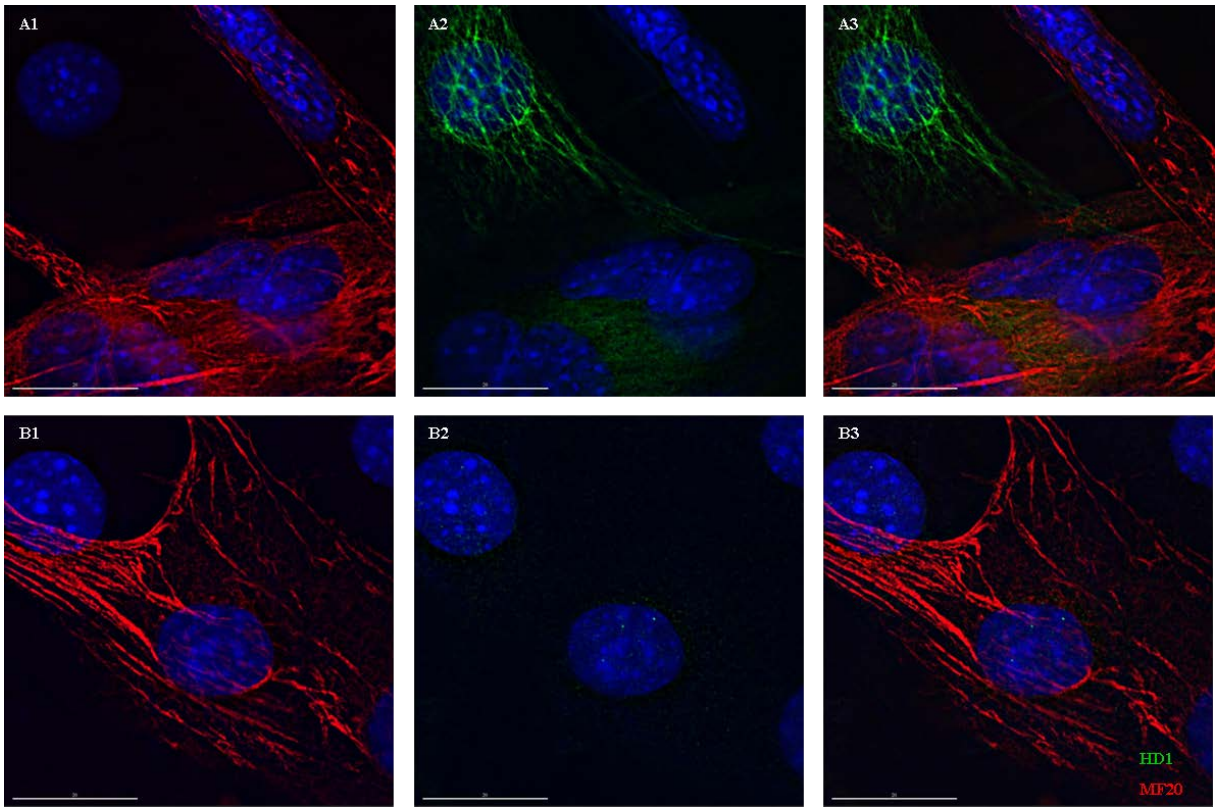

Figure 47. C2C12 +*hDes* (DM +bix) stained with HD1 and MF20. C2C12 +*hDes* **(A)** *hDes*E245D and **(B)** *hDes*R350P cells incubated 6 days in DM +BIX-01294. The cells were stained with both MF20, red **(A1, B1)** and HD1, green **(A2, B2)**. **(A3, B3)** Merge; blue, DAPI; scale bars, 20 μm.

4. Discussion

4.1 The experimental system employed in the study

4.1.1. Optimisation of the C2C12 growth and differentiation procedures

With respect to the cell culture maintenance I would like to briefly reflect on some particular issues concerning culturing of the C2C12 cells. Namely, the procedure for C2C12 cells maintenance in the cell culture as well as differentiation outlined in the methods section 2.2.1 was a result of various trial-and-error steps and thereby optimisations in the general cell maintenance and passaging procedures. C2C12 cell line was generated from the original C2 muscle cells first isolated by Yaffe and Saxel (1977) by subcloning (Blau et al. 1983). Since then there has been a vast amount of published material about these cells demonstrating that they are used as a standard model system for studies on muscle cell biology. Therefore they appeared as the most suitable cell model for the study presented in this thesis.

The first important point was concerning the optimal cell density for cell passaging. Namely, it is essential to note that these cells need to be passaged at somewhat lower (up to 80%) densities as it is crucial to prevent them from becoming too dense. The reason behind it is that once they reach higher densities they change their morphology to resemble the cells which have initiated differentiation. Once they are passaged after reaching such state they appear to grow faster than before. Under those conditions they could be eventually subcultured up to 1: 800 whereby already after five days they would reach complete confluence. Due to these reasons the procedure was eventually standardised so the cells were subcultured 1: 20 and 1: 30 every three days. The cells were always subcultured in two different dilutions as there appeared to have been some minor variations in the cell growth whereby at times they would have grown and gone through their cell cycle somewhat faster. Higher dilutions (than 1: 30) were also eventually avoided as the cells would then appear to grow in clusters. Thereby their local densities after several days of growth would have increased rapidly whereas there would have still been many areas in the dish where there were few or no cells.

The procedure for cell differentiation was also further optimised. For example, cell differentiation was found to be the most effective (i.e., the largest number of fused, multinucleated cells have been observed) in dishes of 6 cm diameter. The reason for such more efficient differentiation in dishes of a smaller size could be an effect of different

alignment of cells due to the size of the dish or the different ratio of medium per area of the dish due to its different height. In addition, the height of the medium in the dish would also effect the O_2 diffusion. As the amount of medium per area of a 10 cm dish was higher than in a 6 cm dish the availability of nutrients per cell was higher in the case the larger Petri dish. The main trigger for C2C12 differentiation is the serum starvation and therefore differentiation medium (DM) contains 2% horse serum whereas growth medium (GM) contains 10% FCS. In addition to the lower percentage of the horse serum used in DM it also has a lower amount of growth factors compared to the FCS as it is obtained from an adult animal.

As C2C12 cells can be differentiated in a Petri dish they do indeed appear to be a powerful tool in muscle cell biology and hence have been implemented since the clone was first generated (Blau et al. 1983). As we wanted to examine the effects of the desmin mutants onto the myoblasts differentiation we have transfected the cells with the particular desmin constructs and followed the cells through differentiation. In order to specifically detect the transfected desmin mutants we also needed to generate antibodies which would specifically recognise it.

4.1.2. Analyses of colocalisation of different antibodies

During the *in vivo* analyses of the *hDes*-transfected C2C12 cells in ICC a problem arose due to the lack of complete colocalisation of antibodies binding to different epitopes on the same protein. Such problem was demonstrated in case with two different vimentin antibodies, Vim3B4 and VimCT (figure 18, section 3.1.5). The initial aim in this study was to generate a rabbit *hDes*-specific antibody (HD1 in this case) and use it in ICC on murine C2C12 cells together with an antibody which could recognise both *m/hDes* (i.e., D9). As the two desmin variants differ in very few amino acids (appendix 2), the approach appeared appropriate.

Therefore, in the ICC with the two antibodies one would have expected a complete colocalisation of the HD1 antibody signals with those from D9. However, that was not always the case as indicated on the example in the figure 27 (section 3.3.1). Baring that in mind one could propose several possible reasons which could account for such discrepancy. One of the possible causes would be due to the effect of the masking of the antibody binding to the epitope. Namely, although the two epitopes are on the opposite sides (head and tail domains) of desmin the effects of blocking of their binding to the epitopes could occur due to their

association at the stage of ULF formation (section 1.1.5, figure 2). As the association of dimers at the stage of tetramer formation is antiparallel, the two epitopes would come closer to each other than one originally thought (Herrmann et al. 2009). Furthermore, as indicated in figure 27 the apparent lack of colocalisation was often observed in cases of filaments stretching over the nucleus. A similar point was demonstrated in the colocalisation study with vimentin antibodies which bind to the different epitopes on the protein, one in the tail domain, VimCT, and the other in the coil 2, Vim3B4 (figure 18, section 3.1.5). In this case, some filaments stretching over the cell nucleus were stained with only one of the two antibodies. Thereby one could hypothesize that the potential epitope availability and position of antibody binding could have further been affected by the IF geometry, i.e., its bending in this case.

Therefore due to the colocalisation problem of the D9 and HD1 antibodies (depicted in figure 27, section 3.3.1) we have attempted to generate the *mDes*-specific antibodies (MD1, MD2) using two different epitopes in the head domain as it was the case with HD1 (section 3.1.2, figure 9). The reason why two different epitopes were chosen, as compared to that of HD1, was due to their higher immunogenicity in case of *mDes*. Namely, the HD1 epitope in *mDes* contained one serine (S) less and had alanine (A) to threonine (T) substitution. Therefore, the peptide used for HD1 generation contained amino acids with two additional hydroxyl groups (as compared to the *mDes* epitope) making it more immunogenic. In addition, there would have been a clear obstacle in antibodies competing for the same epitope region if the same epitope would have been used for generating a *mDes*-specific antibody.

Another clearly technical problem which could have affected the difference in the antibodies staining efficiencies was the fluorophore calibration. Namely, the fluorophore exposure times could not have been mutually calibrated as the strength of one fluorophore was not affected and could not have been linearly correlated to the other. In addition, the deconvolution process is automated and calculates the extent of the out-of-focus light of the two fluorophore channels independently. The similar problem, i.e., uncorrelated fluorophores light emission, also persisted with the confocal microscopy, which does not require deconvolution as the light beam is already focused. Therefore, the microscopy technical problems could not have caused the lack of complete colocalisation of signals (data not shown).

Another alternative to the use of *h/mDes*-specific antibodies was addressed by attempting to use vimentin antibodies in addition. The two IF proteins are known to form heterodimers *in*

vitro (Wickert et al. 2005), which has also been found to occur *in vivo* in hamster kidney cells, BHK21 (Quinlan and Franke 1982). Thereby the cell line has been used to determine if antibodies binding to different epitopes on vimentin could be used to stain the endogenous desmin/vimentin network. The purpose of use of vimentin antibodies in ICC with the desmin mutant was to avoid the possible effects of epitope masking even in the case when the epitopes are located on distant parts of the protein.

However, it has been demonstrated in the case of BHK21-C13 cells, which stem from a clone of the original cell line, that staining of the two networks in not fully identical (figure 17, section 3.1.5). Even more so, when two antibodies binding to different epitopes on vimentin were used there appeared to have been preferential binding of one or the other antibody to particular IF segments. In that respect, one could consider some cases where there some amino acid modifications, such as SUMOrylations of phosphorylations, which would have hindered the antibody binding to the particular epitope. The cases of partial epitope masking is not uncommon for ICC with antibodies against IF proteins. In particular, in analyses by Tunnah et al. (2005), epitopes of lamin B1 detected by some antibodies were masked in a subset of tissues. The same antibodies from the study were also successfully used for the protein detection in the WB. In case of desmin antibodies, as previously indicated and depicted in figure 18b (section 3.1.5), such cases were usually observed in areas above the cell nucleus. This particular example demonstrates that there were vimentin filaments stained with either Vim3B4 or VimCT antibodies whereas some IFs were stained with both of them. Such heterogeneity with respect to the staining patterns of the two antibodies would indicate that the epitope masking is an unlikely cause behind the different staining pattern of the individual vimentin IFs in this case.

Finally, one could also address the need for generating an antibody specific for the transfected protein, as opposed to adding a peptide tag to a *hDes*WT or mutant desmin protein. Such approach would have allowed the analyses to be conducted in the conditions nearer to the native ones. Namely, the mCherry-tagged *hDes*R350P, as well as the *hDes*WT form of the tagged protein to a lower extent, is quickly degraded in the cells. In the WB it has been shown that there were both N- and C-terminal fractions of the mCherry-tagged desmin. This has been demonstrated by the WB of the pellets from the C2C12 cells transfected with the mCherry-tagged desmin variants (figure 36, section 3.3.5). In particular, there are two additional lower molecular weight (Mw) bands below the full length desmin in the HD1 WB, compared to the

WB with D9. As the epitope of one of the antibodies, HD1, is located on the head domain whereas the epitope of D9 is in the tail domain the reason why the two lower Mw bands are lost from the D9 WB would likely be due to the protein degradation from the C-terminus (i.e., the tail domain). However, as only the corresponding highest Mw band is detected by the mCherry antibody degradation likely occurs from both sides of the fusion proteins.

4.1.3 Other technical obstacles and limitations

In case of ICC procedure with antibodies raised against the *hDes*WT (*hDes*R350) and the mutant (*hDes*R350P) epitopes additional treatment with 2 M urea was performed (section 3.1.4, figure 16). The reason for such modification in the standard ICC protocol used with other antibodies was due to the necessity for the epitope retrieval. Namely, as the epitope of the protein detected by the antibody was located in the coil 2B region it was likely masked when the standard ICC procedure was used. Therefore the staining appeared in the form of large, punctuated marks located through the cytosol (data not shown). The 2 M urea treatment was used in an attempt to denature the coiled coil structure sufficiently to release the epitope but not to denature other components in the cell. Further increase in urea concentration or additional repetition of rinsing in the 2M urea therefore led to disruption of other cell structure, including the native IF network (data not shown). Such procedure has been previously successfully applied in ICC analyses of other IF proteins (Franke et al 1983).

Another obstacle during the ICC procedure arose with respect to differentiating C2C12 cells on glass cover slips. Namely, as it has been indicated in the original paper of when C2 cell line were generated (Yaffe and Saxel 1977), the cells appear to retract or curve up upon differentiation whereby they start detaching from the cover slips. Further differentiation on collagen-, matrigel- or other forms of coated cover slips was insufficient to keep the differentiating cells attached. Finally, activating the glass of the cover slips using the chrome-sulphuric acid was sufficient to keep a significant proportion of differentiating cells still attached to the cover slips. In case of double ICC with MF20-HD1 statistics (section 3.4.5, figure 46) the cells were differentiated only for three days prior to the ICC and statistical analyses. As MHC is expressed already three days after initiation of differentiation such analyses was commonly performed in other studies (such as in Ling et al. 2012a). Therefore, as the cell retraction largely started four to five days after initiation of differentiation (data not shown) the statistical analyses were performed on the cells fixed after three days of initiation of differentiation.

With respect to the cell fractionation procedure several other points would need to be briefly addressed in this section. One of the points needing some discussion is the use of protein concentration in the LIB to scale the loading of the samples on the gel. Although the relative amounts of different soluble (i.e., digitonin- or LIB-extracted) protein might differ between C2C12 (GM) and (DM) cells the scaling of sample loading to the protein amounts in the LIB appeared to have been the best way to do so. Namely, the LIB fractions had the lowest amounts of detergents which could interfere with the Bradford assay measurements (digitonin also appeared to affect the 595nm absorption of the samples, data not shown) and a relatively high amount of protein. As the cell material was collected directly from the Petri dish scaling the protein loading to the cell number could have also not been done.

In addition to the fractionation of cells with respect to the solubility of their IF proteins (i.e., extractions with the LIB and HIB) an additional extraction using digitonin was performed prior to those procedures. Digitonin is a detergent with a sterol moiety which makes it more specific to break holes into cholesterol-containing membranes, such as cell plasma membrane (Fiskum et al. 1980). Due to such specificity of this detergent the digitonin fractions in the procedure would have contained only the most soluble, cytosolic proteins. Therefore as the mitotic A-type lamins, which are dispersed throughout the cytosol, would have already been extracted in the digitonin fraction those found in LIB of C2C12 (GM) but not of (DM) cells do not represent the soluble mitotic lamins in those cells. They would in fact reflect the different A-type lamin distribution in the nucleus and hence different chromatin organisation in the two stages of the cells.

In addition, one could also address the characteristics of proteins extracted in different fractions. The protein remaining in the pellet is considered to be largely IF protein which is a part of the filament networks. As it could have been seen (such as in figure 34, section 3.3.4) *hDes*R350P was also extracted only in the pellet fraction. However only a small subfraction of cells contained this protein in filaments whereby in higher (above 10) passages almost no C2C12 +*hDes*R350P cells contained HD1-stained filaments (data not shown). However, at this higher passage *hDes*R350P was also only found in the pellet fraction of the cells (figure 40C, section 3.4.1). Therefore this fraction would appear to contain the other forms of insoluble IF-proteins: not only those forming filaments but also those forming compact, highly insoluble aggregates.

4.2 The impact of the desmin mutants on the endogenous IF network of C2C12 cells

4.2.1 Mild mutants being incorporated into the filaments

In the work presented two different desmin mutants were analysed and compared to the *hDes*WT. *hDes*E245D has been previously demonstrated to behave similarly to the *hDes*WT with respect to its filament forming capacities (Bär et al. 2005b). Therefore, it was proposed that the effects of this mutation would only manifest themselves in the final stages of the IF network formation or in a muscle-type cellular scenario (figure 6B, section 1.3.1). Based on the results of the current study (section 3.3.2) one could only point out the differences in its distribution in differentiating cells (section 3.4.5). Namely, the percentage of differentiating (i.e., MF20-possitive cells) cells which contained HD1-stained filaments was the same in those cells compared to the cells transfected with *hDes*WT. However, some effects of this mutant compared to the *hDes*WT were evident, which is further discussed in section 4.3.1.

Although the transfected *hDes*E245D was found to form perinuclear accumulations as detected by diffuse staining at several instances (one drastic example was given on figure 28B) it was predominantly found to be integrated into the endogenous filaments (figure 28A). These filaments have also colocalised with vimentin IFs (figure 28C). They have persisted even in higher (over 15) passages upon transfection and the cells expressing *hDes*E245D appeared only marginally irregular or otherwise different from those in *hDes*WT-transfected cells.

As a matter of fact, the *hDes*E245D was subsequently found to introduce a cryptic splice site, whereby the truncated version, rather than the full length mutant desmin, was concluded to be behind the disease phenotype (Clemen et al. 2009). However, there was no clear observation that the same occurs in the C2C12 cells. Namely, upon fractionation only a single band corresponding to the size of full-length desmin has been detected by both the antibodies binding to the head- (HD1) and the other to the tail- (D9) domain (figure 34, section 3.3.4). Therefore, the diffuse staining of the *hDes*E245D was very unlikely due to the presence of a putative desmin truncation product.

4.2.2 Asymmetric distribution of severe mutants upon cell division

On the other hand, the effects of the *hDes* R350P appear to be far more complex. One of the possible causes for such drastic effects of this particular mutation was that the amino acid arginine (R) was substituted with proline (P). Whereas arginine contains a side chain with a

positively charged guanidinium group at its end, proline is a secondary amine and thereby a cyclic amino acid. Due to its cyclic nature the amino acid is characterised by the rigid angles and thereby is commonly found in turns between α-helices or β-sheets but not inside them. Once located in an α-helix, as the case in this mutant, it introduces a kink in the secondary amino acid structure. Yet one should be cautious about extrapolating from these facts. For example, another P mutation also occurs in an α-helix, i.e., *hDes*A360P, and appears to be far less deleterious for IF formation as it allows it to get up to the stage of radial compaction (figure 6B, section 1.3.1).

Another clear observation, as also documented by several WBs (such as on figure 34, section 3.3.4), was that the amount of this particular mutant protein is significantly lower in C2C12 cells than either of the other transfected desmin proteins, *hDes*WT or the *hDes*E245D. Additional observation (data not shown) was that in later (after 10) passages very few of the *hDes*R350P-transfected cells contained any HD1-possitive IF staining. This was observed in each of the several different transfections in the C2C12 cells. In each the protein was lost by further cell passaging. Some of the possible causes for such effect could be due to the mutant degradation or its lower expression and different distribution. However, as the observation was recurrent in different transfection experiments, and was only observed with this particular mutant, its lower expression or varied distribution in different cells seem to be unlikely as potential causes. To confirm that the observations were indeed the result of *hDes*R350P transfection plasmid DNA the $Vim^{-/-}$ fibroblasts were used as a positive transfection control. The experiment has demonstrated that upon transfection of *hDes*R350P into these cells its distribution was distinctly different in all cells as compared to that obtained with the *hDes*WT transfection (compare in figure 37A and B, section 3.3.6).

What has been extensively presented in the section 3.3.3 was the apparent asymmetric distribution of *hDes*R350P in different transfected C2C12 cells. As the phenotype could have occurred due to asymmetric distribution upon cell division or different extent of mutant protein degradation and/or expression it was labelled with a neutral term in order not to presuppose the actual cause behind it. Attempts for live cell imaging of the mCherry-tagged *hDes*R350P failed (section 3.3.5) and hence the cause behind the phenotype could not have been determined. Furthermore, no quantitative analyses could be obtained due to the further variability with respect to the phenotype itself. Namely, the variable distances between the pairs of cells manifesting the observed phenotype or minor differences in local staining

efficiency with either HD1 or D9 antibodies hindered the attempts to statistically analyse the observations. Therefore the data has been presented at length (section 3.3.3) in order to indicate the observed heterogeneity and to describe it as thoroughly as possible.

4.2.3 The mutant desmin protein is not entirely segregated from the wt one

With respect to one of the main topics of this work, the question of desmin mutant segregation from the wt protein, one could extrapolate on the data obtained. Namely, at a ratio 1:3 (*hDes*WT/R350P) the *hDes*R350P was still found to have a dominant negative effect on desmin filaments formation *in vitro* (Bär et al. 2005a). Furthermore, the phenotype of the *hDes*R350P transfection in Vim$^{-/-}$ fibroblasts is distinctly different from that of the *hDes*WT, indicating that the observed filament formation capacity of the *hDes*R350P observed in C2C12 cells is not intrinsic for the protein itself. *hDes*R350P was also found to form filaments with the endogenous vimentin protein (figure 31B and D, section 3.3.3) indicating it is not entirely segregated from the endogenous desmin or vimentin IF networks. The likely reason for the discrepancy between the observations in the two cell lines could be due its capacity to coassemble with the endogenous vimentin and/or desmin IFs.

However, the question of the mechanisms a muscle cell has to cope with the deleterious effects of the mutation still remains open. Namely, the phenotype of the *hDes*R350P discussed in detail indicates that the cells have difficulties coping with the effects of the mutated protein. As the cells do appear to form both desmin and vimentin IFs which contain *hDes*R350P the *in vivo* data would suggest that the *hDes*WT and the *hDes*R350P proteins are at least not fully segregated one from the other.

However, the data obtained by IP (figure 38, section 3.3.7) could argue differently as the *mDes* was not co-IPed with the *hDes* variants. As that was also the case with the *hDes*WT IP, the likely cause for this apparent segregation might simply be in different timing of the transcription and translation, and thereby dimer and tetramer assembly, of endogenous and transfected desmin. Namely, as the gene promoter of the transfected desmin gene (β-actin promoter) is different than that of the endogenous one, the transcription and subsequently translation of the two desmin variants would not necessarily occur at exactly the same time. Thereby, the smaller units of the IFs (i.e., such as tetramers) would be assembled from predominantly single desmin species. Finally, one should also note that no *hDes*R350P was detected in the IP of the respective sample. The cause for this apparent lack of the bound

protein could be due to the effect of a very low amount of *hDes*R350P already in the RIPA sample (figure 38, section 3.3.7). The previous data on the effects of increasing the amount of *hDes*R350P on assembly of *hDes*WT IFs (Bär et al. 2005a) indicate that the two species could form higher order structures *in vitro* at particular ratios. Although the results from the IP would argue the opposite occurs in cells one should be cautious about interpreting these data since in the IP of the *hDes*WT no endogenous *mDes*WT was co-IPed either.

4.3 Differentiation of C2C12 cells expressing mutant desmin

Before discussing the effects of the desmin mutations on C2C12 cell differentiation one should also briefly address the issue of plasmid choice for the analyses. Initially pHβAPr-1-neo plasmid appeared appropriate as it was designed for genes which need to be constitutively expressed as it contained a β-actin gene promoter (Gunning et al. 1987). However, β-actin mRNA is downregulated in differentiating C2C12 (Shimokawa et al., 1998) indicating that upon differentiation the expression of the *hDes* mRNA might also decrease. Yet as reported in the original paper (Gunning et al. 1987) the gene expression from this vector is not affected by C2C12 differentiation. Nevertheless, all of the presented analyses of the differentiating cells containing the transfected desmin mutants were compared to the ones from *hDes*WT-transfected C2C12 cells.

4.3.1 Effects of G9a inhibitor and geneticin treatments onto C2C12 differentiation

Due to the loss of *hDes*R350P from the cells during differentiation we have also attempted differentiating the cells in the presence of the selection marker, G418. Thereby the differentiating cells would have likely retained the protein more efficiently than without the drug, which might appear to be the case for C2C12 +*hDes*E245D cells (figure 40, section 3.4.1). On the other hand, the total amount of desmin in C2C12 +*hDes*R350P (DM+G418) cells is several fold higher than in the (DM) ones whereas the amounts of the transfected desmin are comparably similar. This result indicates that although the overall amount of *hDes*R350P in these cells is somewhat higher the relative (i.e., the percentage of the total) amount of it is lower. Such effect could arise due to the difference in differentiation as C2C12 (DM) express several fold higher amounts of desmin as compared to the (GM) cells (figure 21, section 3.2.2). With respect to the number of HD1- and MF20- double positive cells treatment of cells with G418 appeared to have opposite effects on different cell lines. Namely,

whereas in case of the *hDes*WT and *hDes*E245D-transfected cells the fraction of double-positive cells increased or remained the same, in the differentiating cells in *hDes*R350P it was reduced compared to the respective untreated differentiating cells.

Another drug that has been implemented in the current study is an inhibitor of G9a methyltransferase, BIX-01294 (bix). In addition to its role as a histone methyltransferase, G9a maintains myoblasts in undifferentiated state by methylating MyoD (as described in Ling et al. 2012a). The same study reported its use for a control reagent added to the cells to enhance their differentiation. There have been additional studies demonstrating other effects of BIX-01294 on muscle cell differentiation (Ling et al. 2012b), as well as on differentiation of other cell types (Culmes et al. 2013), indicating that the drug could be a powerful tool in driving the cells into differentiation. In order to attempt to enhance the differentiation of transfected C2C12 cells the drug was used in a subset of experiments. The treatment with the drug did not appear to lead to higher expression of desmin except in the case of C2C12 +*hDes*R350P cells (figure 39C, section 3.4.1), which would have been one of the indicators of more efficient differentiation. On the other hand, the overall expression of the differentiation marker MHC either remained the same, as in case of the C2C12 cells transfected with either of the desmin mutants, or was even lower, as in case of the untransfected and *hDes*WT transfected cells, as compared to the untreated cells (figure 45, section 3.4.5).

However, the most drastic effect of the drug treatment was with respect to the amount of HD1- and MF20-double positive cells in case of the C2C12 expressing the mutant proteins (figure 46, section 3.4.4). One should also note that there was a significantly higher fluctuation in the number of double positive cells among C2C12 +*hDes*E245D (DM +bix/+G418) compared to the other samples (note the errors bars on figure 46). As the BIX-01294 drug has been implemented in trace amounts (2.5nM) one could speculate about a stochastic effect of the drug whereby only a subpopulation of the cells would have received the efficiently effective treatment.

The reduction of the number of HD1- and MF20-double positive cells among C2C12 +*hDes*E245D by BIX-01294 treatment might be caused by the marginally better efficiency of cells without the transfected protein to better differentiate as opposed to the cells expressing the mutant desmin. This point is further supported by the effects the drug has on *hDes*R350P-transfected cells as the drug treatment also led to the reduction of the number of MF20- and

HD1-double positive cells. However, one should also note that G9a is a histone methyltransferase whereby its inhibition could also lead to other effects on the chromatin as its role is not limited to the genes and factors involved in muscle cell differentiation. In addition, it should also be noted that the increase of the amounts of BIX-01294 5-fold in the course of a 6-day differentiation experiment appeared to completely inhibit differentiation as determined by the cell morphology (data not shown).

4.3.2 Presence of hDesR350P could stimulate either differentiation or cell proliferation in C2C12 cells

In the final points of the discussion on the presented results one could outline the general phenotype of the cells transfected with the mutant *hDes*R350P and thereby propose the mechanism of causing such effects in the transfected cells. On the one hand, the *hDes*R350P, unlike *hDes*WT and the *hDes*E245D variants, appears to stimulate the cell proliferation or their delay in differentiation-associated changes. This conclusion is evident from the fact that their distribution of A-type lamins upon fractionation does not appear to change significantly upon induction to differentiation (figure 44, section 3.4.3) as compared to the other transfected cells. The amount of more soluble (i.e., LIB and Sup-extracted) A-type lamins is nevertheless relatively lower in DM C2C12 +*hDes*R350P cells, as compared to the respective GM cells. This difference indicates that the failure to change their A-type lamin distribution, which appears to accompany differentiation (as in figures 19 and 20, section 3.2.1), might also reflect the state of only a subset of cells.

On the other hand, the amounts of MHC in cells transfected with either of the desmin mutants were higher than in untransfected or *hDes*WT-transfected cells (figure 45, section 3.4.4). Therefore, whereas on the one hand presence of *hDes*R350P in these cells would appear to delay their differentiation (A-type lamins fractionation results) it would also appear to stimulate their differentiation (the amount of MF20 in cell extracts). The low percentage of HD1- and MF20-double positive C2C12 +*hDes*R350P cells further suggest a possible link between the two apparently opposite results. Namely, on the one hand some of the cells in a population would appear to retain the mutant protein and they appear to be inefficient in promoting differentiation. On the other hand the cells with low amounts of this particular mutant protein have a higher chance to differentiate. These cells could be differentiating even more efficiently than the untransfected or *hDes*WT-transfected cells, as indicated by the higher amounts of total MHC in the cells transfected with the desmin mutants (figure 45, section 3.4.4).

These conclusions would also correlate to what is observed with mutants in other proteins causing related diseases. Such is the case with lamin A mutants causing Emery-Dreifuss muscular dystrophy which appear to inhibit *in vitro* differentiation of C2C12 cells (Favreau et al. 2004). Thereby one could conclude that in order to attempt to dispose of the mutant desmin protein, the cells expressing it would need to delay their differentiation. An effect analogous to the proposed model was also observed with the treatment of cultured myoblasts and myotubes with prion toxic peptide, PrP106-126 (Brown et al. 1998). The toxicity of this peptide was considerably higher in myotubes as compared to the myoblasts. Such an observation could be explained by the fact that the myoblasts, unlike myotubes, are undergoing cell proliferation whereby they could discard the toxic or aggregation-prone peptides through the process of cell division. A further support in favour of such hypothesis comes from the studies of treating astrocytes with the same peptide. Namely, in case of these cells, treatment with this peptide also induces a release of cytokines and thereby stimulates astrocyte proliferation. These studies would indicate that presence of some aggregation-prone proteins, such as some desmin mutants in this case, could delay differentiation by induction of cell proliferation. Thereby, as in case of the lamin A mutant, which causes Emery-Dreifuss Muscular Dystrophy (Favreau et al. 2004), desmin mutants might also delay differentiation.

4.4 Conclusions and the outlook

The final conclusion from the study, as discussed in the previous section, is that the effects of the presence of *hDes*R350P mutant in myoblasts could have opposite effects on the cell differentiation. The asymmetric *hDes*R350P distribution in transfected myoblasts further suggests a model of how this double effect could occur whereby the cells accumulating the mutant protein would fail to differentiate. On the other hand, accumulation of mutant protein in only a subpopulation of cells could give rise to a fraction of mutant-free cells. Once these cells fuse they would nevertheless still be expressing the mutant protein which could start accumulating over time and, given the late onset of the disease, eventually lead to the fatal phenotypes. Yet one should bear in mind that the presented data were obtained from a cell culture model scarcely mimicking the actual situation in the adult muscle cells. For example, the loss of *hDes*R350P from cells by further passaging indicates a strong toxic effect of the protein on the cell viability. However, having a subpopulation of C2C12 cells still integrating the mutant into their endogenous IFs indicates that the cells do have some innate mechanisms which would allow them to tolerate the mutant protein.

Therefore, additional support for the proposed mechanisms and further elucidation of the actual mode of pathogenesis are still needed. To achieve that one should first attempt to generate a mutant desmin protein fused to a fluorescent tag which could be used for the live cell imaging. In addition, one would also need a more specific *mDes* antibody to be able to precisely differentiate the two species of desmin, the *hDes*WT and the transfected mutants. In that respect, another alternative to perform further experiments in more native conditions would be to subclone the *hDes* epitope of HD1 into *mDes* sequence. This form of fusion protein could be subsequently used for transfection into C2C12 cells. As previously indicated, the same set of experiments using the *hDes*A360P mutant could also be performed as additional control. Finally, the experiments so far were performed on a cell culture model and the results were attempted to be correlated to the observations on the samples from desminopathies patients. Thereby similar analyses could be performed on the heterozygous and homozygous *mDes*R349P knock-in mice (group of Prof. Rolf Schröder, Neuropathology institute, Erlangen). By pursuing such analyses one would get a more reliable insight into the actual pathogenesis process in the case of desminopathies.

5. References

Bär H., Fischer D., Goudeau B., Kley RA., Clemen CS., Vicart P., Herrmann H., Vorgerd M. and Schröder R. (2005a) Pathogenic effects of a novel heterozygous R350P desmin mutation on the assembly of desmin intermediate filaments in vivo and in vitro. *Hum Mol Genet*, 14 (10): 1251-1260.

Bär H., Mücke N., Kostareva A., Sjöberg G., Aebi U. and Herrmann H. (2005b) Severe muscle disease-causing desmin mutations interfere with *in vitro* filament assembly at distinct stages. *Proc Nat Acad Sci USA*, 102 (42): 15099-15104.

Bär H., Kostareva A., Sjöberg G., Sejersen T., Katus HA. And Herrmann H. (2006) Forced expression of desmin and desmin mutants in cultured cells: Impact of myogenic missense mutations in the central coiled-coil domain on network formation. *Exp Cell Res*, 312 (9): 1554-1565.

Bellin RM., Huiatt, TW., Critchley RM. and Robson RM. (2001) Synemin may function to directly link muscle cell intermediate filaments to both myofibrillar Z-lines and costameres. *J Biol Chem*, 276 (34): 32330-32337.

Blau HM., Chiu CP. and Webster C. (1983) Cytoplasmic activation of human genes in stable heterokaryons. *Cell* 32: 1171-1180.

Brown DR., Schmidt B., Groschupc MH. and Kretzschmar HA. (1998) Prion protein expression in muscle cells and toxicity of a prion protein fragment. *Eur J Cell Biol*, 75: 29-37.

Brown DR. (2001) Microglia and prion disease. Microsc Res Tech 54: 71–80.

Clemen CS., Fischer D., Reimann J., Eichinger L, Müller CR., Müller HD., Goebel HH. And Schröder R. (2009) How Much Mutant Protein Is Needed to Cause a Protein Aggregate Myopathy in Vivo? Lessions from an Exeptional Desminopathy. *Hum Mutat*, 30 (3): E490-E499.

Culmes M., Eckstein HH., Burgkart R., Nüssler AK., Guenther M., Wagner E. and Pelisek J. (2013) Endothelial differentiation of adipose-derived mesenchymal stem cells is improved by epigenetic modifying drug BIX-01294. *Eur J Cell Biol*, 92 (2): 70-79.

Favreau C., Higuet D., Courvalin JC. And Buendia B. (2004) Expression of a Mutant Lamin A That Causes Emery-Dreifuss Muscular Dystrophy Inhibits In Vitro Differentiation of C2C12 Myoblasts. *Mol Cell Biol*, 24 (4): 1481-1492.

Fiskum G., Craig SW., Decker GL. and Lehninger AL. (1980) The cytoskeleton of digitonin-treated rat hepatocytes. *Proc Nat Acad Sci USA*, 77 (6): 3430-3434.

Franke WW., Schmid E., Osborn M. and Weber K. (1978) Different intermediate-sized filaments distinguished by immunofluorescence microscopy. *Proc Natl Acad Sci USA*, 75 (10): 5034-5038.

Franke WW., Schmid E., Wellsteed J., Grund C., Gigi O. and Geiger B. (1983) Change of the cytokeratin filament organization during the cell cycle: selective masking of an immunologic determinant in interphase PtK2 cells. *JCB*, 97 (4): 1255-1260.

Geisler N., Kaufmann E. and Weber K. (1982) Proteinchemical characterization of three structurally distinct domains along the protofilament unit of desmin 10nm filaments. *Cell*, 30 (1): 277-286.

Granger BL. And Lazarides E. (1980) Synemin: a new high molecular weight protein associated with desmin and vimentin filaments in muscle. *Cell*, 22 (3): 727-738.

Gruenbaum Y., Margalit A., Goldman RD., Shumaker DK. And Wilson KL. (2005) The nuclear lamina comes of age. *Nat Rev Mol Cell Biol*, 6 (1): 21-31.

Goldfarb LG., Park KY., Cervenakova L., Gorokhova S., Lee HS., VasconcelosO., Nagle JW., Semino-Mora C., SivakumarK., Dalakas MC. (1998) Missense mutations in desmin associated with familial cardiac and skeletal myopathy. *Nat Genet*, 19: 402–403

Gunning P., Leavitt J., Muscat G., Ng SY. And Kedes L. (1987) *Proc Natl Acad Sci USA* 84 (14): 4831-4835.

Herrmann H. and Aebi U. (2000) Intermediate filaments and their associates: multi-talented structural elements specifying cytoarchitecture and cytodynamics. *Curr Opin Cell Biol*, 12 (1): 79-90.

Herrmann H. and Aebi U. (2004) INTERMEDIATE FILAMENTS: Molecular Structure, Assembly Mechanism, and Integration Into Functionally Distinct Intracellular Scaffolds. *Annu Rev Biochem*, 73: 749-789.

Herrmann H., Bär H., Kreplak L., Strelkov SV. And Aebi U. (2007) Intermediate filaments: from cell architecture to nanomechanics. *Nat Rev Mol Cell Biol*, 8 (7): 562-573.

Herrmann H., Fouquet B. and Franke WW. (1989) Expression of intermediate filament proteins during development of Xenopus laevis. II. Identification and molecular characterization of desmin. *Development*, 105 (2): 299-307.

Herrmann H., Strelkov SV., Burkhard P. and Aebi U. (2009) Intermediate filaments: primary determinants of cell architecture and plasticity. *J Clin Invest*, 119 (7): 1772-1783.

Ishikawa H., Bischoff R. and Holtzer H. (1968) Mitosis and intermediate-sized filaments in developing skeletal muscle. *J Cell Biol*, 38 (3): 538-555.

Konieczny P., Fuchs P., Reipert S., Kunz WS., Zeöld A., Fischer I., Paulin D., Schröder R. and Wiche G. (2008) Myofiber integrity depends on desmin network targeting to Z-discs and costameres via distinct plectin isoforms. *J Cell Biol*, 181 (4): 667-681.

Lazarides E. (1980) Intermediate filaments as mechanical integrators of cellular space. *Nature*, 283 (5744): 249-256.

Ling BM., Bharathy N., Chung TK., Kok WK., Li S., Tan YH., Rao VK., Gopinadhan S., Sartorelli V., Walsh MJ. And Taneja R. (2012a) Lysine methyltransferase G9a methylates the transcription factor MyoD and regulates skeletal muscle differentiation. *Proc Nat Acad Sci USA*, 109 (3): 841-846.

Ling BM., Gopinadhan S., Kok WK., Shankar SR., Gopal P., Bharathy N., Wang Y. and Taneja R. (2012b) G9a mediates Sharp-1–dependent inhibition of skeletal muscle differentiation. *Mol Biol Cell*, 23 (24): 4778-4785.

Muralikrishna B., Dhawan J., Rangaraj N. and Parnaik VK. (2001) Distinct changes in intranuclear lamin A/C organization during myoblast differentiation. *J Cell Sci*, 114 (22): 4001-4011.

Parry DA. (2005) Microdissection of the sequence and structure of intermediate filament chains. *Adv Protein Chem*, 70: 113-142.

Perry DA. and Steinert PM. (1999) Intermediate filaments: molecular architecture, assembly, dynamics and polymorphism. *Q Rev Biophys*, 32 (2): 99-187.

Pollard TD. And Borisy GG. (2003) Cellular motility driven by assembly and disassembly of actin filaments. *Cell*, 112 (4): 453-465.

Quinlan RA. and Franke WW. (1982) Heteropolymer filaments of vimentin and desmin in vascular smooth muscle tissue and cultured baby hamster kidney cells demonstrated by chemical crosslinking. *Proc Nat Acad Sci USA*, 79: 3452-3456.

Sanger JM. and Sanger WS. (2008) The Dynamic Z-bands of Striated Muscle Cells. *Sci Signal*, 1 (32): pe37.

Schröder R. and Schoser B. (2009) Myofibrillar Myopathies: A Clinical and Myopathological Guide. *Brain Pathol*, 19 (3): 483-492.

Schweitzer SC., Klymkowsky RM., Bellin, RM., Robson RM., Capetanaki Y. and Evans RM. (2001) Paranemin and the organisation of desmin filament networks. *J Cell Sci*, 114 (6): 1079-1089.

Selcen D, Ohno K and Engel AG (2004) Myofibrillar myopathy: clinical, morphological and genetic studies in 63 patients. *Brain*, 127 (2):439-451.

Sharma S., Mücke N., Katus HA., Herrmann H. and Bär H. (2009) Disease mutations in the "head" domain of the extra-sarcomeric protein desmin distinctly alter its assembly and network-forming properties. *J Mol Med*, 87 (12): 1207-1219.

Shimokawa T., Kato M., Ezaki O. and Hashimoto S. (1998) Transcriptional Regulation of Muscle-Specific Genes During Myoblast Differentiation. *Biochem Biophys Res Commun.*, 246 (1): 287-292.

Steinert PM. and Roop DR. (1988) Molecular and cellular biology of intermediate filaments. *Annu Rev Biochem* 57: 593-625.

Titeux M., Brocheriou V., Xue Z., Gao J., Pellissier JF., Guicheney P., Paulin D. and Li Z. (2001) Human synemin gene generates splice variants encoding two distinct intermediate filament proteins. *Eur J Biochem*, 268 (24): 64356435-6449.

Tunnah D., Sewry CA., Vaux D., Schirmer EC. And Morris GE. (2005) The apparent absence of lamin B1 and emerin in many tissue nuclei is due to epitope masking. *J Mol Histol*, 36 (5): 337-344.

van Spaendonck-Zwarts K., van Hessem L., Jongbloed JD., de Walle HE., Capetanaki Y., van der Kooi AJ., van Langen IM., van den Berg MP. and van Tintelen JP (2010) Desmin-related myopathy: a review and meta-analysis. *Clin Genet*, 80 (4): 354–366.

Walter MC., Reilich P., Huebner A., Fischer D., Schröder R., Vorgerd M., Kress W., Born C., Schoser BG., Krause KH., Klutzny U., Bulst S., Frey JR. and Lochmüler H.(2007) Scapuloperoneal syndrome type Kaeser and a wide phenotypic spectrum of adultonset, dominant myopathies are associated with the desmin mutation R350P. *Brain*, 130 (6):1485–1496.

Waterman-Storer CM. and Salmon ED. (1997) Microtubule dynamics: treadmiling comes around again. *Curr Biol*, 7 (6): 369-372.

Wickert U., Mücke N., Wedig T., Müller SA., Aebi U. and Herrmann H. (2005) Characterization of the in vitro co-assembly process of the intermediate filament proteins vimentin and desmin: mixed polymers at all stages of assembly. *Eur J Cell Biol*, 84 (2-3): 379-391.

Wilhelmsen K., Ketema M., Truong H. and Sonnenberg A. (2006) KASH-domain proteins in nuclear migration, anchorage and other processes. *J Cell Sci*, 119 (24): 5021-5029.

Yaffe D. and Saxel O. (1977) Serial passaging and differentiation of myogenic cells isolated from dystrophic mouse muscle. *Nature*, 270 (5639): 725-727.

6. Appendices

Appendix 1: List of abbreviations

%	Percent
^{o}C	Degree Celsius
µg, µl, µM	Micro-gram, -liter, -molar
Bix	BIX-01294
C2C12 +hDesmin	C2C12 stably expressing a particular hDesmin variant
CD	Consensus domains/motifs
conc.	Concentration
DAPI	4´-6-Diamidino-2-phenylindol
ddH2O	Double-distilled water
DGC	Dystrophin-glycoprotein complex
DM	Differentiation medium
DNA	Deoxyribonucleic acid
E. Coli	*Escherichia Coli*
EM	Electron microscopy
FCS	Fetal calf serum
fr.	Fraction (of antibody eluate)
GAPDH	Glyceraldehyde-3-Phosphate Dehydrogenase
GFAP	Glial fibrillary acidic protein
GM	Growth medium
h	Hour
hDes	Human desmin
HE	Hematoxylin-eosin
HGPS	Hutchinson-Gilbert progeria syndrome
HRP	Horse radish peroxidise
ICC	Immuno-cytochemistry
IF	Intermediate filaments
INM	Inner nuclear membrane
IP	Immunoprecipitation
mCherry-*hDes*	mCherry-tagged *hDes* (N-terminally)
mDes	Mouse desmin

m/hDes	Mouse and/or human desmin
min	Minute
MF	Microfilaments
MFM	Myofibrillary myopathy
MHC	Myosin heavy chain
monoAb	Monoclonal antibody
ms	Mouse
MT	Microtubules
Mw	Molecular weight
ONM	Outer nuclear membrane
p.	Passage
PCD	Pre-coil domain
PCR	Polymerase chain reaction
pH	Power of hydrogen (concentration of hydrogen ions in solution)
polyAb	Polyclonal antibody
rb	Rabbit
RT	Room temperature
s	Second
SHC	Sequence homology classes
ULF	Unit length filament
WB	Western blot
WT	Wild type (i.e., normal)

Appendix 2: h/mDesmin amino acid sequences alignment

Sequence alignment of amino acid composition of mouse and human desmin proteins. The amino acids that were the same in the two sequences have grey background whereas the ones that differ, with the same or different type of chemical group in the amino acid, are labelled in red and yellow respectively. One amino acid difference (hDesminS81) has green background.

```
         1                                                  50
mDesmin MSQAYSSSQR VSSYRRTFGG APGFSLGSPL SSPVFPRAGF GTKGSSSSMT
hDesmin MSQAYSSSQR VSSYRRTFGG APGFPLGSPL SSPVFPRAGF GSKGSSSSVT

         51                                                 100
mDesmin SRVYQVSRTS GGAGGLGSLR SSRLGTTRAP .SYGAGELLD FSLADAVNQE
hDesmin SRVYQVSRTS GGAGGLGSLR ASRLGTTRTP SSYGAGELLD FSLADAVNQE

        101                                                 150
mDesmin FLATRTNEKV ELQELNDRFA NYIEKVRFLE QQNAALAAEV NRLKGREPTR
hDesmin FLTTRTNEKV ELQELNDRFA NYIEKVRFLE QQNAALAAEV NRLKGREPTR

        151                                                 200
mDesmin VAELYEEEMR ELRRQVEVLT NQRARVDVER DNLIDDLQRL KAKLQEEIQL
hDesmin VAELYEEELR ELRRQVEVLT NQRARVDVER DNLLDDLQRL KAKLQEEIQL

        201                                                 250
mDesmin REEAENNLAA FRADVDAATL ARIDLERRIE SLNEEIAFLK KVHEEEIREL
hDesmin KEEAENNLAA FRADVDAATL ARIDLERRIE SLNEEIAFLK KVHEEEIREL

        251                                                 300
mDesmin QAQLQEQQVQ VEMDMSKPDL TAALRDIRAQ YETIAAKNIS EAEEWYKSKV
hDesmin QAQLQEQQVQ VEMDMSKPDL TAALRDIRAQ YETIAAKNIS EAEEWYKSKV

        301                                                 350
mDesmin SDLTQAANKN NDALRQAKQE MMEYRHQIQS YTCEIDALKG TNDSLMRQMR
hDesmin SDLTQAANKN NDALRQAKQE MMEYRHQIQS YTCEIDALKG TNDSLMRQMR

        351                                                 400
mDesmin ELEDRFASEA NGYQDNIARL EEEIRHLKDE MARHLREYQD LLNVKMALDV
hDesmin ELEDRFASEA SGYQDNIARL EEEIRHLKDE MARHLREYQD LLNVKMALDV

        401                                                 450
mDesmin EIATYRKLLE GEESRINLPI QTFSALNFRE TSPEQRGSEV HTKKTVMIKT
hDesmin EIATYRKLLE GEESRINLPI QTYSALNFRE TSPEQRGSEV HTKKTVMIKT

        451             470
mDesmin IETRDGEVVS EATQQQHEVL
hDesmin IETRDGEVVS EATQQQHEVL
```

Appendix 3: Amino acids

Amino acid	three-letter code	single-letter code
Glycine	Gly	**G**
Proline	Pro	**P**
Alanine	Ala	**A**
Valine	Val	**V**
Leucine	Leu	**L**
Isoleucine	Ile	**I**
Methionine	Met	**M**
Cysteine	Cys	**C**
Phenylalanine	Phe	**F**
Tyrosine	Tyr	**Y**
Tryptophan	Trp	**W**
Histidine	His	**H**
Lysine	Lys	**K**
Arginine	Arg	**R**
Glutamine	Gln	**Q**
Asparagine	Asn	**N**
Glutamic Acid	Glu	**E**
Aspartic Acid	Asp	**D**
Serine	Ser	**S**
Threonine	Thr	**T**